COUPLED HYDROLOGIC AND BIOGEOCHEMICAL PROCESSES CONTROLLING ARSENIC IN AQUIFERS OF SOUTHEAST ASIA

A DISSERTATION

SUBMITTED TO THE DEPARTMENT OF GEOLOGICAL AND

ENVIRONMENTAL SCIENCES

AND THE COMMITTEE ON GRADUATE STUDIES

OF STANFORD UNIVERSITY

IN PARTIAL FULFILLMENT OF THE REQUIREMENTS

FOR THE DEGREE OF

DOCTOR OF PHILOSOPHY

Matthew Polizzotto

April 2007

ABSTRACT

Arsenic contamination of groundwater in Southeast Asia represents the largest mass poisoning in history: nearly 100 million people are routinely drinking hazardous concentrations of arsenic. While arsenic is native to the sediments, its mechanism for release to the aqueous phase and its subsequent residence time in groundwater remain unresolved. In addition, the human-induced effects on arsenic concentrations are currently a topic of intense debate. The research presented in this thesis elucidates the coupled hydrological and biogeochemical processes controlling arsenic concentrations within aquifers of Southeast Asia. In addition, in this work, field research in Bangladesh and Cambodia serve as end-member examples of how land use may influence arsenic concentrations.

Nearly half of the 130 million people in Bangladesh drinks water with unsafe arsenic levels. Various theories have been put forth regarding the modes of arsenic release to the aqueous phase, ranging from the oxidative or reductive degradation of arsenic-bearing solids to competitive ligand displacement by phosphate. Reductive dissolution of Fe(III) (hydr)oxides and concomitant arsenic release has become the most widely accepted explanation of high arsenic groundwater concentrations. In order to evaluate the potential mechanisms of arsenic desorption to groundwater, spectroscopic and laboratory batch incubation experiments were conducted with aquifer sediments from Munshiganj, Bangladesh. Two significant pools of solid-phase arsenic were detected, though these two pools vary markedly in their potential for arsenic desorption. Arsenic-bearing iron sulfides, while comprising over 50% of the solid-phase arsenic, are not subject to redox transformation in the strongly reducing groundwater. Alternatively, a

highly labile, and thus mobile, arsenic phase persists in the aquifer. Importantly, contrary to what was the prevailing paradigm, Fe(III) (hydr)oxides are not detected in the aquifer materials and proxies of active microbial processes are inconsistent with Fe(III) reduction at well depth.

A comprehensive analysis of geochemical and hydrological conditions in Bangladesh suggests that arsenic may be released in the surface or near-surface environment and then transported to depth. Groundwater residence times are sufficiently short to necessitate continued input of arsenic in order to maintain observed concentrations. The only portion of the sediment profile with conditions conducive to arsenic desorption/dissolution is in the near-surface environment, and annual sediment deposition provides a means for sustained input of arsenic to groundwater. Thus, on the bases of coupled hydrologic, biogeochemical, and sedimentary processes, arsenic concentrations in groundwater can be maintained indefinitely.

In order to unequivocally determine the processes controlling arsenic concentrations in groundwater and to evaluate how anthropogenic changes in land use influence arsenic concentrations, I conducted a multifaceted field study within the Mekong Delta of Cambodia to detail the hydrology and biogeochemistry of the surface and subsurface environments. In the field area, central surface water ponds and wetlands overly the flood plain aquifer, and the Mekong and Bassac Rivers bound the wetlands on either side. Hydraulic gradients reveal seasonal reversals in groundwater flow directions, but net yearly flow from interior surface water (ponds and wetlands) through the aquifer and to the Mekong River; these flow patterns are supported by steady-state flux calculations as well as water budgets defined from changes in surface water levels,

evaporation rates, and rainfall. Spatial concentration profiles of arsenic and associated biogeochemical indicators (e.g., bicarbonate and ammonium) illustrate arsenic desorption within the initial portion (0 to 4 m depth) of the recharge flow path and minimal retardation within the aquifer. Seasonal changes in near-river groundwater arsenic, ammonium, calcium, magnesium, and sulfate concentrations are coincident with changes in flow directions, indicating that hydrology and geochemistry are linked at both the inlet and outlet of the aquifer.

Similarities in geologic deposition, aquifer source rock, regional hydrological gradients, and groundwater geochemistry between Cambodia and Bangladesh suggest that common processes control arsenic within the groundwater throughout Southeast Asia. Within our field area of the Mekong Delta in Cambodia, where anthropogenic land use alterations are negligible, natural hydrologic variations between rivers and adjacent wetlands drive both biogeochemical arsenic release to the shallow pore water and centurial-scale transport through the underlying aquifer back to the river. Arsenic influxes via sedimentation are equivalent to effluxes via groundwater discharge, and thus, groundwater arsenic concentrations are in steady-state and have persisted for millennia. However, human-induced changes in land use that disrupt the hydrologic regime or arsenic source material will have important consequences for arsenic in the aquifer, as evidenced by comparisons between the subsurface systems of Cambodia, where groundwater flow is natural, and Bangladesh, where flow paths have been distorted by extensive groundwater pumping for irrigation. Whereas arsenic concentration profiles from Cambodia reflect transport through the aquifer and discharge to rivers, arsenic concentrations are more spatially variable in Bangladesh and enhanced aquifer flushing

from irrigation pumping may be causing arsenic concentrations to decrease. Therefore, the results of this thesis suggest that policy makers in Southeast Asia must consider hydrological and biogeochemical information, as well projected changes in land use, when evaluating the long-term viabilities of groundwater resources.

TABLE OF CONTENTS

CHAPTER 1

Introduction

1.1. RESEARCH MOTIVATION

As many as 20 percent of the world's people do not have adequate access to drinking water sources untainted by biological or chemical contamination, and with increasing population and the ever expanding human footprint on natural resources, this number is expected to grow. Limited supply of safe drinking water most adversely affects the poorest people who have few options for improving their drinking water sources (UN, 2006). Natural and anthropogenic contamination of water can pose a serious hazard to human and ecosystem health, and therefore, understanding the threats to water supplies is vital for the protection of these resources.

Owing to both high population density and poor infrastructure, South and Southeast Asia presents a region of the world where people have insufficient drinking water sources and improper sanitation (WHO/UNICEF, 2004; WHO/UNICEF, 2005). As a result, life expectancies are significantly lower and infant morality rates are significantly higher in this region than in developed nations. Traditionally, the majority of people have obtained their domestic water supply from surface water sources such as rivers and ponds, but due to poor sanitation and rapid population growth, surface waters are increasingly contaminated with water-borne diseases. Accordingly, over the past forty years there has been a concentrated effort to use groundwater as the primary source of domestic water, as this water system is relatively devoid of disease-causing pathogens. Tragically, however, much of the groundwater in Southeast Asia is naturally contaminated with arsenic, and long-term exposure has resulted in arsenicosis and cancers (Smith et al., 2000; Yu et al., 2003). Thus, when it is left untreated, groundwater poses risks to human health as well and cannot be truly considered a viable source for

drinking and irrigation water. Because the latency period for cancer from arsenic poisoning is on the order of decades (Yoshida et al., 2004) and because pathogen-laden surface water remains the only alternative, arsenic-contaminated groundwater is still widely consumed throughout Southeast Asia. As many as 100 million people in the region are estimated to routinely drink water with arsenic concentrations greater than the World Health Organization recommended limit of 10 μg/L (Smith et al., 2000; Ahmed et al., 2006).

Although arsenic contamination of groundwater in Southeast Asia represents "the largest mass poisoning in human history" (Smith et al., 2000), the processes responsible for controlling arsenic within the subsurface of the region are poorly understood. The erratic distribution of arsenic has proven puzzling, and discerning overarching mechanisms influencing the fate and transport of arsenic has been convoluted by human impacts to the natural environment (Harvey et al., 2006). It is critical that we develop an understanding of processes governing groundwater arsenic concentrations; improvements in our understanding and predictive capacities may serve to benefit millions of people.

Contaminants in surface and subsurface waters are controlled by a host of physical, chemical, and biological processes, each of which can exert an influence over a range of spatial and temporal scales, from the molecular scale to the field scale, and from nanoseconds to millennia. Because arsenic dynamics are modulated by a complexity of factors and distinct processes, effectively predicting and controlling the fate of arsenic in the environment requires an integration of approaches. The research presented in this thesis seeks to link the hydrologic and biogeochemical factors responsible for the mass arsenic contamination of groundwater in Southeast Asia. Such an integration has

previously proven elusive and the research presented in Chapters 2 through 5 incorporates spectroscopic, laboratory, and field data to bridge both spatial and temporal scales. Field sites in Bangladesh (Chapters 2 and 3) and Cambodia (Chapters 4 and 5) also serve as end-members in terms of human impacts to the natural environment and illustrate how land use is intimately connected to arsenic in groundwater. Because Southeast Asia includes some of the most densely populated nations, the issues surrounding water resources in this region impact more people than anywhere else in the world. It is hoped that the results of this research will be accessible and useful to policy makers concerned with improving water resources in Southeast Asia, and that the conclusions will serve as a basis for predicting future changes to arsenic concentrations that occur as a result of development and land use alterations.

1.2. BACKGROUND

1.2.1. Southeast Asian Natural Environment and Water Use

The low-latitude and low-elevation nations that comprise Southeast Asia are geologically young, formed following the transport and deposition of eroded Himalayan sediments. From West Bengal, India to southeastern China, large meandering rivers – including the Ganges, Brahmaputra, Meghna, Irrawaddy, Salween, Mekong, and Red Rivers – dominate the landscape (and the livelihood) of the region. The rivers carry massive sediment loads and are home to a diverse array of flora and faunal species (e.g. Berg et al., 2001; Ta et al., 2002; Goodbred et al., 2003; Ahmed et al., 2004).

River stage levels fluctuate dramatically throughout the year, with as much as 10 m differences between the wet and dry seasons. Water levels are typically highest in the

late summer and early fall, following Himalayan snowmelt and monsoonal rains. Rivers often breach their banks during high stages, flooding the surrounding areas and leaving overbank deposits of clay-rich sediments that overlay deeper aquifer sands. Nutrients deposited with sediments during flooding have created fertile, arable lands, and accordingly, agricultural and subsistence living is pervasive throughout rural areas, supporting high population densities. Local rains are governed by the monsoon and occur in brief, but intense, ~3-month periods throughout the year.

The abundance of accessible river and pond water and a lack of financial resources throughout Southeast Asian countries have resulted in the widespread consumption of unhealthy surface water. For instance, in Bangladesh, over 25% of the population does not use "improved" water sources, with "improved" defined here to include piped water, tubewells, protected wells, rainwater, and bottled water; staggeringly, in Cambodia, up to 66% do not use improved water sources (WHO/UNICEF 2004; WHO/UNICEF, 2005).

In an effort to minimize the health risks associated with the mass use of "unimproved" drinking water sources (which include unprotected dug wells, springs, and direct surface water), international aid groups, nongovernmental organizations, and local governments have combined to install shallow tubewells for groundwater retrieval. In Bangladesh alone, 4 million wells have been installed that could potentially serve 95% of the population (WHO, 2004); in Cambodia, over 40,000 wells had been installed as of 2004 (Fredericks, 2004), and the number continues to grow.

Natural arsenic contamination of groundwater in Southeast Asian aquifers, however, is slowly poisoning many of the millions of people who currently rely on

groundwater for drinking. While knowledge about contamination of groundwater has spread into rural areas, strategies for mitigating the problem have lagged. Rainwater harvesting, surface water filtration, groundwater (arsenic) filtration, and aeration of shallow wells have each been utilized, but in general, none of the present methods appear acceptable as a widely distributed, long-term solution. Groundwater use is currently the most widely adopted means of obtaining 'clean' drinking water. Thus, understanding processes controlling arsenic concentrations within the groundwater is vital.

1.2.2. Processes Controlling Arsenic in the Environment

Arsenic is a contaminant in many groundwater systems throughout the world (Nordstrom, 2002). High concentrations of arsenic in drinking water can lead to arsenicosis, a condition that may include skin lesions, paralysis, blindness, and bladder, lung, skin, kidney, liver, and prostate cancers (Yamauchi and Fowler, 1994). For these reasons, and for its extensive presence in the environment, arsenic ranks as the top priority contaminant by the CERCLA, ahead of other notable poisons such as lead, mercury, and vinyl chloride (CERCLA, 2005). The World Health Organization has recommended a maximum allowed concentration of As in drinking water of 10 μg/L (WHO, 2004); it is estimated that over 100 million people worldwide are regularly exposed to drinking water above this level (Smedley and Kinniburgh, 2002; Yu et al., 2003; Ahmed et al., 2006).

Anthropogenic sources of arsenic, such as mine drainage, agricultural pesticides, and burning of fossil fuels, typically lead to the greatest concentrations of arsenic in soils and sediments. However, natural sources of arsenic, although typically much lower in

total concentration, are having devastating global impacts on human health (*e.g.* Nickson et al., 2000; Welch, et al., 2000; Smedley et al., 2002). Primary sources of arsenic are prominently sulfide minerals, but these are not often labile without changes in redox conditions (Eary, 1992; Nesbitt et al. 1995). In oxidized environments, arsenic exists dominantly as the arsenate anion (AsO_4^{3-} [As(V)]) and is usually (strongly) adsorbed on mineral surfaces (Mok and Wai, 1994; Waychunas et al., 1993; Fendorf et al., 1997; Manning et al., 1998; Ladeira et al., 2001; Farquhar et al., 2002). Arsenite (AsO_3^{3-} [As(III)]), a reduced form of arsenic, typically exhibits a strong preference for adsorption on iron (hydr)oxides (Manning et al., 1998; Raven et al., 1998; Sun and Doner, 1998; Dixit and Hering, 2003), and tends to adsorb more extensively at higher pH (adsorption maximum's are usually near pH 8.5). Although arsenite binds extensively to ferric (hydr)oxides, it forms weaker complexes than arsenate (Herbel et al., 2006; Kocar et al., 2006) and thus tends to be more mobile. Arsenite is also three to five times more toxic than arsenate, but each of the inorganic forms is much more hazardous than organic arsenic species in low temperature environmental systems (Yamauchi and Fowler, 1994).

The particular speciation of arsenic greatly affects its mobility in soils and sediments, and varying environmental conditions may influence arsenic adsorption/desorption on soil and sediment minerals (Masscheleyn et al., 1991). Numerous processes have been postulated to promote arsenic desorption/dissolution, including oxidation of arsenic-bearing sulfides (Nesbitt et al., 1995), reductive dissolution of arsenic-bearing ferric (hydr)oxides (Cummings et al., 1999), arsenate reduction to arsenite, desorption at high pH > 8.5 (Frost and Griffin, 1977; Darland and Inskeep, 1997; Jackson and Miller, 2000), and ion displacement by phosphate (Darland

and Inskeep, 1997; Peryea and Kammereck, 1997), carbonate (Appelo et al., 2002), silicic acid (Waltham and Eick, 2002), and natural organic matter (Redman et al., 2002). However, arsenic release to the aqueous phase is typically promoted most extensively by changes in redox conditions. Reductive dissolution of primary sorbents, particularly ferric (hydr)oxides, and arsenate reduction to arsenite trigger the release of arsenic into the aqueous phase. The problem of arsenic contamination in groundwater as a result of anaerobic arsenic displacement is particularly acute in aquifers of sedimentary basins (Smedley and Kinniburgh, 2002).

As a result of the onset of these triggers (high pH, competitive ligand displacement, and anaerobic release), over the past half century increases in solution phase arsenic in drinking water have been recorded throughout the world, most notably in Bangladesh and West Bengal, India (where arsenic affects up to 100 million people), but also throughout Southeast Asia (>1 million people), China (>1 million people), South America (>3 million people), and in more localized areas of Europe and the United States (>1 million people) (Nordstrom, 2002; Smedley and Kinniburgh, 2002; Yu et al., 2003; Polya et al., 2005; Berg et al., 2006; Ahmed et al., 2006).

1.2.3. Arsenic in Southeast Asia

Hazardous concentrations of arsenic have been detected in groundwater from countries throughout Southeast Asia, including India, Bangladesh, Myanmar, Thailand, Laos, Nepal, Cambodia, and Vietnam (Kadushkin et al., 2004). To date, the majority of research concerning arsenic has been conducted in the Ganges-Brahmaputra Delta of West Bengal, India and Bangladesh, where the problem is most severe and arsenic

contamination of drinking water adversely affects nearly half of the population (Smith et al., 2000; Yu et al., 2003). Recently, in an effort to discover the extent of the situation, studies have also been conducted in the Vietnamese Red River Delta and the Mekong River Delta of Cambodia and Vietnam (Berg et al., 2001; Polya et al., 2003; Stranger et al., 2005; Polya et al., 2005; Berg et al., 2006).

Due to similarities in geologic source material, depositional history, regional hydrologic gradients, and current monsoonal climate, it is generally accepted that similar processes may control arsenic throughout Southeast Asia. The arsenic affected areas are massive deltas, formed from the erosion of the Himalayas following the rise in sea level 6,000 to 10,000 years ago (Ta et al., 2002; Goodbred et al., 2003). Arsenic is derived from arsenic-bearing sulfide minerals in the Himalaya that are then oxidized before and/or during transport (Galy and France-Lanord, 1999); arsenic-laden weathering products, ferric (hydr)oxides in particular, are then deposited in the sediment basins.

As a consequence of the similarities in environmental and geological settings, aquifer characteristics are also comparable throughout Southeast Asia. High arsenic groundwaters are found in Holocene aquifers dominated by fine grey sands, and the sediments contain dispersed, near crustal-average, solid-phase arsenic concentrations (Smedley and Kinniburgh, 2002; Swartz et al., 2004). In these aquifers dissolved arsenic is associated with reducing, circumneutral pH groundwater dominated by Ca^{2+} and HCO_3^- ions (McArthur et al., 2001; Berg et al., 2001; Swartz et al., 2004; Buschmann et al., 2007).

Despite their importance on environmental quality and human health, the processes controlling arsenic concentrations in Southeast Asia remain unresolved.

Researchers have postulated that arsenic desorption/dissolution from sediments is due to the oxidation of arsenic-bearing sulfides (Chowdhury et al., 1999) or ion displacement from aquifer mineral surfaces by fertilizer-derived phosphate (Acharyya et al., 1999), but these mechanisms are now generally discounted. Instead, it has been widely believed that dissolved arsenic is a product of the microbial reduction of Fe within aquifer sediments (Nickson et al., 1998; Nickson et al., 2000; McArthur et al., 2001; Berg et al., 2001; Dowling et al., 2002; Harvey et al., 2002; Islam et al., 2004; Polya et al., 2005; Berg et al., 2006). Data to support the reductive dissolution mechanism have predominantly been obtained from aqueous chemistry. Groundwater typically has high Fe^{2+} concentrations (Nickson et al., 2000; McArthur et al., 2001; Dowling et al., 2002; Harvey et al., 2002; Swartz et al., 2004), and dissolved arsenic often correlates with chemical species indicative of biological activity including ammonium and dissolved inorganic carbon (Dowling et al., 2002; Harvey et al., 2002).

In order to characterize aquifer sediments, particularly phases hosting arsenic, numerous techniques have been utilized. X-ray diffraction, electron microprobe analysis, transmission electron microscopy (Akai et al., 2004), scanning electron microscopy (Nickson et al., 2000; Akai et al., 2004), extractions (Swartz et al., 2004; Horneman et al., 2004), color (van Geen et al., 2003a), reflectance and magnetic properties (Horneman et al., 2004), and X-ray absorption spectroscopy (Gault et al., 2003; Gault et al., 2005; Rowland et al., 2005) have been employed to characterize sediment solid-phases, although to date Fe(III) (hydr)oxides – the potential source of arsenic – have not been detected from aquifer materials associated with high dissolved arsenic, nor has solid-phase arsenic been adequately speciated before the research presented here. Finally,

laboratory microcosm experiments have been conducted to isolate mechanisms of arsenic release (Akai et al., 2004; Islam et al., 2004; van Geen et al., 2004). In each case, researchers found arsenic to be released from sediments with the onset of reducing conditions, and microbial reduction stimulated arsenic liberation. However, none of the studies used Holocene aquifer sediments from where groundwater concentrations are highest, but instead researchers used near-surface sediments or deep clays. In my thesis, I fill in this gap and show rapid abiotic arsenic desorption from Holocene aquifer sands in batch experiments.

Although there is general agreement for microbial reductive dissolution as the mechanism leading to high arsenic concentrations, the organic carbon source fueling this process has been intensely debated. Organic carbon was first speculated to be derived from aquifer sedimentary peat deposits (McArthur et al., 2001; McArthur et al., 2004; Berg et al., 2006). In contrast, on the basis of ^{3}H and ^{14}C isotopic analyses, it has also been argued that labile dissolved organic carbon from surface ponds stimulates microbial activity following its transport to the aquifer (Harvey et al., 2002). This dispute has highlighted questions concerning the role of hydrological processes influencing arsenic within the subsurface; in particular, sedimentary carbon requires relatively stagnant groundwater, while surface-derived labile dissolved organic carbon necessitates substantial groundwater flow. Furthermore, the suggestion that the recent widespread irrigation with groundwater has modified hydrologic flow and resulted in surface-derived organic carbon being brought to depth remains contentious (Harvey et al., 2002; van Geen et al., 2003b; Aggarwal et al., 2003; Harvey et al., 2003; McArthur et al., 2004).

Recently, the hydrologic and geochemical processes governing arsenic in the subsurface have been refined further. The spatial variability of arsenic has been reported (van Geen et al., 2003a), and arsenic and iron release to solution have been shown to be decoupled (Horneman et al., 2004; van Geen et al., 2004; van Geen et al., 2006). Additionally, hydrologic modeling has indicated that in Bangladesh prior to irrigation pumping, groundwater residence times were 44-84 y, but with the onset of irrigation, groundwater residence times were 26-38 y, allowing surface water to reach the depths of wells in under forty years (Harvey et al., 2006).

Despite concerted effort to deduce the causal process liberating arsenic to groundwater, a unifying model has yet to be developed, and as a result, a number of questions concerning arsenic remain unanswered. Both laboratory and field investigations have focused on isolated rather than interrelated processes, thereby limiting our understanding of arsenic fate and transport. The spatial variance in arsenic concentrations has yet to be explained. Additionally, given high recharge rates and relatively low aquifer solid-phase concentrations, it is puzzling that arsenic remains in the groundwater and has not been flushed from the system. Therefore, development of a coupled hydrologic and geochemical model describing arsenic in groundwater is critically needed not only to mitigate the current contamination problem, but also to predict where arsenic concentrations may ultimately prove hazardous.

1.3. SCOPE OF RESEARCH

The research presented in this thesis seeks to discern the dominant factors controlling arsenic concentrations in Southeast Asian aquifers. Field, laboratory, and

spectroscopic investigations are integrated in order to probe a range of spatial scales, from the molecular level to the field scale. The main objective of this work is to create a model unifying the hydrological and biogeochemical factors that influence arsenic in groundwater. In particular, I hope to (i) determine the mechanism(s) responsible for arsenic liberation to the aqueous phase; (ii) resolve existing puzzles concerning the spatial distribution of arsenic; (iii) improve the ability to predict arsenic concentrations; and (iv) create a basis for understanding how human actions may alter arsenic concentrations. Studies have been performed from field sites in Bangladesh, where human-induced land use changes are pervasive throughout the country, and Cambodia, where human disturbances to the environment are negligible.

The chapters in this thesis describe research that has evolved as the understanding of arsenic in Southeast Asia has improved. The aim of the work in Chapter 2 was to use spectroscopic techniques and laboratory analyses to confirm the theory that arsenic is released from aquifer sediments during the reductive dissolution of ferric (hydr)oxides in Bangladesh; however, the experimental results from these studies indicate that the original hypothesis is incomplete. Accordingly, I investigated other possible mechanisms governing the release of native arsenic into groundwater systems. Chapter 3 represents this line of investigation, and my assimilation of disparate data demonstrates that arsenic is released to solution outside of the aquifer, and it is likely transported through the aquifer by hydrologic flow. Because natural groundwater flow patterns in Bangladesh have been distorted due to pervasive pumping for irrigation, tracking the transport of arsenic in the subsurface is challenging. In Cambodia, groundwater pumping is negligible, and Chapter 4 presents the hydrology and geochemistry of a field site from

where land use perturbations are minimal and arsenic is controlled only by natural processes. Finally, Chapter 5 illustrates a unified model describing arsenic behavior in the groundwater of Cambodia, and it is shown that anthropogenic land use changes will alter arsenic concentrations in aquifers throughout Southeast Asia. A brief summary of each research chapter is given below.

Chapter 2: Solid-Phases and Desorption Processes of Arsenic within Bangladesh Sediments

Reductive dissolution of ferric (hydr)oxides and concomitant arsenic release is the most widely accepted explanation of high arsenic groundwater concentrations in Bangladesh. However, this conclusion is based almost solely on aqueous chemistry data, and little attention has been paid to controls by solid phases on groundwater flow and residence times. The research presented in Chapter 2 investigates solid phase speciation and arsenic release processes of sediments from a field site in Munshiganj, Bangladesh. In contrast to expectations, ferric (hydr)oxides were not detected within the sandy aquifer sediments, and solid-phase arsenic is predominantly found in detrital and authigenic sulfide minerals. Furthermore, in batch microcosm experiments, arsenic rapidly desorbs from aquifer sediments, indicating that arsenic retardation in flowing groundwater is minimal. Arsenic and iron speciation from soils indicate a zone of active reduction, and therefore, the near-surface is a potential location of arsenic release.

Chapter 3: Processes Conducive to the Release and Transport of Arsenic into Aquifers of Bangladesh

Studies concerning the causes of arsenic in Southeast Asian groundwater have typically focused on isolated processes (e.g. desorption, reductive dissolution, transport) and as a result, have often overlooked process coupling (reactive transport) that may influence arsenic concentrations. Moreover, solid-phase speciation and hydrology have seldom been examined in detail. The research in Chapter 3 seeks to rectify many of the misleading assumptions and takes a holistic view of the processes influencing arsenic by combining existing hydrological and biogeochemical data. My research establishes that for arsenic to be maintained in the aquifer under current groundwater flow conditions, it must be generated from a source that is hydraulically upgradient from the aquifer sediments. Within soils and near-surface sediments, seasonally fluctuating redox conditions promote arsenic liberation from the solid- to the aqueous-phase and lead to subsequent transport to depth with groundwater recharge. Arsenic concentrations in aquifers are maintained by annual deposition of Himalayan sediments. Furthermore, anisotropy in hydrologic conductivity and gradients rectifies the puzzling spatial variation in arsenic concentrations, resulting from groundwater flow and arsenic transport patterns.

Chapter 4: Coupled Hydrologic and (Bio)geochemical Processes Controlling Arsenic Cycling in the Mekong Delta, Cambodia

The hydrologic influence on arsenic in Bangladeshi groundwater has been fiercely debated, in part because pervasive well pumping for irrigation has resulted in convoluted groundwater flow paths. Additionally, throughout Southeast Asia, little data exists on hydrologic processes occurring at the scale of the spatial variation in arsenic concentrations. Moreover, in nearly all studies, hydrological and geochemical factors are considered separately. In order to consider a less convoluted hydrologic regime, and

thereby isolate groundwater flow paths and arsenic distribution in recharge waters, in Chapter 4 I describe a regional geochemical and hydrological evaluation performed within the upper region of the Mekong River Delta, Cambodia. In Cambodia, groundwater pumping is negligible, and therefore, natural hydraulic gradients are undisturbed by irrigation pumping. In fact, hydraulic gradients throughout the field area are constrained by the Mekong River and interior wetlands, which are separated by a natural levee. Net annual groundwater flow is from interior wetlands, through the underlying aquifer, and to the Mekong River; vertical and horizontal fluxes indicate steady-state groundwater flow. Spatial distributions of dissolved chemical species suggest biotically-controlled arsenic release at recharge zones, with subsequent arsenic transport along recharge flowpaths into the underlying aquifer.

Chapter 5: Contributions of Natural Arsenic Cycling and Human Disturbance to History's Largest Mass Poisoning

Similarities in geologic deposition, aquifer source rock, regional hydrological gradients, and groundwater chemistry throughout the aquifers of Southeast Asia suggest that the processes controlling arsenic in the subsurface are common throughout the region. However, these processes, as well as the anthropogenic influence on arsenic concentrations within Southeast Asian aquifers, remain unresolved. The research in Chapter 5 presents a unifying hydrologic and geochemical model describing the fate and transport of arsenic within the Mekong Delta of Cambodia. Seasonally-shifting hydrologic gradients drive both biogeochemical arsenic release from near-surface sediments and arsenic transport through the aquifer. Arsenic influx to the system *via* sediment deposition and efflux *via* groundwater transport out of the aquifer are at steady-

state. Comparisons of land use practices and environmental conditions found in different river deltas reveal that throughout Southeast Asia, arsenic contamination of groundwater has existed prior to anthropogenic disturbance of the surface or subsurface environment. Nevertheless, land use changes such as pumping for irrigation, sediment removal, and upstream river damming will each impact arsenic concentrations in groundwater.

Summary

The sum research presented in this thesis reveals that in Southeast Asia, arsenic is liberated to solution from near-surface sediments and is subsequently transported into aquifers by groundwater flow. In both Bangladesh and Cambodia, influxes of arsenic are sufficient to maintain dissolved arsenic concentrations despite arsenic removal from aquifers during groundwater discharge. However, while the distribution of arsenic concentrations reflects natural groundwater flow patterns in Cambodia, analyses in Bangladesh indicate that arsenic concentrations have been impacted by irrigation pumping there. Thus, land use changes that distort the natural hydrologic regime alter arsenic concentrations, and in order to predict where hazardous arsenic concentrations occur, an integrated understanding of hydrology, biogeochemistry, and land use practices is required.

1.4. REFERENCES

Acharyya, S. K., Chakraborty, P., Lahiri, S., Raymahashay, B. C., Guha, S., and Bhowmik, A. (1999) Arsenic poisoning in the Ganges delta. *Nature* **401**, 545.

Aggarwal, P. K., Basu, A. R., and Kulkarni., K. M. (2003) Comment on "Arsenic mobility and groundwater extraction in Bangladesh" (I). *Science* **300**, 584b.

Ahmed, K. M., Bhattacharya, P., Hasan, M. A., Akhter, S. H., Alam, S. M. M, Bhuyian, M. A. H., Imam, M. B., Khan, A. A., and Sracek, O. (2004) Arsenic enrichment in groundwater of the alluvial aquifers in Bangladesh: an overview. *Appl. Geochem.* **19**, 181-200.

Ahmed, M. F., Ahuja, S., Alauddin, M., Hug, S. J., Lloyd, J. R., Pfaff, A., Pichler, T., Saltikov, C., Stute, M., and van Geen, A. (2006) Ensuring safe drinking water in Bangladesh. *Science* **314**, 1687-1688.

Akai, J., Izumi, K., Fukuhara, H., Masuda, H., Nakano, S., Yoshimura, T., Ohfuji, H., Anawar, H.M., and Akai, K. (2004) Mineralogical and geomicrobiological investigations on groundwater arsenic enrichment in Bangladesh. *Appl. Geochem.* **19**, 215-230.

Appelo, C. A. J., Van der Weiden, M. J. J., Tournassat, C., and Charlet, L. (2002) Surface complexation of ferrous iron and carbonate on ferrihydrite and the mobilization of arsenic. *Environ. Sci. Technol*. **36**, 3096-3103.

Berg, M., Tran, H. C., Nguyen, T. C., Pham, H. V., Schertenlieb, R., and Giger, W. (2001) Arsenic contamination of groundwater and drinking water in Vietnam: A human health threat. *Environ. Sci. Technol*. **35**, 2621-2626.

Berg, M., Stengel, C., Trang, P. T. K., Viet, P. H., Sampson, M. L., Leng, M., Samreth, S., and Fredericks, D. (2006) Magnitude of arsenic pollution in the Mekong and Red River Deltas — Cambodia and Vietnam. *Sci. Tot. Environ.* **372**, 413-425.

Buschmann, J., Berg, M., Stengel, C., and Sampson, M. L. (2007) Arsenic contamination in Cambodia: confined risk areas controlled by 'mirco-topography' in the Upper Mekong Delta. *Environ. Sci. Technol*. in press.

CERCLA (Comprehensive Environmental Response, Compensation, and Liability Act) (2005) http://www.atsdr.cdc.gov/cercla/05list.html, Agency for Toxic Substances and Disease Registry, Department of Health and Human Services.

Chowdhury, T. R., Basu, G. K., Samanta, G., Chanda, C. R., Mandal, B. K., Dhar, R. K., Biswas, B. K., Lodh, D., Ray, S. L., and Chakraborti, D. (1999) Arsenic poisoning of Bangladesh groundwater. *Nature* **401**, 545-546.

Cummings, D. E., Caccavo, F. Jr., Fendorf, S., and Rosenzweig, R. F. (1999) Arsenic mobilization by the dissimilatory Fe(III)-reducing bacterium Shewanella alga BrY. *Environ. Sci. Technol*. **33**, 723-729.

Darland, J. E. and Inskeep, W. P. (1997) Effects of pH and phosphate competition on the transport of arsenate. *J. Environ. Qual*. **26**, 1133-1139.

Dixit, S. and Hering, J. G. (2003) Comparison of arsenic(V) and arsenic(III) sorption onto iron oxide minerals: implications for arsenic mobility. *Environ. Sci. Technol*. **37**, 4182-4189.

Dowling, C. B., Poreda, R. J., Basu, A. R., Peters, S. L., and Aggarwal, P. K. (2002) Geochemical study of arsenic release mechanisms in the Bengal Basin groundwater. *Water Resour. Res.* **38**, 1173, doi: 10.1029/2001WR000968.

Eary, L. E. (1992) The solubility of amorphous As_2S_3 from 25 to 90°C. *Geochim. Cosmochim. Acta* **56**, 2267-2280.

Farquhar, M. L., Charnock, J. M., Livens, F. R., and Vaughan, D. J. (2002) Mechanisms of arsenic uptake from aqueous solution by interaction with goethite, lepidocrocite, mackinawite, and pyrite: an x-ray absorption spectroscopy study. *Environ. Sci. Technol*. **36**, 1757-1762.

Fendorf, S., Eick, M. J., Grossl, P., and Sparks, D. L. (1997) Arsenate and chromate retention mechanisms on goethite. 1. Surface structure. *Environ. Sci. Technol*. **31**, 315-320.

Fredericks, D. (2004) *Situation analysis: arsenic contamination of groundwater in Cambodia.* Unpublished Report to Arsenic Inter-Ministerial Sub-Committee, Cambodia, July 2004, 54 p.

Frost, R. R. and Griffin, R. A. (1977) Effect of pH on adsorption of arsenic and selenium from landfill leachate by clay minerals. *Soil Sci. Soc. Am. J*. **41**, 53-57.

Galy, A. and France-Lanord, C. (1999) Weathering processes in the Ganges-Brahmaputra basin and the riverine alkalinity budget. *Chemical Geology* **159**, 31-60.

Gault, A. G., Polya, D. A., Charnock, J. M., Islam, F. S., Lloyd, J. R., and Chatterjee, D. (2003) Preliminary EXAFS studies of solid phase speciation of As in a West Bengali sediment. *Mineral. Mag.* **67**, 1183-1191.

Gault, A. G., Islam, F. S., Polya, D. A., Charnock, J. M., Boothman, C., Chatterjee, D., and Lloyd, J. R. (2005) Microcosm depth profiles of arsenic release in a shallow aquifer, West Bengal. *Mineral. Mag.* **69**, 855-863.

Goodbred, S. L., Kuehl, S. A., Steckler, M. S., and Sarker, M. H. (2003) Controls on facies distribution and stratigraphic preservation in the Ganges-Brahmaputra delta sequence. *Sed. Geo.* **155**, 301-316.

Harvey, C. F., Swartz, C. H., Badruzzaman, A. B. M., Keon-Blute, N., Niedan, V., Brabander, D., Oates, P. M., Ashfaque, K. N., Islam, S., Hemond, H. F., and Ahmed, M.F. (2002) Arsenic mobility and groundwater extraction in Bangladesh. *Science* **298**, 1602-1606.

Harvey, C. F., Swartz, C., Badruzzaman, A. B. M., Keon-Blute, N., Niedan, V., Brabander, D., Oates, P. M., Ashfaque, K. N., Islam, S., Hemond, H. F., and Ahmed, M. F. (2003) Response to comments on "Arsenic mobility and groundwater extraction in Bangladesh". *Science* **300**, 584d.

Harvey, C. F., Ashfaque, K. N., Yu, W., Badruzzaman, A. B. M., Ali, M. A., Oates, P. M., Michael, H., Neumann, R. B., Beckie, R., Islam, S., and Ahmed, M. F. (2006) Groundwater flow and arsenic biogeochemistry in Bangladesh: an analysis of transience and coupling. *Chemical Geology* **228**, 112-136.

Herbel, M. and Fendorf, S. (2006) Biogeochemical processes controlling the speciation and transport of arsenic within iron coated sands. *Chemical Geology*, **228**, 16-32.

Horneman, A., van Geen, A., Kent, D. V., Mathe, P. E., Zheng, Y., Dhar, R. K., O'Connell, S., Hoque, M. A., Aziz, Z., Shamsudduha, M., Seddique, A. A., and Ahmed, K. M. (2004) Decoupling of As and Fe release to Bangladesh groundwater under reducing conditions. Part I: Evidence from sediment profiles. *Geochim. Cosmochim. Acta* **68**, 3459-3473.

Islam, F. S., Gault, A. G., Boothman, C., Polya, D. A., Chatterjee, D., and Lloyd, J. (2004) Direct evidence of arsenic release from Bengali sediments due to metal-reducing bacteria. *Nature* **430**, 68-71.

Jackson, B. P. and Miller, W. P. (2000) Effectiveness of phosphate and hydroxide for desorption of arsenic and selenium species from iron oxides. *Soil Sci. Soc. Am. J.* **64**, 1616-1622.

Kadushkin, A., Siddiqui, Z., and Shipin, O. (2004) Groundwater quality assessment and management in selected countries of East and South-East Asia. *Water Resour. J.* **216**, 83-108.

Kocar, B. D., Herbel, M. J., Tufano, K. J., and Fendorf, S. (2006) Contrasting effects of dissimilatory iron(III) and arsenic(V) reduction on arsenic retention and transport. *Environ. Sci. Technol.* **40**, 6715-6712.

Ladeira, A. C. Q., Ciminelli, V. S. T., Duarte, H. A., Alves, M. C. M., and Ramos, A. Y. (2001) Mechanism of anion retention from EXAFS and density functional calculations: Arsenic (V) adsorbed on gibbsite. *Geochim. Cosmochim. Acta* **65**, 1211-1217.

Manning, B. A., Fendorf, S. E., and Goldberg, S. (1998) Surface structures and stability of arsenic (III) on goethite: spectroscopic evidence for inner-sphere complexes. *Environ. Sci. Technol.* **32**, 2383-2388.

Masscheleyn, P. H., Delaune, R. D., and Patrick, W. H. Jr (1991) Effect of redox potential and pH on arsenic speciation and solubility in a contaminated soil. *Environ. Sci. Technol*. **25**, 1414-1419.

McArthur, J. M., Ravenscroft, P., Safiulla, S., and Thirlwall, M. F. (2001) Arsenic in groundwater: Testing pollution mechanisms for sedimentary aquifers in Bangladesh. *Water Resour. Res.* **37**, 109-117.

McArthur, J. M., Banerjee, D. M., Hudson-Edwards, K. A., Mishra, R., Purohit, R., Ravenscroft, P., Cronin, A., Howarth, R. J., Chatterjee, A., Talukder, T., Lowry, D., Houghton, S., and Chadha, D. K. (2004) Natural organic matter in sedimentary basins and its relation to arsenic in anoxic ground water: the example of West Bengal and its worldwide implications. *Appl. Geochem.* **19**, 1255-1293.

Mok, W. M. and Wai, C. M. (1994) Mobilization of arsenic in contaminated river waters. p. 99-118. In Nriagu, J. O. (ed.). *Arsenic in the Environment. Part I. Cycling and Characterization*. Vol. **26**, Wiley Series in Advances in Environmental Science and Technology, Wiley-Interscience, 430 p.

Nesbitt, H. W., Muir, I. J., and Pratt, A. R. (1995) Oxidation of arsenopyrite by air and air-saturated, distilled water, and implications for mechanism of oxidation. *Geochim. Cosmochim. Acta*. **59**, 1773-1786.

Nickson, R., McArthur, J., Burgess, W., Ahmed, K. M., Ravenscroft, P., and Rahman, M. (1998) Arsenic poisoning of Bangladesh groundwater. *Nature* **395**, 338.

Nickson, R. T., McArthur, J. M., Ravenscroft, P., Burgess, W. G., and Ahmed, K.M. (2000) Mechanism of arsenic release to groundwater, Bangladesh and West Bengal. *Appl. Geochem.* **15**, 403-413.

Nordstrom, D. K. (2002) Worldwide occurrences of arsenic in ground water. *Science* **296**, 2143-2144.

Peryea, F. J. and Kammereck, R. (1997) Phosphate-enhanced movement of arsenic out of lead arsenate- contaminated topsoil and through uncontaminated subsoil. *Water, Air, and Soil Pollution* **93**, 243-254.

Polya. D. A., Lythgoe, P. R., Abou-Shakra, F., Gault, A. G., Brydie, J. R., Webster, J. G., Brown, K. L., Nimfopolous, M. K., and Michailidis, K. M. (2003) IC-ICP-MS and IC-ICP-HEX-MS determination of arsenic speciation in surface and groundwaters: preservation and analytical issues. *Mineral. Mag.* **67**, 247-262.

Polya, D. A., Gault, A. G., Diebe, N., Feldman, P., Rosenboom, J. W., Gilligan, E., Fredericks, D., Milton, A. H., Sampson, M., Rowland, H. A. L., Lythgoe, P. R., Jones, J. C., Middleton, C., and Cooke, D. A. (2005) Arsenic hazard in shallow Cambodian groundwaters. *Mineral. Mag.* **69**, 807-823.

Raven, K. P., Jain, A., and Loeppert, R. H. (1998) Arsenite and arsenate adsorption on ferrihydrite: kinetics, equilibrium, and adsorption envelopes. *Environ. Sci. Technol*. **32**, 344-349.

Redman, A. D., Macalady, D. L., and Ahmann, D. (2002) Natural organic matter affects arsenic speciation and sorption onto hematite. *Environ. Sci. Technol*. **36**, 2889-2896.

Rowland, H. A. L., Gault, A. G., Charnock, J. M., and Polya, D. A. (2005) Preservation and XANES determination of the oxidation state of solid-phase arsenic in shallow sedimentary aquifers in Bengal and Cambodia. *Mineral. Mag.* **69**, 825-839.

Smedley, P. L. and Kinniburgh, D. G. (2002) A review of the source, behaviour and distribution of arsenic in natural waters. *Appl. Geochem.* **17**, 517-568.

Smedley, P. L., Nicolli, H. B., Macdonald, D. M. J., Barros, A. J., and Tullio, J. O. (2002) Hydrogeochemistry of arsenic and other inorganic constituents in groundwaters from La Pampa, Argentina. *Appl. Geochem*. **17**, 259-284.

Smith, A. H., Lingas, E. O., and Rahman, M. (2000) Contamination of drinking-water by arsenic in Bangladesh: a public health emergency. *Bulletin World Health Organization* **78**, 1093-1103.

Stanger, G., Truong, T. V., Ngoc, K. S. L. T. M., Luyen, T. V., and Thanh, T. T. (2005) Arsenic in groundwaters of the Lower Mekong. *Environ. Geochem. Health* **27**, 341-357.

Sun, X. and Doner, H. E. (1998) Adsorption and oxidation of arsenite on goethite. *Soil Sci*. **163**, 278-287.

Swartz, C. H., Blute, N. K., Badruzzman, B., Ali, A., Brabander, D., Jay, J., Besancon, J., Islam, S., Hemond, H. F., Harvey, C. F. (2004) Mobility of arsenic in a Bangladesh aquifer: inferences from geochemical profiles, leaching data, and mineralogical characterization. *Geochim. Cosmochim. Acta*, **68**, 4539-4557.

Ta, T. K. O., Nguyen, V. L., Tateishi, M., Kobayashi, I., Tanabe, S., and Saito, Y. (2002) Holocene delta evolution and sediment discharge of the Mekong River, southern Vietnam. *Quaternary Sci. Rev*. **21**, 1807-1819.

UN (United Nations) (2006) *Water, A Shared Responsibility: The United Nations World Water Development Report 2.* United Nations Educational, Scientific and Cultural Organization, Paris and Berghahn Books, New York. 584 p.

van Geen, A., Zheng, Y., Versteeg, R., Stute, M., Horneman, A., Dhar, R., Steckler, M., Gelman, A., Small, C., Ahsan, H., Graziano, J. H., Hussain, I., and Ahmed, K. M.

(2003a) Spatial variability of arsenic in 6000 tube wells in a 25 km^2 area of Bangladesh. *Water Resour. Res.* **39**, 1140, doi: 10.1029/2002WR001617.

van Geen, A., Zheng, Y., Stute, M., and Ahmed, K. M. (2003b) Comment on "Arsenic mobility and groundwater extraction in Bangladesh" (II). *Science* **300**, 584c.

van Geen, A., Rose, J., Thoral, S., Garnier, M., Zheng, Y., Bottero, J. Y. (2004) Decoupling of As and Fe release to Bangladesh groundwater under reducing conditions. Part II: Evidence from sediment incubations. *Geochim. Cosmochim. Acta* **68**, 3475-3486.

van Geen, A., Zheng, Y., Cheng, Z., Aziz, Z., Horneman, A., Dhar, R. K., Mailloux, B., Stute, M., Weinman, B., Goodbred, S., Seddique, A. A., Hoque, M. A., and Ahmed, K. M. (2006) A transect of groundwater and sediment properties in Araihazar, Bangladesh: further evidence of decoupling between As and Fe mobilization. *Chemical Geology* **228**, 85-96.

Waltham, C. A. and Eick, M. J. (2002) Kinetics of arsenic adsorption on goethite in the presence of sorbed silicic acid. *Soil Sci. Soc. Am. J*. **66**, 818-825.

Waychunas, G. A., Rea, B. A., Fuller, C. C., and Davis, J. A. (1993) Surface chemistry of ferrihydrite: Part 1. EXAFS studies of the geometry of coprecipitated and adsorbed arsenate. *Geochim. Cosmochim. Acta*. **57**, 2251-2269.

Welch, A. H., Westjohn, D. B., Helsel, D. R., and Wanty, R. B. (2000) Arsenic in ground water of the United States: Occurrence and geochemistry. *Ground Water*. **38**, 589-604.

WHO (World Health Organization) (2004) Guidelines for Drinking-Water Quality. Third Edition. Vol. 1: Recommendations. World Health Organization, Geneva.

WHO/UNICEF (World Health Organization/ United Nations Children's Fund) (2004) *Meeting the MDG Drinking Water and Sanitation Target. A Mid-term assessment of Progress*. New York, Geneva.

WHO/UNICEF (World Health Organization/ United Nations Children's Fund) (2005) Water for Life: Making it Happen. Geneva.

Yamauchi, H. and Fowler B. A. (1994) Toxicity and metabolism of inorganic and methylated arsenicals. In Nriagu, J. O. (ed.). *Arsenic in the Environment. Part II. Cycling and Characterization*. Vol. **27**, Wiley Series in Advances in Environmental Science and Technology, Wiley-Interscience, 293 p.

Yoshida, T., Yamauchi, H., and Fan Sun, G. (2004) Chronic health effects in people exposed to arsenic via the drinking water: dose – response relationships in review. *Tox. Appl. Pharm.* **198**, 243-252.

Yu, W. H., Harvey, C. M., and Harvey, C. F. (2003) Arsenic in groundwater in Bangladesh: A geostatistical and epidemiological framework for evaluating health effects and potential remedies. *Water Resour. Res.* **39**, 1146, doi: 10.1029/2002WR001327.

CHAPTER 2

Solid-Phases and Desorption Processes of Arsenic within Bangladesh Sediments

ABSTRACT

Arsenic is a contaminant in the groundwater of Bangladesh and West Bengal, India, where an estimated 57 million people may be drinking water with unsafe arsenic levels. The source of arsenic appears to be natural, solid-phase arsenic in the sediments, and various theories have been put forth regarding the modes of arsenic release, ranging from the oxidative or reductive degradation of arsenic-bearing solids to competitive ligand displacement by phosphate. Currently, however, reductive dissolution of Fe(III) (hydr)oxides and concomitant arsenic release is the most widely accepted explanation of high arsenic groundwater concentrations. Using micro-X-ray fluorescence elemental mapping and micro-X-ray absorption near-edge structure spectroscopy, we detect arsenic-bearing sulfides in the aquifer sediments from our field site in Munshiganj, Bangladesh. Reduction of Fe and As in surface soil layers is apparent, but Fe(III) (hydr)oxides are not detected in the Holocene aquifer materials. Rapid abiotic desorption of arsenic from sediments is observed in batch experiments, and positive controls with ferrihydrite dismiss the role of ferric (hydr)oxides in arsenic retention within the aquifer sediments. Based on our laboratory results, we do not see evidence for ferric (hydr)oxide reductive dissolution at well-depths in the Holocene aquifer. In contrast, our data suggest that arsenic is only released via redox cycling in surface soils/sediments and thus must then be transported to well-depth through the sandy aquifer.

2.1. INTRODUCTION

Arsenic is a contaminant in the groundwater of Bangladesh and West Bengal, India, and an estimated 57 million people may be drinking water with arsenic concentrations above the World Health Organization standard of 10 μg/L (Yu et al., 2003). In an effort to reduce the number of diseases due to surface water consumption, the Bangladesh government initiated a widespread project to obtain drinking water through groundwater retrieval in the late 1960s. Water-borne diseases have since decreased, but recent incidences of arsenicosis and cancer have resulted due to arsenic poisoning (Yu et al., 2003).

Bangladesh is a country sitting on kilometers of eroded Himalayan sediments, transported and deposited by the Ganges, Brahmaputra, and Meghna Rivers (Acharyya et al., 2000; Anawar et al., 2002), and it is believed that arsenic concentrations in groundwater are the consequence of the release of natural arsenic from these sediments (Acharyya et al., 1999; Chowdhury et al., 1999; Nickson et al., 2000; McArthur et al., 2001; Anawar et al., 2002; Harvey et al., 2002). Though regional variations are present, Bangladesh sediments typically consist of a thick Pleistocene orange sand aquifer, overlain by a clay aquitard, a thick dark-gray sandy Holocene aquifer, and a 0 – 5 m clay layer cap of overbank deposits (Ahmed et al., 2004). Throughout the country, groundwater arsenic concentrations decrease with depth (Yu et al., 2003), and at some intensive study sites the concentration profile has been found to peak between depths of 28 – 45 m in the Holocene aquifer. Concentrations are below detection limits in the Pleistocene aquifer (McArthur et al, 2001). Solid phase arsenic concentrations are relatively uniform with depth and are typically below 3 μg/g in the aquifer sands (Swartz

et al., 2004), but average ~ 20 μg/g (Meharg et al., 2003) and can be as high as 800 μg/g (Breit et al, 2004) in the surficial clay layer. Well depths vary but tubewells in central Bangladesh generally tap groundwater in the Holocene aquifer at depths of ~ 30 m.

Currently, the mechanism of arsenic release remains unclear. Initial theories suggested that ion displacement by fertilizer-derived phosphate (Acharyya et al., 1999) or oxidation of arsenic-bearing sulfides (Chowdhury et al., 1999) has resulted in the partitioning of arsenic in the aqueous phase. However, these hypotheses have been discounted as viable mechanisms within the aquifer. Phosphate concentrations decrease with depth and do not correspond with arsenic levels (McArthur et al., 2001). Following the oxidative dissolution of sulfide minerals, resulting ferric (hydr)oxides would rapidly scavenge any concomitantly released arsenic (Mok and Wai, 1994). Furthermore, it has been proposed that primary sulfide grains are completely oxidized prior to deposition, and, therefore, sulfides detected within the aquifer materials are authigenic, formed following microbial sulfogenesis (McArthur et al., 2001).

The most widely accepted theory to date is that arsenic is released from aquifer sediments during the microbial reductive dissolution of ferric (hydr)oxides (Nickson et al., 1998; Nickson et al., 2000; McArthur et al., 2001; Dowling et al., 2002; Harvey et al., 2002). Though yet to be detected in sediments from the Holocene aquifer at depths where groundwater arsenic concentrations are highest, Fe(III) (hydr)oxides are presumed to be derived from the weathering of micas, iron sulfides, and other primary Fe-bearing minerals. Support for reductive dissolution of iron (hydr)oxides has been gleaned from the low redox potential (< 90 mV) of the aquifer, high dissolved Fe content (Nickson et al., 2000; McArthur et al., 2001; Dowling et al., 2002; Harvey et al., 2002; Swartz et al.,

2004), injection-withdrawal experiments (Harvey et al., 2002), and correlations of arsenic with methane, ammonium, and dissolved inorganic carbon (DIC) – indicators of biological activity (Dowling et al., 2002; Harvey et al., 2002).

Despite the support for the reductive dissolution theory, the organic carbon source fueling this process remains contentious. McArthur and colleagues (2001) argue that dissolved organic carbon is from sedimentary peat deposits within the aquifer. Alternatively, Harvey et al. (2002) have shown that groundwater dissolved organic carbon (DOC) ages are 3000 – 5000 y while dissolved inorganic carbon is substantially younger. Microbial processes in the aquifer are thought to be driven by young, labile organic carbon drawn down from surface waters. Tritium concentrations suggest that groundwater flow is rapid in the upper 30 m of the Holocene aquifer and since the onset of extensive dry-season irrigation with groundwater, surface to groundwater travel times have decreased from ~ 80 years or more to less than 40 years today (Harvey et al., 2006).

Conclusions concerning arsenic release have largely been drawn from observations of solution-phase chemistry. Recent studies have used X-ray diffraction (XRD), electron probe X-ray microanalysis (EPMA), transmission electron microscopy (TEM) (Akai et al., 2004), scanning electron microscopy (SEM) (Nickson et al., 2000; Akai et al., 2004), extractions (Swartz et al., 2004; Horneman et al., 2004), color (van Geen et al., 2003a) and reflectance and magnetic properties (Horneman et al., 2004) to rectify this limitation; however, in general, solid-phases remain incompletely characterized or even identified. Microcosm incubation experiments with aquifer materials have been conducted, and while reductive dissolution has been observed from sediments from what appear to be the Pleistocene aquifer and oxidized portions of the

Holocene aquifer (Akai et al., 2004; Islam et al., 2004; van Geen et al., 2004), it has not been shown for the reducing Holocene aquifer sediments where groundwater arsenic concentrations are typically highest (i.e. > 50 μg/L and often ≥ 600 μg/L).

Despite the broad consensus that reductive dissolution of ferric (hydr)oxides is the dominant mechanism of arsenic release within Bangladesh aquifers, a number of unexplained observations linger. Arsenic concentrations are spatially variant; wells separated by less than 100 m may provide water with drastically different levels (van Geen et al., 2003a). Also, solid-phase arsenic concentrations in the aquifer sands are lower than world averages for sedimentary basins (Smedley and Kinniburgh, 2002), and given surface water recharge rates, it is curious that arsenic has not already been flushed from the system.

In order to better understand the solid-phase influences on solution-phase arsenic concentrations, as well as begin to address some of the remaining puzzles concerning arsenic distributions, we have initiated studies examining sediments from the Bangladesh aquifers and surface clay layer. Solid materials have been characterized by element-specific spectroscopic techniques. In addition, arsenic desorption microcosm experiments were conducted. From our results, we propose that, contrary to general beliefs, arsenic is not being released in place within the aquifer but is released in the near-surface zone where variable redox conditions exist, and it is then drawn to depth following its liberation from the solid phase.

2.2. MATERIALS AND METHODS

2.2.1. Site Description and Sediment Handling

Sediment samples were obtained from the Munshiganj district of Bangladesh, 30 km south of Dhaka and 7 km north of the Ganges River. Our field site is typical of the region and includes a surficial clay, a Holocene aquifer of gray sand, an aquitard of marine clay, and a deep burnt-orange sandy Pleistocene aquifer. Core extraction procedures, groundwater aqueous chemistry, and bulk solid-phase analyses are summarized in Swartz et al. (2004). Arsenic concentrations in the groundwater increase with depth to a maximum at ~30 m and then decrease with increasing depth; solid-phase arsenic concentrations in both aquifers are below 3 μg/g (Swartz et al., 2004).

Cores were retrieved in April 2000, January 2002, January 2003, and May 2003, and sediments were obtained to a depth of approximately 165 m. The core-ends were sealed in the field with paraffin wax to minimize contact with the atmosphere. Sediment sub-samples for spectroscopic analyses were collected at depths of 5 m, 10 m, 15 m, 20 m, 30 m, and 60 m, and put into crimp-sealed serum vials under an N_2 atmosphere. The samples were shipped from Bangladesh and stored at 4^{o}C upon arrival. Soil samples were obtained in May, 2003 by driving a PVC pipe into rice paddy soils and the core-ends were sealed in the field. Soil and sediment core segments were removed for laboratory and spectroscopic experiments, homogenized in 2.5 cm (for surface soil) or 30 cm (for aquifer sediments) sections, and transferred into crimp-sealed serum vials under anaerobic conditions (N_2:H_2, 95:5) in a polyethylene glovebag (Coy Labs, Grasslake, MI).

2.2.2. Elemental Distributions and Arsenic Speciation

Solid-phase As concentrations in the Holocene and Pleistocene aquifers are below 3 μg/g and cannot be detected by conventional spectroscopic techniques. Spatial distributions for As, Fe, Cu, and Zn were determined on sediment samples from 5, 10, 15, 20, 30, 60, 105, and 165-m depths by micro x-ray fluorescence (μ-XRF) elemental mapping. Experiments were conducted on undulator beamline 13-ID-C at the Advanced Photon Source, Argonne National Laboratory, Argonne, IL, USA. The ring operated at 7 GeV and current was maintained at ~100 mA through periodic electron injection. Energy selection was maintained by a Si (111) monochromator. All sample preparation was conducted anaerobically (N_2:H_2, 95:5). Sediments were spread on clear plastic slides and covered with Kapton tape for analyses under in situ and anaerobic conditions. Slides were rastered in 5 - 15 μm steps around a 5 x 6 μm X-ray beam and fluorescent X-rays were measured with a 16-element solid-state energy-dispersive Ge detector. As, Fe, Cu, and Zn were detected simultaneously with their fluorescent X-ray intensities proportional to the number of atoms under the incident beam. Incident and transmitted intensities were measured with in-line ionization chambers.

Arsenic "hotspots" in the elemental maps were analyzed with micro x-ray absorption near-edge structure (μ-XANES) spectroscopy to determine arsenic speciation. Sample spectra were collected from –50 to +100 eV about the As K_α edge of 11867 eV and compared to XANES spectra of standards, including arsenate (Na_3AsO_4), arsenite (As_2O_3), orpiment (As_2S_3), realgar (AsS), and arsenopyrite (FeAsS). Spectra were calibrated to the edge position of sodium arsenate, which was set at 11,874 eV. Using WINXAS (Ressler, 1998), spectra were then normalized and background removed. First-

derivatives of the processed spectra were taken, smoothed with a cubic spline interpolation (SigmaPlot, SPSS Inc.), and used to deduce the speciation of arsenic. Edge-position, as deduced by first-derivative peaks, is indicative of arsenic species (Rochette et al., 1998; Hansel et al., 2002).

Arsenic concentrations within grains were determined by comparison to a thin film standard. For sulfidic arsenic (see below), the proportion of total arsenic bound in sulfides in the sediments was approximated by considering spheres of sulfides (as confirmed by μ-XANES) with volumes based on radii in the 2-dimensional maps; the density of pyrite was used and arsenic was assumed to be 1% of the total sulfide mass, the approximate average arsenic concentration of a typical 10-35 μm grain in our maps. Total sulfides were summed over the μ-XRF maps (totaling > 1000 points with the x-ray beam) at each depth and averaged for the total amount of sediment analyzed. Abundances of sulfide-bound arsenic were compared to total sediment concentrations.

2.2.3. Iron XAS Analysis

Bulk Fe speciation of aquifer sediments from depths of 5, 10, 15, 20, 30, 60, and 165 m was analyzed by X-ray absorption spectroscopy. Experiments were conducted on beamline 4-3 (an 8-pole wiggler) for extended x-ray absorption fine structure (EXAFS) and on beamline 2-3 (bending magnet) for X-ray absorption near-edge structure (XANES) spectroscopic analyses at the Stanford Synchrotron Radiation Laboratory (SSRL). The ring operated at 3 GeV with current generally between 50 and 100 mA. Samples were mounted 45 degrees to the incident x-ray beam. Incident and transmitted

intensities were measured with in-line ionization chambers and fluorescent x-rays were determined with a Lytle detector equipped with a 3μx Mn filter and Soller slits.

All sample preparation was conducted anaerobically (N_2:H_2, 95:5). Sediments were packed into dedicated Teflon sample holders and covered with Kapton tape for analyses under in-situ and anaerobic conditions. Energy selection was maintained by a Si (220) monochromator and energy calibration was performed by assigning a K_α edge position of 7111.0 eV to an in-line Fe(0) metal foil standard. The incident beam was detuned ~50% to reduce contributions from upper-order harmonic energies. Energy scans for XANES analysis were collected from 7050 eV to 7300 eV and 3 to 4 scans were averaged per sample; data processing was conducted as described above. Energy scans for EXAFS analyses were collected from –200 to +1000 eV about the Fe foil edge (set at 7111.0 eV) and 5 to 6 scans were averaged per sample. Using EXAFSPAK (George, 1993), sample fluorescence spectra were averaged, background subtracted, and normalized. A spline function was fit through the absorption envelope and subtracted from each spectrum. The resulting EXAFS function (χ) was transformed from eV to *k*-space ($Å^{-1}$) and weighted by k^3.

EXAFS and XANES spectra of model compounds were obtained and analyzed in the same manner as unknowns. Known samples included ferrihydrite, goethite, hematite, lepidocrocite, magnetite, siderite, vivianite, biotite, hornblende, mackinawite, pyrrhotite, and pyrite. Ferrihydrite, goethite, lepidocrocite, and mackinawite were synthesized according to typical methods (Morse and Arakaki, 1993; Schwertmann and Fechter, 1994; Schwertmann and Cornell, 2000), and the remainder of the model compounds were obtained from the Stanford University Mineral Collection. XANES linear combination

fitting with models was performed to determine the composition of Fe species (in percent of total Fe) in the unknown samples. Fits were optimized over an energy range of 7100 to 7150 eV. Qualitative examination of EXAFS spectra was used to constrain components for XANES linear combination fitting; iterative EXAFS and XANES analyses allowed for mineral identification of spectra that were not otherwise unique based on solely EXAFS or XANES spectra.

2.2.4. Arsenic Displacement Experiments

Arsenic release from 30 m sediments was examined in batch experiments with 5 g of drained sediment and 10 mL of solution in 20 mL serum vials; these sediments were chosen because 30 m is the depth of the highest aqueous As concentrations at our field site (Swartz et al, 2004). Solutions of 18 MΩ water and 1.5 mM DOC (as lactate) were autoclaved and made anoxic by boiling and cooling under a stream of O_2-free N_2. Lactate was added as an electron donor to some vials to study biotic processes. Ferrihydrite-coated sand (1% Fe(III) by weight) was synthesized according to previous methods (Hansel et al, 2003) and was added to select sediments giving 0.04 and 0.20 total weight percent Fe(III); ferrihydrite-coated sands were used rather than ferrihydrite suspensions to better approximate the natural environment and to increase the accuracy of addition of small quantities of Fe(III). Sediment and Fe-coated sand samples for abiotic controls were sterilized by gamma irradiation (2855 R/min for 14 hours). All glassware was autoclaved prior to experimentation and sterile techniques were employed. Reactions were initiated and sampled under anaerobic conditions (N_2:H_2, 95:5) in a

glovebag. The sediment slurries including water, lactate, or Fe(III) and water were crimp-sealed with butyl rubber stoppers and shaken (140 rpm) at 20^{o}C in darkness.

Two sets of experiments were run. In one, sampling was performed after 2, 4, 7, and 12 d. In the second set of experiments, vials were sampled after 16 and 29 d. Vials were allowed to settle for 1 h and then supernatant was extracted; 8 mL of solution was removed from the vials with a sterile syringe and was replaced with 8 mL of fresh solution with another sterile syringe. Aqueous samples were passed through a 0.20 μm filter and acidified (to 0.17 M) with concentrated trace metal grade hydrochloric acid. Samples were stored at 4^{o}C until analysis.

Solution-phase arsenic concentrations were analyzed by hydride generation inductively-coupled-plasma atomic emission spectroscopy (HG-ICP-AES). In order to reduce any arsenate to arsenite, 3 mL of sample was mixed with 3 mL concentrated trace metal grade hydrochloric acid, 1 mL 8% urea, and, following 10 min of reaction time, 1 mL 16% KI. The mixture was allowed to sit for at least 1 hour and then further reacted with 6 N HCl and 0.6% NaBH4/0.5% NaOH. The resulting arsine gas was measured by ICP-AES. Detection limits were 5 μg/L arsenic for the pre-reacted sample. Aqueous concentrations of Al, Ca, Fe, Mn, P, S, and Si were measured by ICP-AES subsequent to As measurements, and quality control standards were monitored throughout the course of the analyses.

2.3. RESULTS

2.3.1. Spectroscopy of Aquifer Sediments

2.3.1.1. Arsenic

Solid-phase arsenic concentrations are below 3 μg/g in the Holocene and Pleistocene aquifer sediments at our field site (Swartz et al., 2004), and therefore prove challenging for many conventional spectroscopic techniques. Here we investigated arsenic in the sediments using μ-X-ray fluorescence (μ-XRF) elemental mapping combined with As μ-X-ray absorption near edge structure (μ-XANES) spectroscopy. Elemental maps (Figure 2.1) illustrate that arsenic exists in discrete sediment grains; in our analyses, we detected As-bearing grains with diameters of 5 μm and greater.

Arsenic is concentrated in grains up to 100 μm in diameter (Figure 2.1A-C) and exists in different oxidation states throughout the aquifer sediments (Figure 2.1). Arsenate, arsenite, and reduced As coordinated with S (orpiment-like) were detected in a large grain from a depth of 30 m in the Holocene aquifer (Figure 2.1A). Copper and zinc were also abundant and correlated strongly with arsenic (Figure 2.2) with R^2 values of 0.77 and 0.82, respectively. The arsenic speciation and association with chalcophiles suggests partial oxidation of sulfidic grains. Arsenic also existed in wholly sulfidic grains, exceeding 100 μm in diameter and having arsenopyrite and orpiment-like spectral signatures (Figure 2.1B). Grains with oxidized arsenic were detected in the Holocene aquifer sediments; the 100 μm grain shown in Figure 2.1C is from a depth of 5 m and arsenic exists primarily as arsenate.

Despite the large As-bearing grains described above, arsenic was most commonly found in small sulfidic grains throughout the samples we analyzed from the Holocene and Pleistocene aquifers. As in Figure 2.1D, grains were between 10 and 35 μm in size, and As was generally coordinated with S. Based on the occurrences of these small As-bearing sulfides (not including partially oxidized sulfides) in the μ-XRF maps of the

aquifer sediments, the total As abundance in the sediments, and assuming that As comprises roughly 1% of the mass of the grains, these As-sulfides constitute greater than 60% of the total arsenic in the aquifer sediments.

2.3.1.2. Iron

The composition of Fe in the dark gray Holocene sediments varied little with depth. EXAFS and XANES spectra from sediments between 5 m and 60 m are virtually indistinguishable from one another and appear to be dominated by Fe-bearing primary minerals such as hornblende and biotite (Figure 2.3). Quantitative fitting of XANES and EXAFS spectra (in combination) and reveals hornblende (49-59%) and biotite (21-45%), as the dominant phases of iron, with no consistent depth-dependent variations (Table 2.1). Significant proportions of ferric (hydr)oxides, such as ferrihydrite and hematite, are not supported by the linear combination fitting; Fe(III) present within the sediments can be accounted for by that in magnetite and Fe bearing silicates. Thus, if ferric (hydr)oxides are present, they reside near our detection limit (detection limit is 5% of the total iron in the sample). Finally, small discrepancies between fitted and experimental XANES spectra at ~7128 eV cannot be accounted for by inclusion (or subtraction) of ferric (hydr)oxide phases but may rather be due to additional Fe-bearing silicates such as illite (O'Day et al., 2004).

Sediments from the Pleistocene aquifer, which are burnt-orange in color, in contrast have a distinctly different Fe composition than those from the Holocene aquifer (Figure 2.3). Sediments from a depth of 165 m contain ferric (hydr)oxides in addition to Fe in primary minerals; excellent fits were obtained using horneblende (31%) and

goethite/ferrihydrite (69% in combination) to reproduce the Pleistocene sediment spectrum.

2.3.2 Spectroscopy of Surface Soil

2.3.2.1. Arsenic

Concentrations of solid-phase arsenic are higher in the surface soils than in the aquifer sediments, ranging from roughly 25 μg/g at the surface to 10 μg/g at 36 cm depth. Arsenic concentrations were sufficiently low, however, to make bulk As XANES spectroscopy difficult for resolving oxidation states. Thus, soil phases were also investigated using μ-XRF and μ-XANES spectroscopy. Arsenic oxidation states were consistent at different μ-XRF 'hotspots' from the same depth, suggesting that average μ-XANES spectra are representative of the bulk oxidation state for a given depth.

Solid-phase arsenic becomes more reduced with depth in the soil (Figure 2.4). Arsenate is the dominant arsenic species at a depth of 5 cm, but an arsenite peak becomes more apparent at 20 cm and 36 cm depth while the arsenate peak diminishes. One particular 25 μm As-bearing grain from a depth of 36 cm (Figure 2.5) was composed of more reduced arsenic than otherwise detected. The more reduced grain from 36 cm is dominated by arsenite with arsenic sulfide as well and has the highest concentrations of As in the map.

2.3.2.2. Iron

Like arsenic, solid-phase iron is also more reduced with increasing depth in the surface soil (5 – 36 cm). In Figure 2.6, normalized first-derivative XANES spectra from

varying depths are superimposed on each other to illustrate changes in Fe oxidation state; the inset serves to enlarge the changing regions in the energy scans. A peak at higher energy (7127 eV) decreases with depth indicating loss of Fe(III), while growth of the lower energy peak at 7120 eV is representative of an increase of Fe(II) at deeper soil levels. The XANES spectra show that Fe speciation is dominated by Fe-bearing silicates such as hornblende, biotite (Figures 2.3 and 2.6), and illite (O'Day et al., 2004). The decreasing Fe(III)/Fe(II) ratios with depth may be due to enhanced Fe reduction with depth or increased Fe oxidation of silicates nearer to the surface (Jeong and Kim, 2003); however, because these soil samples are from an agricultural area and undergo seasonal turnover prior to planting and immediate flooding, it is likely that the decreasing Fe(III)/Fe(II) ratios are in fact due to Fe reduction with depth. Most importantly, though, the varying Fe(III)/Fe(II) ratios demonstrate that active redox processes are occurring within the surface soils.

2.3.3. Batch Experiments

2.3.3.1. Arsenic Desorption

Appreciable concentrations of arsenic rapidly desorbed from the Holocene aquifer sediments (depth of 30 m) during batch experiments examining arsenic release. Incubations of sediments with deionized water released approximately 15% of the total arsenic from the sediments (Figure 6.7A). Stimulation with 1.5 mM dissolved organic carbon (as lactate) produced similar results, releasing > 10% of the total arsenic. Following aqueous phase sampling, fresh solution was added to maintain a constant solid:solution ratio throughout the experiments. The total arsenic released began to

approach a maximum by 12 days. Solution pH remained relatively constant between 7 and 8 throughout the experiments.

To examine the role of biological activity on arsenic release, control experiments were performed with sediments that had been gamma irradiated. Abiotic controls did not result in decreased arsenic release; rather, aqueous concentrations of desorbed As were slightly higher than the experiments without gamma irradiation. This suggests that desorption of arsenic from the 30 m sediments observed here is an abiotic, chemical process. To ensure that sampling and solution addition did not inhibit any potential biological activity, a set of parallel experiments were run for 30 d with only one intermediate sampling after 16 days. Again, arsenic was readily desorbed even within sterile controls (Figure 2.7B).

2.3.3.2. Fe(III) Additions

The concentrations of arsenic released in the desorption experiments described above are greater than we would expect if the released arsenic were bound to Fe(III) (hydr)oxides. To examine the effects of Fe(III) on arsenic release, sediment samples were spiked with ferrihydrite-coated sand; 0.04% and 0.2% Fe(III) (weight basis) were achieved. With 0.04% Fe(III), aqueous concentrations of arsenic decreased by ~88% in both the biotic and abiotic experiments with a steady-state achieved in < 2 d (Figure 7a). With additions of 0.2% Fe(III), arsenic in the aqueous phase was not detectable. Thus, these ferric iron addition experiments suggest that any arsenic released is not controlled by Fe (hydr)oxides.

2.3.3.3. Elemental Correlations

Throughout the entire set of batch experiments (including biotic and abiotic reactions, and with and without the addition of Fe(III)) arsenic release was strongly correlated with phosphorous release (R^2 = 0.81, Figure 2.8). Phosphate, arsenate and arsenite strongly adsorb to Fe(III) (hydr)oxides in inner sphere complexes (Fendorf et al., 1997; Manning et al., 1998), but are only weakly adsorbed to many other minerals such as silicates (Manning and Goldberg, 1997). The nonlinearity at high concentrations of both P and As is likely due to the formation of secondary phosphate mineral phases.

Aside from phosphorous, no other strong elemental correlations with arsenic were observed. However, when omitting the results of Fe(III) additions, it is noted that arsenic co-varies with Ca (R^2 = 0.94), Si (R^2 = 0.79), Fe (R^2 = 0.84), and Mn (R^2 = 0.78, data not shown) (Figure 2.9). These elements have significantly different reactivities towards Fe(III) (hydr)oxides than As, and therefore do not co-vary in the Fe(III) addition experiments. The correlations of Ca, Si, Fe, and Mn with As in the experiments without Fe(III) further suggest that chemical desorption is the primary mechanism observed in these experiments. Furthermore, the concentrations of Ca, Si, Fe, Mn, P, and As released were not in the same proportions as those that exist in the groundwater (Swartz et al., 2004), indicating that release in these experiments was not simply due to dilution of any pre-existing groundwater remaining with the sediments but was in fact due to desorption from sediments.

2.4. DISCUSSION

2.4.1. Arsenic in Holocene Aquifer Sediments

Two dominant pools of arsenic in the Holocene aquifer sediments of Bangladesh are revealed: arsenic in sulfide minerals (greater than 60% of the total solid phase arsenic) and weakly adsorbed arsenic (15% of the solid-phase arsenic as retrieved in the batch experiments). Currently, microbial reductive dissolution of Fe(III) (hydr)oxides and concomitant release of arsenic is the most widely accepted mechanism for the cause of high aqueous arsenic concentrations in Bangladesh aquifers. Our results suggest that an alternative process (or set of processes) must be postulated to explain high dissolved arsenic.

Based on the oxidation state, grain size (~100 μm), and As correlations with the chalcophiles Cu and Zn, some of the arsenic bearing sulfide minerals appear detrital, having been transported from the Himalayan source rock, deposited, and buried without complete oxidation. The quantity of As bound in sulfides is in agreement with the crystalline phases targeted in the HF, nitric acid and hot nitric acid sequential extractions of Swartz et al. (2004). Pyrite has been detected previously in aquifer sediments (Nickson et al., 2000) and in the wood flakes of muddy layers (Akai et al., 2004), though sulfides have been rectified as authigenic (McArthur et al., 2001). And, in fact, the abundant sulfide grains ranging in size from 10 to 35 μm observed here are likely authigenic. Detrital, along with authigenic, sulfides therefore appear to account for an appreciable proportion of arsenic within the aquifer sediments.

The Bangladesh Holocene aquifer is strongly reducing and oxidation of sulfides is not an important process at depths of ~30 m where the majority of wells retrieve water.

However, arsenic that is loosely bound and easily desorbed from the sediments, as observed in the batch experiments, may indicate why groundwater arsenic concentrations are high. Solution-phase concentrations in the batch experiments reached concentrations of 100 μg/L. Given that these experiments were conducted with a solid:solution ratio of 1:2, if an equivalent amount of arsenic was desorbed from the sediments in the aquifer, where solid:solution ratios are greater than 1, aqueous arsenic concentrations would approach the high levels observed in the groundwater (640 μg/L at our field site; Swartz et al., 2004).

2.4.2. Reductive Dissolution of Fe(III) (Hydr)oxides

Numerous studies suggest that the reductive dissolution of Fe(III) (hydr)oxides at well-depths in the Holocene aquifer (~30 m near our field site), has led to the high concentrations of arsenic in groundwater. Our results are inconsistent with such a process. We find no indication of reactive Fe(III) oxides in the sediments and positive controls in batch experiments with ferric oxide addition provide further support for a lack of iron controlling arsenic at well-depth—a finding supported by the dark-gray color of the sediments, the sequential extractions of Swartz et al. (2004), and the low redox potential (20 - 90 mV; Harvey et al., 2002). Additionally, the high concentrations of methane (> 1 mM; Harvey et al., 2002) and hydrogen (10 nM; Harvey et al., 2002) in porewaters indicate that Fe(III) reduction is no longer occurring at well-depths, and only methanogenesis is likely (Lovley and Goodwin, 1988; Lovley et al., 1994; Lovley and Anderson, 2000). While it may be possible that Fe(III) (hydr)oxides are below detection limits in the silicate-dominated aquifer, the batch experiments showed that rapid release

of As from the solid-phase was completely inhibited with the addition of 0.2% Fe(III). Thus an appreciable pool of mobile arsenic is not controlled by Fe(III) (hydr)oxides in the Holocene aquifer sediments.

Previous studies involving microcosm sediment incubations demonstrate that microbial processes are coupled to As release. Akai et al. (2004) observed As release from muddy sediments in batch experiments enriched with nutrients and from sandy sediments circulating water flow experiments. Aside from the different mineralogy of the muddy sediments, the experiments of Akai et al. (2004) were initiated under aerobic conditions (Eh ~ 400 mV), potentially allowing Fe(III) (hydr)oxides to form, and are therefore not directly comparable to our studies. Islam et al. (2004) reported arsenic release from unautoclaved sediments under anaerobic conditions; however, based on the presence of aerobic bacteria and > 90% initial solid-phase arsenic as As(V), the sediments used in the study may have been derived from the oxic-anoxic interface, also differing from our experiments. The sediments used in the batch experiments of van Geen et al. (2004) were derived from depths where groundwater concentrations were below 50 μg/L (the Bangladesh national drinking water standard). Additionally, site variations may have provided for dissimilar results between our studies and those of Akai et al. (2004), Islam et al. (2004) and van Geen et al. (2004).

2.4.3. Arsenic in the Pleistocene Aquifer

Ferric iron (hydr)oxides were detected in the Pleistocene aquifer, which is separated from the Holocene aquifer by a 40 m thick clay aquitard at our field site. Arsenic-bearing sulfides were also detected in Pleistocene sediment samples and could be

from a detrital or authigenic source. The sediments are burnt-orange in color and groundwater arsenic concentrations are 4 μg/L (Swartz et al., 2004). Although reductive dissolution of Fe(III) minerals may be occurring (low concentrations (< 2 mg/L) of Fe(II) exist in the Pleistocene groundwater), due to the abundance of ferric (hydr)oxides, it is probable that arsenic is kept out of solution by adsorption to Fe (hydr)oxides in the Pleistocene aquifer.

2.4.4. Arsenic in Soils

Due to monsoonal activity and dry-season irrigation, surface soils we examined have undergone at least two major reduction-oxidation cycles each year (and possibly more based on irrigation and crop cycling). Both solid-phase As and Fe become more reduced with depth in the soils.

Solid-phase arsenic concentrations are typically higher in the soils than in the aquifer materials (Meharg and Rahman, 2003; Swartz et al., 2004), with levels as high as 40 μg/g at the very surface. Meharg and Rahman (2003) demonstrated that high As concentrations in soils were positively correlated with high groundwater As, and suggested that this may be due in part to the irrigation with groundwater. However, solid-phase concentrations in soils were still higher than aquifer materials prior to the onset of irrigation (Ali et al., 2003). In fact, it has been reported that As is approximately 15 μg/g in the suspended sediments of the Ganges River near the Bay of Bengal (Stummeyer et al., 2002). Thus, higher As concentrations in soils are most probably due to a combination of groundwater irrigation and annual deposition bringing additional solid-phase As into the soil system. Moreover, widespread As-rich Fe(III) (hydr)oxide

bands at the near-surface (within the upper 5 m) have solid-phase As concentrations as high as 800 μg/g (Breit et al., 2004), and such high concentrations could not have occurred solely from irrigation, but are likely due to accumulation from depositional sources.

Important depositional sources of arsenic include As associated with Fe (hydr)oxides and detrital sulfide minerals. The presence of As-bearing sulfide grains is supported by the sequential extractions of near-surface materials (Swartz et al., 2004). Furthermore, Stummeyer et al. (2002) found the majority of As in suspended sediments to be hosted in strong acid soluble and insoluble residual phases, both of which were the solid-phase remnants following weak acid and easily reducible fractions in their sequential extraction protocol. Arsenic-bearing sulfide grains in surficial sediments would yield a source of arsenic during oxic cycles, which would then be subject to reductive dissolution during monsoonal and flooding events (Figure 2.10). Upon oxidation, Fe(III) (hydr)oxides would be formed; arsenic in the sulfide matrix would undergo a solid-phase transformation and be adsorbed to and coprecipitated with ferric (hydr)oxides. Arsenic released from Fe(III) minerals, both those newly formed and those deposited, during subsequent reducing periods (flooding events where floodwaters carry high, labile dissolved organic carbon) or competitive ion displacement could be re-sequestered into authigenic sulfide minerals. However, because sulfur would be partially removed via sulfate transport following oxidation, only a portion of the original arsenic could be re-precipitated in sulfidic form; additionally, competition from other ions, such as Fe^{2+}, could limit sequestration of arsenic by sulfide production. Early-diagenetic

fromboidal pyrite in the sediments (Nickson et al., 2000) and remaining detrital sulfides could be re-oxidized during the dry season and thus continue the arsenic cycle.

Such redox activity at the surface is shown by the reduction of Fe and As with depth in the soils. Additionally, the presence of a Mn-oxide layer above an Fe-oxide band (Breit et al., 2004) in the near-surface corresponds to typical redox profile zonation and reflects the seasonal changes in water table, which may vary by over 6 m. As Fe(III) (hydr)oxides are reduced with depth, arsenic is released to solution.

2.4.5. Sources of Arsenic

Aqueous concentrations of arsenic comparable to the maximum groundwater concentrations at our field site (640 μg/L) can be achieved by simply incubating retrieved sediments within deionized water for 12 days. Based on our laboratory studies, at least 15% of the solid-phase arsenic is rapidly desorbed, and greater than 60% of the arsenic is bound in sulfides and therefore unreactive in the strongly reducing aquifer. Reductive processes in the Holocene aquifer at our site did not contribute to arsenic desorption. A likely source of arsenic resulting from biological reduction would likely occur within the surface soils and sediments. Arsenic released within the surface binds only weakly to silicate minerals which dominate the aquifer materials—particularly given the competing ion concentrations within the aquifer and the large mineral grain size (Swartz et al., 2004)—and would thus be easily transported to well depth. While the surface clay layers and soils act as an aquitard, rivers, irrigation channels, and ponds breach the clay layer and thus provide a conduit to the subsurface. Further, the studies of Akai et al. (2004), Islam et al. (2004), and van Geen et al. (2004) show microbial reductive

mobilization of arsenic from near-surface sediments. Therefore, based on existing data, the release of arsenic from surface sediments and subsequent transport to depth is plausible.

The process of arsenic release observed here may not be ubiquitous throughout Bangladesh and West Bengal due to site variations and differing land use practices. However, a map showing the probability of high groundwater arsenic concentrations (BGS and DPHE, 2001) indicates that the highest concentrations of arsenic exist in the Ganges delta of southern Bangladesh, where surface sediments undergo dramatic seasonal changes in water table levels and where rivers and streams provide conduits through breaches in the surface clay layer. Such a mechanism of arsenic release could help further explain the spatial variability noted in groundwater As concentrations. Drastically differing arsenic concentrations from wells as close as 100 m to one another and varying groundwater As depth profiles may in fact be the result of water retrieval from separate hydraulic domains. Additionally, should surface sediments be the ultimate source of arsenic to groundwater, varying mechanisms of arsenic release may appear to be occurring in different locations – sulfide oxidation (Chowdhury et al., 1999), ion displacement by fertilizer-derived phosphate (Acharyya et al., 1999), and microbial reductive processes (Nickson et al., 1998; Nickson et al., 2000; McArthur et al., 2001; Dowling et al., 2002; Harvey et al., 2002; McArthur et al., 2004) may all play roles in the overall release of arsenic.

2.5. CONCLUSIONS

Two pools of arsenic dominate the solid-phase in Holocene aquifer sediments of our field site in Munshiganj. Detrital and authigenic arsenic-bearing sulfide grains comprise greater than 60% of arsenic in the sediments. A second pool consists of arsenic adsorbed on the sand and it gives rise to a labile fraction in which over 15% of the solid-phase arsenic is released in batch incubations. A highly labile fraction is inconsistent with arsenic bound to Fe(III) (hydr)oxides. Moreover, we find no evidence for ferric (hydr)oxides in the Holocene aquifer materials and their presence would be inconsistent with the redox conditions of the aquifer. Finally, ferric (hydr)oxide additions to sediments in batch experiments removed As from solution, illustrating the strong retention expected should such phases control As.

Solid-phase concentrations of arsenic in soil materials are typically higher than those in the aquifer sediments. Due to monsoons and extensive groundwater removal for dry-season irrigation, soils are variably saturated and undergo seasonal redox cycles. Consequently, arsenic may be released from soil minerals at oxic-anoxic boundaries and could be subsequently drawn down from the near-surface through the aquifer to well-depths. These results indicate the need for monitoring soil environments above Bangladesh aquifers, as well as developing a better understanding of the potential transport of arsenic.

2.6. REFERENCES

Acharyya, S. K., Chakraborty, P., Lahiri, S., Raymahashay, B. C., Guha, S., and Bhowmik, A. (1999) Arsenic poisoning in the Ganges delta. *Nature* **401**, 545.

Acharyya, S. K., Lahiri, S., Raymahashay, B. C., and Bhowmilk, A. (2000) Arsenic toxicity of groundwater in parts of the Bengal basin in India and Bangladesh: the role of Quaternary stratigraphy and Holocene sea-level fluctuation. *Environmental Geology* **39**, 231-238.

Ahmed, K. M., Bhattacharya, P., Hasan, M. A., Akhter, S. H., Alam, S. M. M, Bhuyian, M. A. H., Imam, M. B., Khan, A. A., and Sracek, O. (2004) Arsenic enrichment in groundwater of the alluvial aquifers in Bangladesh: an overview. *Appl. Geochem.* **19**, 181-2000.

Akai, J., Izumi, K., Fukuhara, H., Masuda, H., Nakano, S., Yoshimura, T., Ohfuji, H., Anawar, H. M., and Akai, K. (2004) Mineralogical and geomicrobiological investigations on groundwater arsenic enrichment in Bangladesh. *Appl. Geochem.* **19**, 215-230.

Ali, M. M., Ishiga, H., and Wakatsuki, T. (2003) Influence of soil type and properties on distribution and changes in arsenic contents of different paddy soils in Bangladesh. *Soil Science and Plant Nutrition* **49**, 111-123.

Anawar, H. M., Komaki, K., Akai, J., Ishizuka, T., Takahashi, T., Yoshioka, T., and Kato, K. (2002) Diagenetic control on arsenic partitioning in sediments of the Meghna River delta, Bangladesh. *Environmental Geology* **41**, 816-825.

BGS and DPHE (2001) *Arsenic contamination of groundwater in Bangladesh, Vol. 2. Final report*. BGS technical report WC/00/19.

Breit, G. N., Foster, A. L., Perkins, R. B., Yount, J. C., King, T., Welch, A. H., Whitney, J. W., Uddin, N., Muneem, A., and Alam., M. (2004) As-rich ferric oxyhydroxide enrichments in the shallow subsurface of Bangladesh. In Wanty, R. B. and Seal, R. R. II (eds.) *Water-Rock Interactions*. Taylor & Francis Group, London, 1457-1461.

Chowdhury, T. R., Basu, G. K., Samanta, G., Chanda, C. R., Mandal, B. K., Dhar, R. K., Biswas, B. K., Lodh, D., Ray, S. L., and Chakraborti, D. (1999) Arsenic poisoning of Bangladesh groundwater. *Nature* **401**, 545-546.

Dowling, C. B., Poreda, R. J., Basu, A. R., Peters, S. L., and Aggarwal, P. K. (2002) Geochemical study of arsenic release mechanisms in the Bengal Basin groundwater. *Water Resour. Res.* **38**, 1173, doi: 10.1029/2001WR000968.

Fendorf, S., Eick, M. J., Grossl, P., and Sparks, D. L. (1997) Arsenate and chromate retention mechanisms on goethite. 1. Surface structure. *Environ. Sci. Technol.* **31**, 315-320.

George, G. N. (1993) EXAFSPAK. Stanford Synchrotron Radiation Laboratory, Menlo Park, CA.

Hansel C. M., LaForce, M. J., Fendorf, S., and Sutton, S. (2002) Spatial and temporal association of As and Fe species on aquatic plant roots. *Environ. Sci. Technol.* **36**, 1988-1994.

Hansel, C. M., Benner, S., Neiss, J., Dohnalkova, A., Kukkadapu, R. K., and Fendorf, S. (2003) Secondary mineralization pathways induced by dissimilatory iron reduction of ferrihydrite under advective flow. *Geochim. Cosmochim. Acta* **67**, 2977-2992.

Harvey, C. F., Swartz, C. H., Badruzzaman, A. B. M., Keon-Blute, N., Niedan, V., Brabander, D., Oates, P. M., Ashfaque, K. N., Islam, S., Hemond, H. F., and Ahmed, M. F. (2002) Arsenic mobility and groundwater extraction in Bangladesh. *Science* **298**, 1602-1606.

Harvey, C. F., Swartz, C., Badruzzaman, A. B. M., Keon-Blute, N., Niedan, V., Brabander, D., Oates, P. M., Ashfaque, K. N., Islam, S., Hemond, H. F., and Ahmed, M. F. (2003) Response to comments on "Arsenic mobility and groundwater extraction in Bangladesh". *Science* **300**, 584d.

Harvey, C. F., Ashfaque, K. N., Yu, W., Badruzzaman, A. B. M., Ali, M. A., Oates, P. M., Michael, H., Neumann, R. B., Beckie, R., Islam, S., and Ahmed, M. F. (2006) Groundwater flow and arsenic biogeochemistry in Bangladesh: an analysis of transience and coupling. *Chemical Geology* **228**, 112-136.

Horneman, A., van Geen, A., Kent, D. V., Mathe, P. E., Zheng, Y., Dhar, R. K., O'Connell, S., Hoque, M. A., Aziz, Z., Shamsudduha, M., Seddique, A. A., and Ahmed, K. M. (2004) Decoupling of As and Fe release to Bangladesh groundwater under reducing conditions. Part I: Evidence from sediment profiles. *Geochim. Cosmochim. Acta* **68**, 3459-3473.

Islam, F. S., Gault, A. G., Boothman, C., Polya, D. A., Chatterjee, D., and Lloyd, J. (2004) Direct evidence of arsenic release from Bengali sediments due to metal-reducing bacteria. *Nature* **430**, 68-71.

Jeong, G. Y. and Kim, H. B. (2003) Mineralogy, chemistry, and formation of oxidized biotite in the weathering profile of granitic rocks. *Am. Min.* **88**, 352-364.

Lovley, D. R. and Goodwin, S. (1988) Hydrogen concentrations as an indicator of the predominant terminal electron accepting reactions in aquatic sediments. *Geochim. Cosmochim. Acta* **52**, 2993-3003.

Lovley, D. R., Chapelle, F. H., and Woodward, J. C. (1994) Use of dissolved H_2 concentrations to determine distribution of microbially catalyzed redox reactions in anoxic groundwater. *Environ. Sci. Technol.* **28**, 1205-1210.

Lovley, D. R. and Anderson, R. T. (2000) Influence of dissimilatory metal reduction on fate of organic and metal contaminants in the subsurface. *Hydrogeology J.* **8**, 77-88.

Manning, B. A. and Goldberg, S. (1997) Adsorption and stability of arsenic(III) at the clay mineral-water interface. *Environ. Sci. Technol.* **31**, 2005-2011.

Manning, B. A., Fendorf, S. E., and Goldberg, S. (1998) Surface structures and stability of arsenic (III) on goethite: spectroscopic evidence for inner-sphere complexes. *Environ. Sci. Technol.* **32**, 2383-2388.

McArthur, J. M., Ravenscroft, P., Safiulla, S., and Thirlwall, M. F. (2001) Arsenic in groundwater: Testing pollution mechanisms for sedimentary aquifers in Bangladesh. *Water Resour. Res.* **37**, 109-117.

McArthur, J. M., Banerjee, D. M., Hudson-Edwards, K. A., Mishra, R., Purohit, R., Ravenscroft, P., Cronin, A., Howarth, R. J., Chatterjee, A., Talukder, T., Lowry, D., Houghton, S., and Chadha, D. K. (2004) Natural organic matter in sedimentary basins and its relation to arsenic in anoxic ground water: the example of West Bengal and its worldwide implications. *Appl. Geochem.* **19**, 1255-1293.

Meharg, A. A. and Rahman, M. (2003) Arsenic contamination of Bangladesh paddy field soils: implications for rice contribution to arsenic consumption. *Environ. Sci. Technol.* **37**, 229-234.

Mok, W. M. and Wai, C. M. (1994) Mobilization of arsenic in contaminated river waters. p. 99-118. In Nriagu, J. O. (ed.). *Arsenic in the Environment. Part I. Cycling and Characterization*. Vol. **26**, Wiley Series in Advances in Environmental Science and Technology, Wiley-Interscience, 430 p.

Morse, J. W. and Arakaki, T. (1993) Adsorption and coprecipitation of divalent metals with mackinawite (FeS). *Geochim. Cosmochim. Acta* **57**, 3635-3640.

Nickson, R., McArthur, J., Burgess, W., Ahmed, K. M., Ravenscroft, P., and Rahman, M. (1998) Arsenic poisoning of Bangladesh groundwater. *Nature* **395**, 338.

Nickson, R. T., McArthur, J. M., Ravenscroft, P., Burgess, W. G., and Ahmed, K. M. (2000) Mechanism of arsenic release to groundwater, Bangladesh and West Bengal. *Appl. Geochem.* **15**, 403-413.

O'Day, P. A., Rivera, N. Jr., Root, R., and Carroll, S. A. (2004) X-ray absorption spectroscopic study of Fe reference compounds for the analysis of natural sediments. *Am. Min.* **89**, 572-585.

Ressler, T. (1998) *WinXAS*: a program for X-ray absorption spectroscopy data analysis under MS-Windows. *J. Synchrotron Rad.* **5**, 118-122.

Rochette, E. A., Li, G., Fendorf, S. E. (1998) Stability of arsenate minerals in soil under biotically generated reducing conditions. *Soil Sci. Soc. Am. J*. **62**, 1530-1537.

Schwermann, U. and Fechter, H. (1994) The formation of green rust and its transformation to lepidocrocite. *Clay Miner.* **29**, 87-92.

Schwertmann, U. and Cornell, R. M. (2000) *Iron Oxides in the Laboratory: Preparation and Characterization*. Wiley-VCH, New York.

Smedley, P. L. and Kinniburgh, D. G. (2002) A review of the source, behaviour and distribution of arsenic in natural waters. *Appl. Geochem.* **17**, 517-568.

Stummmeyer, J., Marchig, V., and Knabe, W. (2002) The composition of suspended matter from Ganges-Brahmaputra sediment dispersal system during low sediment transport season. *Chem. Geol.* **185**, 125-147.

Swartz, C. H., Blute, N. K., Badruzzman, B., Ali, A., Brabander, D., Jay, J., Besancon, J., Islam, S., Hemond, H. F., and Harvey, C. F. (2004) Mobility of arsenic in a Bangladesh aquifer: inferences from geochemical profiles, leaching data, and mineralogical characterization. *Geochim. Cosmochim. Acta*, **68**, 4539-4557.

van Geen, A., Zheng, Y., Versteeg, R., Stute, M., Horneman, A., Dhar, R., Steckler, M., Gelman, A., Small, C., Ahsan, H., Graziano, J. H., Hussain, I., and Ahmed, K. M. (2003a) Spatial variability of arsenic in 6000 tube wells in a 25 km^2 area of Bangladesh. *Water Resour. Res.* **39**, 1140, doi: 10.1029/2002WR001617.

van Geen, A., Zheng, Y., Stute, M., and Ahmed, K. M. (2003b) Comment on "Arsenic mobility and groundwater extraction in Bangladesh" (II). *Science* **300**, 584c.

van Geen, A., Rose, J., Thoral, S., Garnier, M., Zheng, Y., Bottero, J. Y. (2004) Decoupling of As and Fe release to Bangladesh groundwater under reducing conditions. Part II: Evidence from sediment incubations. *Geochim. Cosmochim. Acta* **68**, 3475-3486.

Yu, W. H., Harvey, C. M., and Harvey, C. F. (2003) Arsenic in groundwater in Bangladesh: A geostatistical and epidemiological framework for evaluating health

effects and potential remedies. *Water Resour. Res.* **39**, 1146, doi: 10.1029/2002WR001327.

2.7. FIGURE CAPTIONS

Figure 2.1. μ-XRF microprobe images of As intensity within grains from Holocene aquifer sediments. Points of highest As intensity are light in color and As speciation is determined from the first-derivative XANES plot at the right. (A) Partially oxidized grain from a depth of 30 m, composed of arsenate, arsenite, and sulfidic arsenic. (B) Grain from 30 m depth dominated by reduced As coordinated with S. (C) Grain from 5 m with arsenate. (D) Grain from 60 m, a typical As-bearing grain found throughout the sediment profile with reduced As coordinated with S.

Figure 2.2. As-Cu and As-Zn correlations in grain depicted in Figure 6.1A.

Figure 2.3. Iron X-ray absorption spectra of sediments from the Holocene (5 – 60 m depth) and Pleistocene (165 m depth) aquifers; (A) k^3-weighted EXAFS, and (B) first-derivative XANES spectra. Sample spectra are shown with solid lines and linear combination fits are represented by dotted lines.

Figure 2.4. First-derivative As XANES spectra of As hotspots in soil from 5 cm, 20 cm, and 36 cm. The sample from 36-cm denoted by * is imaged in Figure 6.5 and is more reduced than the rest of the bulk soil.

Figure 2.5. μ-XRF map of As-bearing grains in surface soil from a depth of 36 cm (X-ray absorption spectra of the sample are shown in Figure 6.4).

Figure 2.6. First-derivative Fe XANES spectra of soil materials. Inset illustrates changes in the spectra at selected energy regions. With decreasing depth, the peak at 7127 eV representative of Fe(III) decreases while the peak at 7120 eV representative of Fe(II) increases.

Figure 2.7. Arsenic desorption batch experiments having sediments from 30 m depth incubated with solutions noted in the legend. (A) Experiments sampled after 2, 4, 7, and 12 d. (B) A second set of experiments examined after 16 and 29 d in order to minimize sample perturbations induced by sampling (as occurred in part A).

Figure 2.8. Correlation of dissolved P with As in batch experiments (data includes all batch experiments).

Figure 2.9. Correlations of dissolved Ca, Si, and Fe with As in batch experiments without additions of Fe(III) (hydr)oxides.

Figure 2.10. Proposed cycling and transport of As. At the surface, detrital sulfides are oxidized forming ferric (hydr)oxides which are then subject to reductive dissolution during anaerobic periods.

Table 2.1. Summary of Fe XANES and EXAFS linear combination fit results for Holocene aquifer sediments. Mineral content is representative of the mole percent of total iron within the sample.

Depth (m)	Hornblende (%)	Biotite (%)	Magnetite (%)
5	49	45	6
10	58	31	11
15	52	42	6
20	53	27	20
30	59	21	20
60	52	39	9

Figure 2.1.

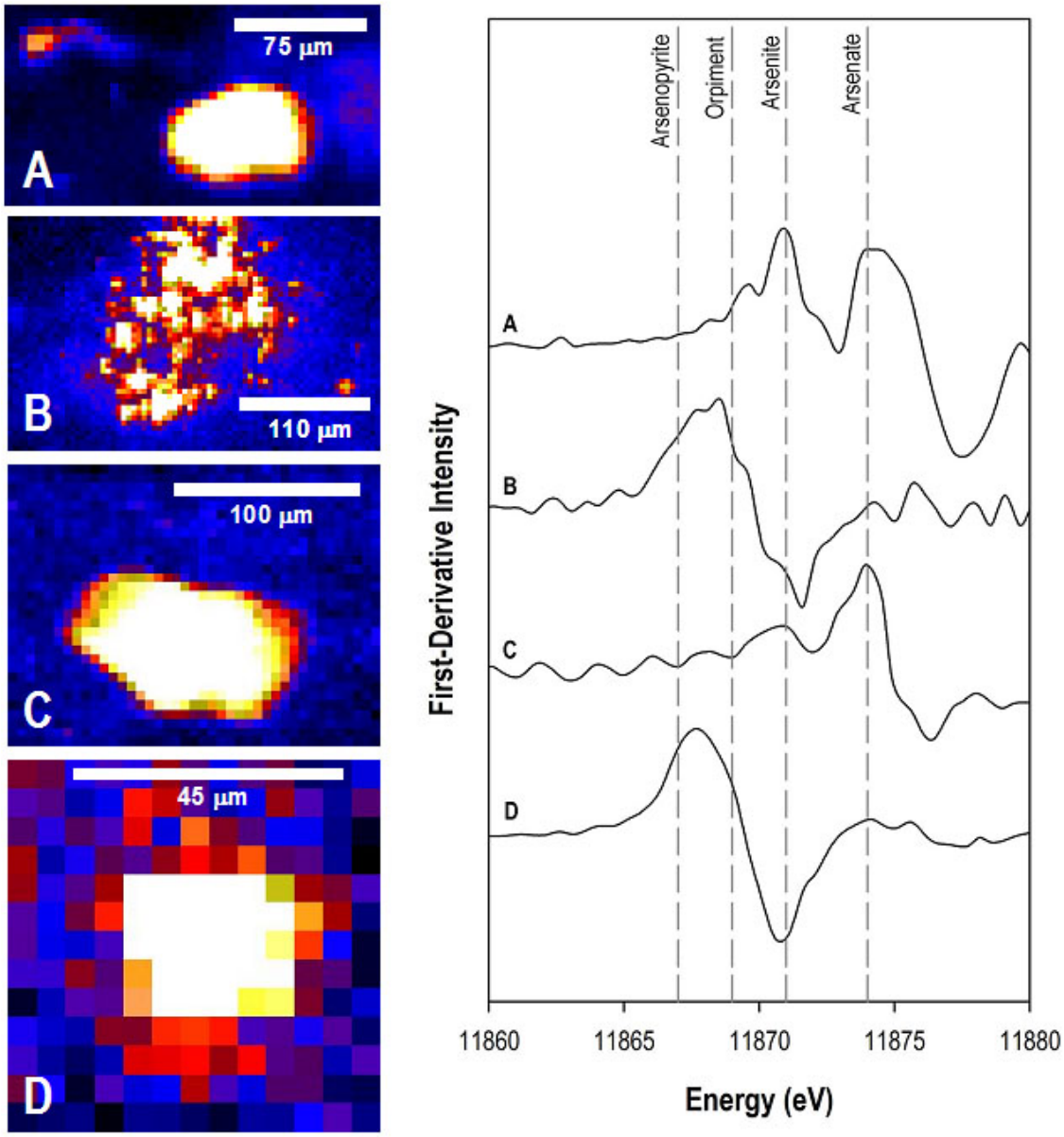
75 µm
A
B
110 µm
100 µm
C
45 µm
D
Arsenopyrite
Orpiment
Arsenite
Arsenate
A
B
C
D
First-Derivative Intensity
11860
11865
11870
11875
11880
Energy (eV)

Figure 2.2.

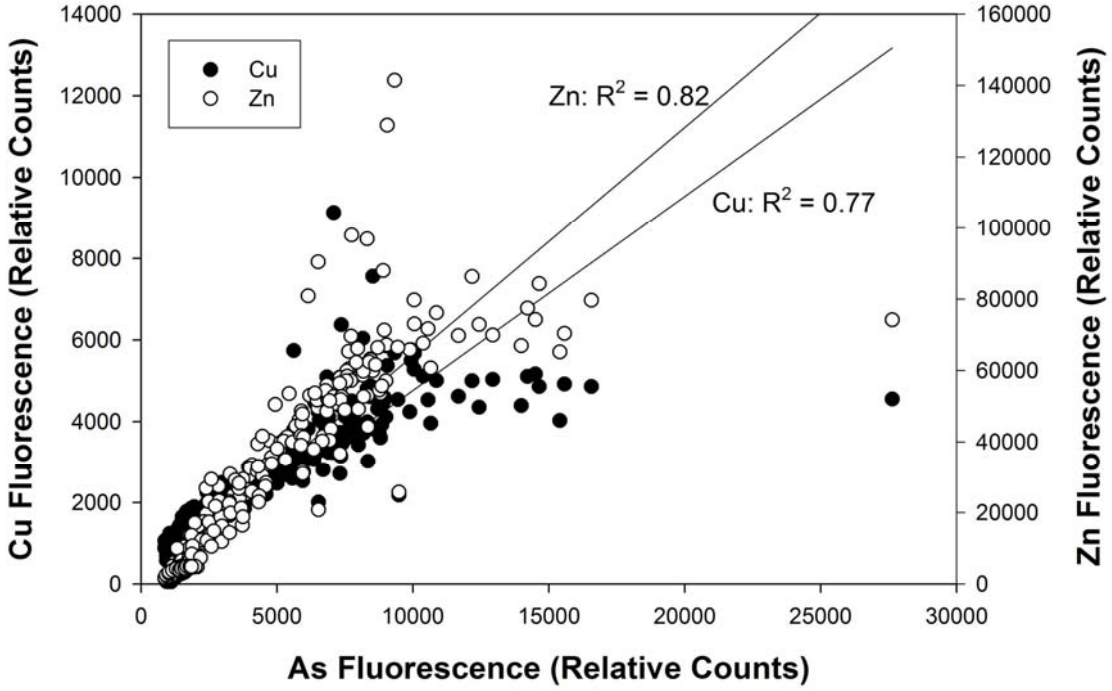
Cu
Zn
Zn: R2 = 0.82
Cu: R2 = 0.77
Cu Fluorescence (Relative Counts)
Zn Fluorescence (Relative Counts)
As Fluorescence (Relative Counts)
0
2000
4000
6000
8000
10000
12000
14000
0
20000
40000
60000
80000
100000
120000
140000
160000
0
5000
10000
15000
20000
25000
30000

Figure 2.3.

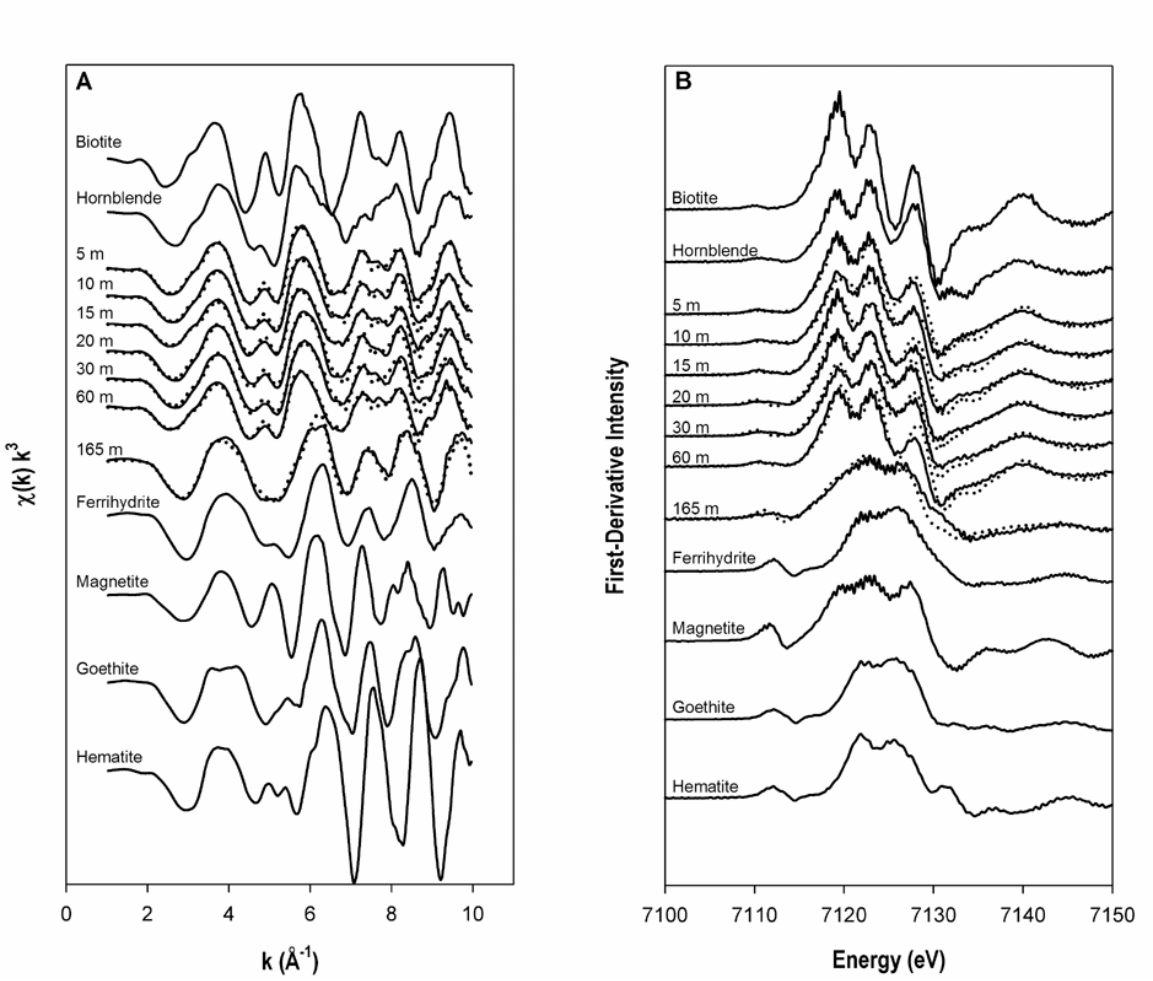
A
Biotite
Hornblende
5 m
10 m
15 m
20 m
30 m
60 m
165 m
Ferrihydrite
Magnetite
Goethite
Hematite
χ(k) k3
0
2
4
6
8
10
k (Å-1)
B
Biotite
Hornblende
5 m
10 m
15 m
20 m
30 m
60 m
165 m
Ferrihydrite
Magnetite
Goethite
Hematite
First-Derivative Intensity
7100
7110
7120
7130
7140
7150
Energy (eV)

Figure 2.4.

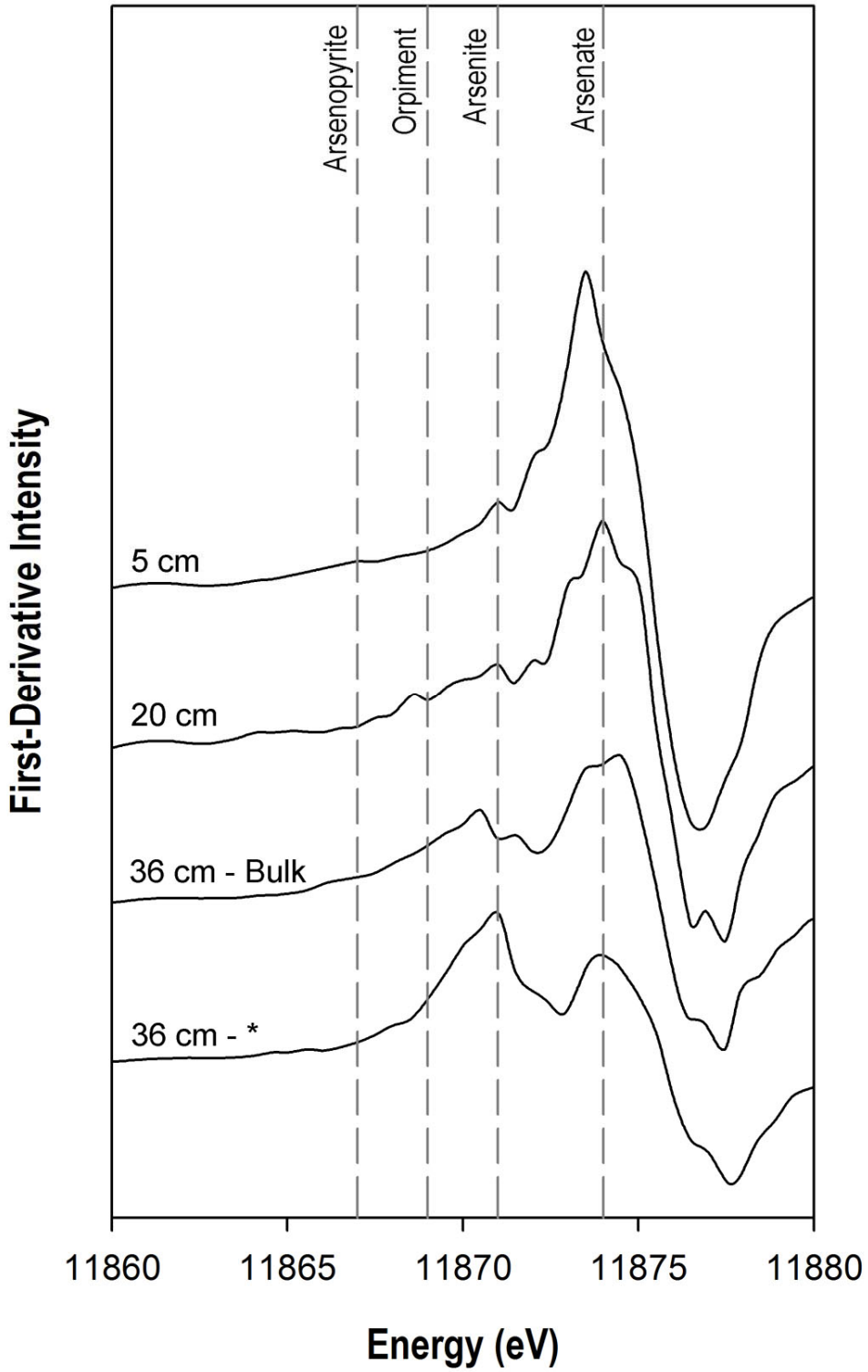
Arsenopyrite
Orpiment
Arsenite
Arsenate
5 cm
20 cm
36 cm - Bulk
36 cm - *
First-Derivative Intensity
11860
11865
11870
11875
11880
Energy (eV)

Figure 2.5.

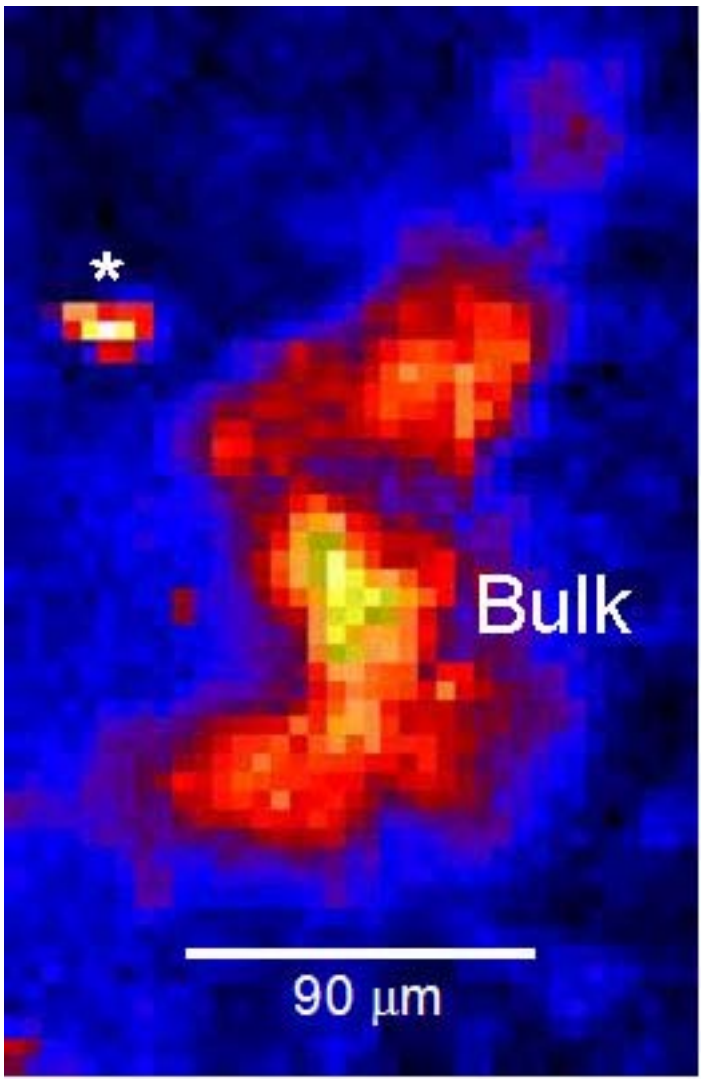

Figure 2.6.

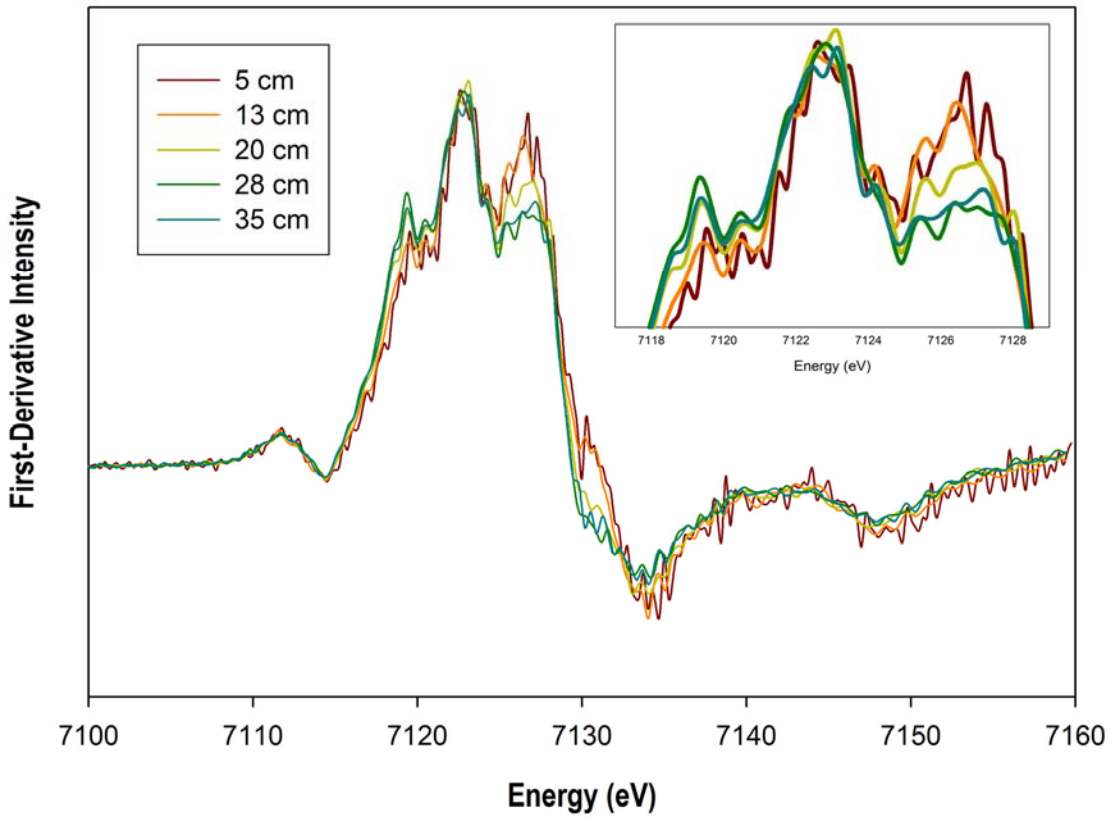
5 cm
13 cm
20 cm
28 cm
35 cm
First-Derivative Intensity
7100
7110
7120
7130
7140
7150
7160
Energy (eV)
7118
7120
7122
7124
7126
7128
Energy (eV)

Figure 2.7.

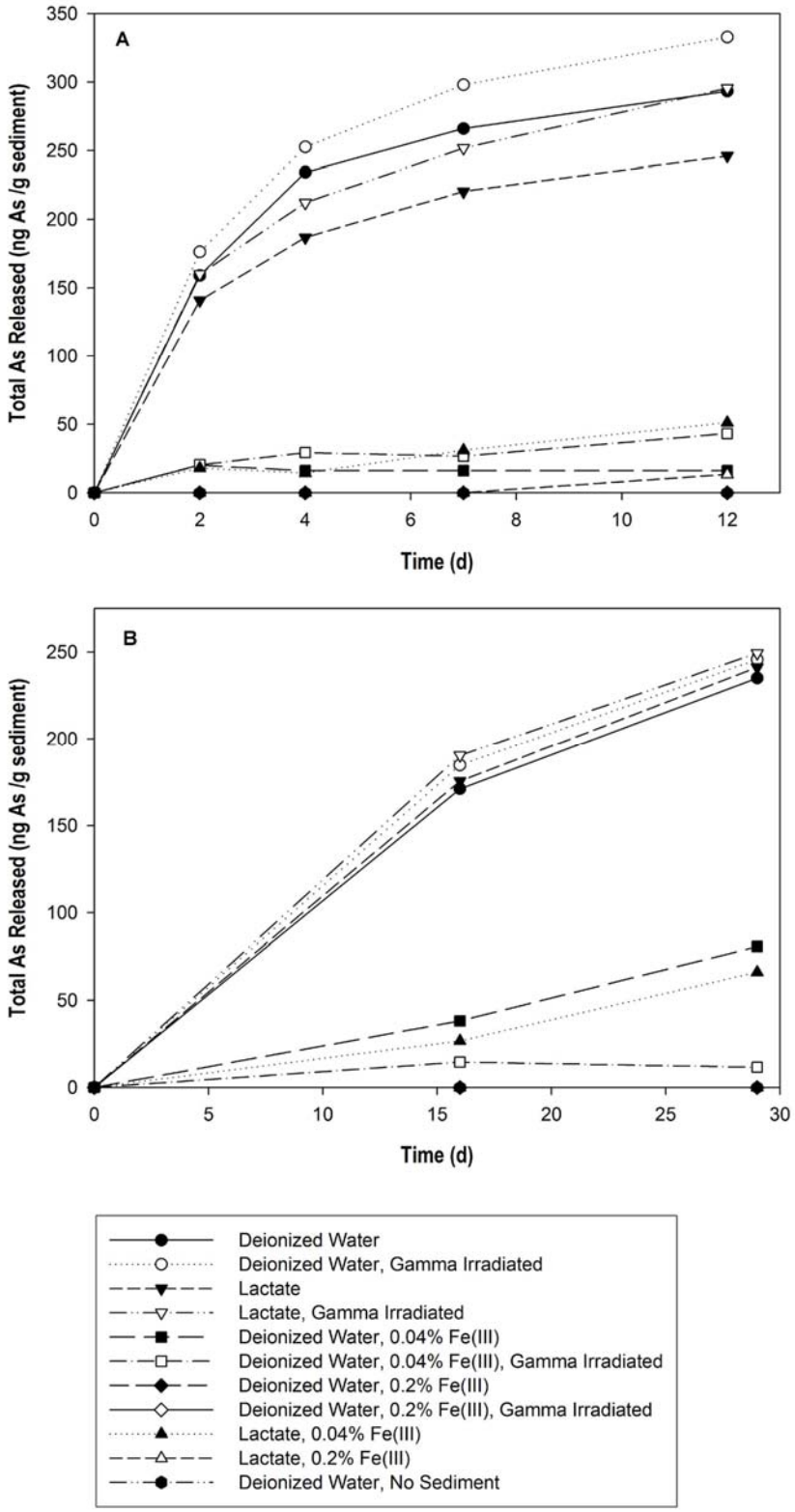
A
Total As Released (ng As /g sediment)
Time (d)
B
Total As Released (ng As /g sediment)
Time (d)
Deionized Water
Deionized Water, Gamma Irradiated
Lactate
Lactate, Gamma Irradiated
Deionized Water, 0.04% Fe(III)
Deionized Water, 0.04% Fe(III), Gamma Irradiated
Deionized Water, 0.2% Fe(III)
Deionized Water, 0.2% Fe(III), Gamma Irradiated
Lactate, 0.04% Fe(III)
Lactate, 0.2% Fe(III)
Deionized Water, No Sediment

Figure 2.8.

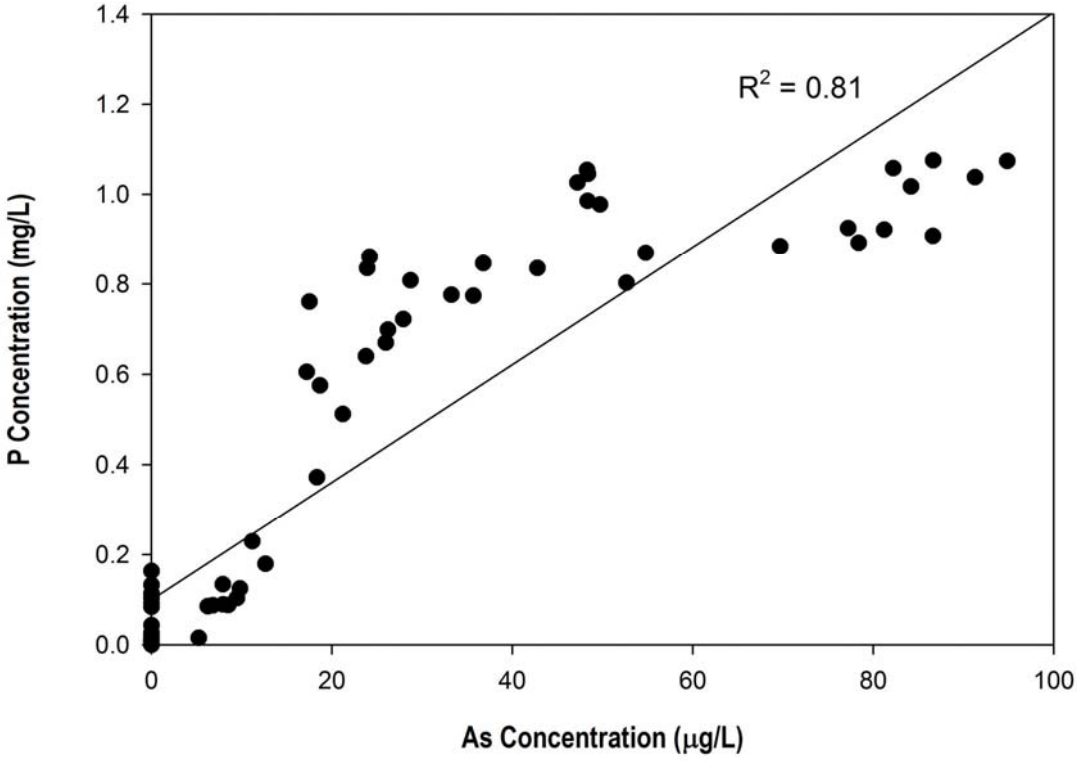
1.4
1.2
1.0
0.8
0.6
0.4
0.2
0.0
P Concentration (mg/L)
R2 = 0.81
0
20
40
60
80
100
As Concentration (μg/L)

Figure 2.9.

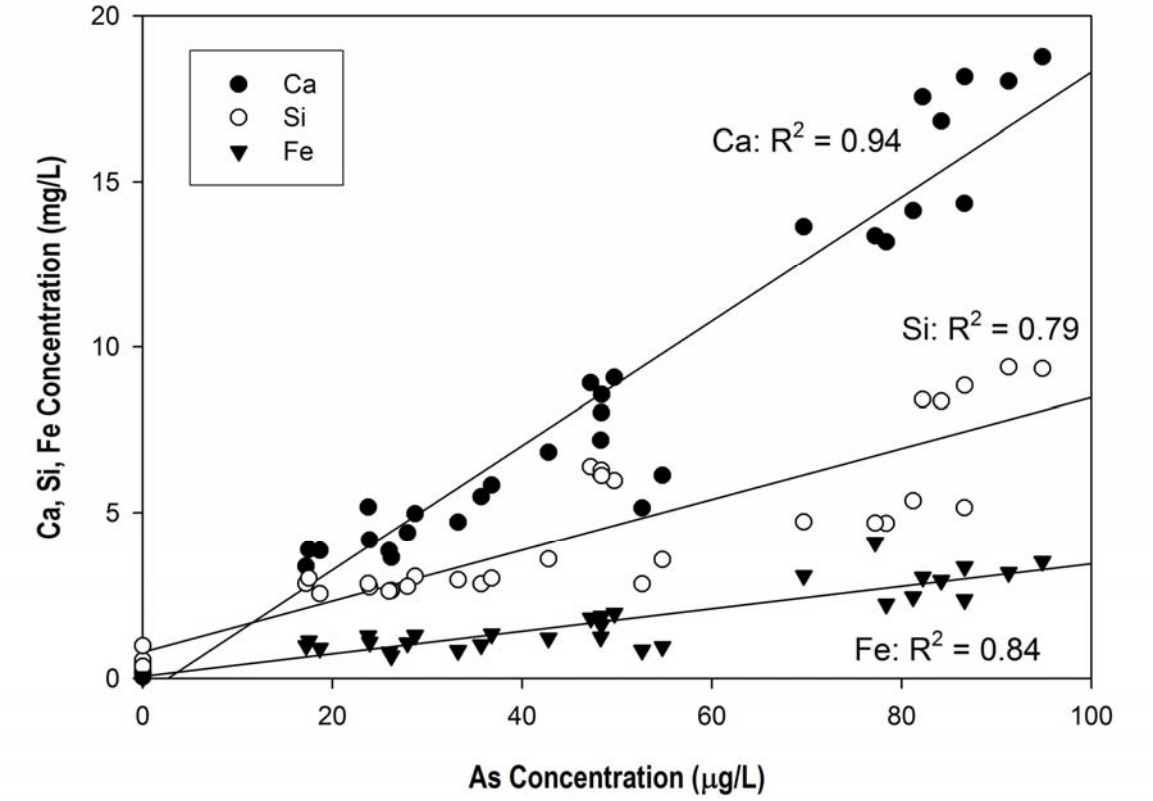
Ca
Si
Fe
Ca: R2 = 0.94
Si: R2 = 0.79
Fe: R2 = 0.84
Ca, Si, Fe Concentration (mg/L)
As Concentration (μg/L)
0
5
10
15
20
0
20
40
60
80
100

Figure 2.10.

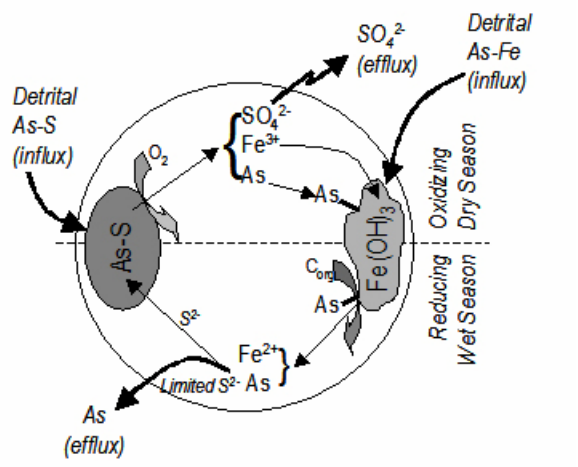
SO_4^{2-} (efflux)
Detrital As-Fe (influx)
Detrital As-S (influx)
SO_4^{2-}
Fe^{3+}
As
O_2
As
As-S
$Fe(OH)_3$
Oxidizing Dry Season
C_{org}
As
Reducing Wet Season
S^{2-}
Fe^{2+}
Limited S^{2-} As
As (efflux)

CHAPTER 3

Processes Conducive to the Release and Transport of Arsenic into Aquifers of Bangladesh

ABSTRACT

Arsenic is a contaminant in the groundwater of Holocene aquifers in Bangladesh, where approximately 57 million people drink water with arsenic levels exceeding the limits set by the World Health Organization. While arsenic is native to the sediments, the means by which it is released to groundwater remains unresolved. Contrary to the current paradigm, ferric (hydr)oxides appear to dominate the partitioning of arsenic in the near-surface but have a limited impact at aquifer depths where wells extract groundwater with high arsenic concentrations. We present a sequence of evidence that taken together suggest that arsenic may be released in the near surface and then transported to depth. We establish that (*i*) the only portion of the sediment profile with conditions destabilizing to arsenic in our analysis is in the surface or near-surface environment; (*ii*) a consistent input of arsenic via sediment deposition exists; (*iii*) retardation of arsenic transport is limited in the aquifers, and (*iv*) groundwater recharge occurs at a rate sufficient to necessitate continued input of arsenic to maintain observed concentrations. Our analyses thus lead to the premise that arsenic is liberated in surface and near-surface sediments through cyclic redox conditions and is subsequently transported to well-depth. Influx of sediment and redox cycling provide a long-term source of arsenic that when liberated in the near-surface is only weakly partitioned onto sediments deeper in the profile and is transported through aquifers by groundwater recharge.

3.1. INTRODUCTION

Resolving the processes responsible for high concentrations of dissolved arsenic is essential for addressing the human health calamity within Bangladesh and West Bengal, India, where we are witnessing the largest mass poisoning in history (Yu et al., 2003). Furthermore, deciphering the processes and conditions responsible for arsenic partitioning to the aqueous phase within the Ganges-Brahmaputra Delta may also help diminish arsenic-induced hazards within deltas throughout subtropical and tropical regions of Asia. Although important work has been done to this end, numerous observations conflict with the prevailing theory that reductive dissolution of iron (hydr)oxides at well-depth (i.e. 30-50 m) results in the high concentration of arsenic within drinking water (Nickson et al., 1998; Nickson et al., 2000; Harvey et al., 2002; Dowling et al., 2002; McArthur et al., 2004). While iron (hydr)oxides have been detected in oxidized upper sediments (Akai et al., 2004), as well as in orange Pleistocene sediments (Horneman et al., 2004; Swartz et al., 2004), they do not appear widespread in the grey Holocene aquifer at depths of (and below) the highest arsenic concentrations (McArthur et al., 2004; Horneman et al., 2004; Swartz et al., 2004). Moreover, proxies for active bacterial metabolism, namely redox potential (BGS and DPHE, 2001; Harvey et al., 2002; Dowling et al., 2002), concentration of dissolved electron acceptors (e.g., sulphate; Figure 3.1) and their products (e.g., methane), and molecular hydrogen (Harvey et al., 2002), are all inconsistent with ongoing ferric-iron reduction at well depths of 30 to 40 m. Finally, solid-phase arsenic concentrations in the aquifer sediments are relatively low (typically < 3 mg/Kg) compared to world averages of sedimentary basins (Smedley and Kinniburgh, 2002); if reductive dissolution of iron (hydr)oxides were the sole cause

of arsenic release, one would expect As concentrations to have declined as Fe(III) minerals were consumed and aquifers flushed. However, arsenic concentrations are highest at well-depths where reactive ferric (hydr)oxides appear exhausted (Horneman et al., 2004; Swartz et al., 2004). Accordingly, in order to help understand the processes controlling arsenic in Bangladesh groundwater, we evaluated the hydrologic and biogeochemical setting, conducted spectroscopic examinations of Holocene aquifer sediments, and performed arsenic release batch experiments incorporating sediments from depths where arsenic groundwater concentrations are highest. Our findings reveal that arsenic must be released upgradient and transported to the aquifer at well-depth, a scenario we postulate is maintained by release in the surface or near-surface soils/sediments through cyclic, seasonal redox cycles.

3.2. MATERIALS AND METHODS

3.2.1. Sediment Samples

Sediment samples were obtained from the Munshiganj district of Bangladesh, 30 km south of Dhaka and 7 km north of the Ganges River. Our field site is located centrally in Bangladesh with geological and hydrological conditions typical of the areas worst affected by arsenic; geochemical conditions are similar to those sites with high dissolved arsenic as discussed in the Bangladesh-wide British Geological Survey study (BGS and DPHE, 2001). The site encompasses 16 km^2 and is thus considerably larger than the dominant scales of spatial heterogeneity (10's to 100's of meters) in dissolved arsenic in the worst-affected areas, yielding findings of wide-spread utility. The

subsurface at our location consists of a surficial clay, a Holocene aquifer of grey sand, a clay aquitard, and a deep burnt-orange sandy Pleistocene aquifer.

Core extraction procedures and groundwater aqueous chemistry were summarized previously (Swartz et al., 2004). Arsenic concentrations in the groundwater increase with depth to a maximum at ~30 m and then decrease with increasing depth; solid-phase arsenic concentrations in the Holocene aquifer are below 3 mg/Kg (Harvey et al., 2002). Sediment sub-samples for spectroscopic analyses were collected from one core at depths of 5, 10, 15, 22, 30, and 60 m and put into crimp-sealed serum vials under an N_2 atmosphere. The samples were shipped from Bangladesh and stored at 4^{o}C upon arrival.

3.2.2. X-ray Microprobe and X-ray Absorption Spectroscopic Analyses

Spatial distributions of As, Fe, Cu, and Zn were determined using X-ray fluorescence (XRF) spectroscopy, and X-ray absorption spectroscopy (XAS) was used to elucidate oxidation and chemical states of arsenic. Experiments were conducted on undulator beamline 13-ID-C at the Advanced Photon Source, Argonne National Laboratory. The ring operated at 7 GeV and current was maintained at ~100 mA through periodic electron injection. Energy selection was performed by a Si (111) monochromator. All sample preparation was conducted under anaerobic conditions (N_2:H_2, 95:5) in a polyethylene glovebag. Sediments were spread on polycarbonate slides and sealed with Kapton tape. Slides were rastered in 5 to 15 μm steps around a 5x6 μm X-ray beam and fluorescent X-rays were measured with a 16-element solid-state energy-dispersive Ge detector. Arsenic, Fe, Cu, and Zn were detected simultaneously with their fluorescent X-ray intensities proportional to the number of atoms under the

incident beam. Incident and transmitted intensities were measured with in-line ionization chambers. Iron XAS was collected and analyzed as described previously to determine the solid-phase speciation (Hansel et al., 2003); detection limits of this approach are approximately 5% of the total iron within the system.

Multiple X-ray fluorescence maps were made on sediments from each depth and thousands of points were analysed. Areas of arsenic concentration in the elemental maps were analyzed with micro-X-ray absorption near-edge structure (μ-XANES) spectroscopy to determine arsenic speciation. The sample spectra were collected from –50 to +100 eV about the As K_α edge of 11867 eV, and speciation was determined through a spectral analysis of first-derivative peaks from the XANES spectra of As standards. Arsenic concentrations within grains were determined by comparison to a thin film standard. The proportion of total arsenic bound in sulfide form in the sediments was approximated by considering spheres of sulfide minerals (as determined by μ-XANES) with volumes based on radii in the 2-dimensional maps; the density of pyrite was used and arsenic was assumed to be 1% of the total sulfide mass.

3.2.3. Arsenic Displacement Experiments

Arsenic release from 30 m sediments was examined in batch experiments with 5 g of sediment and 10 mL of solution in 20 mL serum vials. Solutions of 18 MΩ water and 1.5 mM DOC (as lactate) were autoclaved and made anoxic by boiling and cooling under a stream of O_2-free N_2. Ferrihydrite-coated sand was synthesized according to previous methods (Hansel et al., 2003) and was added to some vials with the natural sediments to give 0.04 and 0.20 total weight percent Fe(III). Sediment and Fe-coated sand samples for

abiotic controls were sterilized by gamma irradiation (2855 R/min for 14 hours). All glassware was autoclaved prior to experimentation and sterile techniques were employed. Reactions were initiated and sampled under anaerobic conditions (N_2:H_2, 95:5) in a glovebag. Sediment slurries including water, lactate, or Fe(III)-oxide and water were sealed and shaken (140 rpm) in darkness, and separate sets of experiments were run for 2 and 16 days. Aqueous samples were acidified with concentrated trace metal grade hydrochloric acid (to achieve 0.17 M acidity) and stored at 4^{o}C until analysis.

Solution-phase arsenic concentrations were analyzed by hydride generation inductively-coupled-plasma optical emission spectroscopy (HG-ICP-OES). In order to reduce any arsenate to arsenite, 3 mL of sample was mixed with 3 mL concentrated trace metal grade hydrochloric acid, 1 mL 8% urea, and, following 10 min of reaction time, 1 mL 16% KI. The mixture was allowed to sit for at least 1 h and then further reacted with 6 N HCl and 0.6% $NaBH_4$/0.5% NaOH. The resulting arsine gas was measured by ICP-OES. Detection limits were 5 μg/L for arsenic.

3.3. RESULTS AND DISCUSSION

The current paradigm within Bangladesh and West Bengal is that Fe(III) (hydr)oxides remain the dominant host of arsenic even at well-depth (i.e., 30 to 50 m) within contaminated aquifers, and that organic carbon derived either from the surface (Harvey et al., 2002) or from detrital material (Nickson et al., 1998; Nickson et al., 2000; McArthur et al., 2004) is stimulating reductive dissolution of the iron phases and concomitant release of arsenic. Here we explore operative redox processes impacting arsenic partitioning between the solid and aqueous phase using multiple lines of data,

inclusive of detailed spectroscopic measurements, batch experiments, and field observations.

3.3.1. Aquifer Redox Processes

Aqueous arsenic concentrations in Bangladesh aquifers often reach a maximum within the first 50 m below the surface, and at our site we find a distinct peak at ~30 m depth (Figure 3.1; BGS and DPHE, 2001). Groundwater at 30 to 40 m depth often has high methane concentrations (> 1 mM) and very low redox potentials (BGS and DPHE, 2001; Harvey et al., 2002; Dowling et al., 2002), and at our field site in the Munshiganj district of Bangladesh 10 nM H_2 was observed at 38 m depth (Harvey et al., 2002). Given that dissimilatory iron reduction, the primary means of iron reduction, precedes methane generation in sediment diagenesis (or aquifer redox profiles), active iron reduction occurred at an earlier stage in diagenesis (Lovley and Anderson, 2000) as opposed to the present time. Furthermore, the H_2 concentration at 38 m is 10 to 100 times higher than representative of dissimilatory Fe(III) reduction and is instead indicative of CO_2 reduction to methane, consistent with the high methane values recorded (Lovley and Anderson, 2000).

3.3.2. Associations of Arsenic in the Solid-Phase. In sediments from 30 m depth, the approximate depth of the maximum dissolved As at our field site and the average well-depth in the region (Harvey et al., 2002), we find arsenic within sulfide grains exceeding 100 μm in diameter (Figure 3.2). Grain-size, association with copper and zinc (chalcophiles), and weathering progress of the sulfides suggest detrital origin. For

example, analysis of a 150 μm grain illustrates sulfidic arsenic (Figure 3.2A), with local arsenic concentrations as high as 50 g/Kg (5%) within the grain. Another large grain (Figure 3.2B) exhibiting oxidation, as indicated by arsenate and arsenite species, is in association with sulfidic arsenic (Figure 3.2B), and Cu and Zn correlate strongly with arsenic (R^2 values of 0.77 and 0.82, respectively); occlusion in quartz or other primary silicates may, in part, be responsible for their preservation. Sulfidic grains with arsenic concentrations of ~1% and diameters of 15 to 35 μm occur throughout the Holocene sediment borehole samples obtained at our field site, including depths ranging from 5 to 60 m, and are likely of authigenic origin. While we observe concentrated arsenate- and arsenite-bearing grains within aquifer sediments, arsenic-bearing sulfides (detrital and authigenic) represent the largest solid-phase arsenic fraction within the investigated aquifer sediments, accounting for up to 60% of the total arsenic (based on spatial analysis using X-ray microprobe/XAS and supported by chemical extractions; Swartz et al., 2004). Additionally, small fromboidal pyrite, presumably diagenetic, was observed in surficial (< 9 m) Holocene sediments (Nickson et al., 2000), and we find acid volatile sulfides at our field site in Munshiganj (Harvey et al., 2002).

3.3.3. Arsenic Desorption from Aquifer Sediments

A paucity of ferric (hydr)oxides has been observed in extraction (Swartz et al., 2002) and reflectance (Horneman et al., 2004) experiments and, albeit with detection limits restricted to about 5% of the total Fe within the sampled region, we did not detect iron (hydr)oxides in Holocene aquifer sediments using both bulk- and micro-XAS. Most importantly, current redox conditions are inconsistent with dissimilatory iron reduction

being the dominant electron accepting process. Thus, because reactive Fe(III) (hydr)oxides are predominantly depleted from the Holocene aquifer, adsorption of aqueous arsenic is limited to phases such as the silicate and carbonate minerals which have a low surface area and a relatively weak affinity for arsenic. Laboratory batch experiments (ours in Figure 3.3; and van Geen et al., 2004) and previous *in situ* injection-withdrawal tests (Harvey et al., 2002) both reveal rapid desorption of arsenic from the sediments, indicating that arsenic is more labile than would be expected if it were bound to ferric (hydr)oxides. Arsenic is released from grey Holocene sediment solids by the simple addition of water and thus amendment with labile organic carbon (e.g. lactate (Figure 3.3) or acetate (van Geen et al., 2004)) is not necessary to invoke rapid desorption of arsenic. In contrast, arsenic remains in the solid-phase with the addition of ferric (hydr)oxide to sediment incubations (Figure 3.3). Consequently, the weakly adsorbed (labile) phase of arsenic within the Holocene aquifer, constituting approximately 20% of the initial solid-phase As in our experiments, can be easily liberated and transported during groundwater movement.

3.3.4. Groundwater Flow and Arsenic Transport

Groundwater tritium concentrations at our site (Harvey et al., 2003), and across Bangladesh (Aggarwal et al., 2002), indicate a residence time of typically less than 50 years in the upper 30 m, consistent with the rate of irrigation withdrawal (Harvey et al., 2003; Harvey et al., 2006). Three scenarios may therefore explain the current aqueous arsenic concentrations: (*i*) groundwater flow was much slower in the past such that arsenic was not flushed from the Holocene aquifer, (*ii*) geochemical conditions have

recently shifted to mobilize arsenic, or (*iii*) dissolved arsenic is provided by a source that is hydrologically upgradient of the sampling wells. Surface sediments, which typically have higher solid-phase arsenic concentrations than the aquifer materials (Mehoarg and Rahman, 2003; Breit et al., 2004; Swartz et al., 2004), can provide a source of arsenic, potentially maintaining constant aqueous arsenic concentrations downgradient in areas where groundwater velocities and/or solid-phase arsenic concentrations are modest. Assuming a downward component of groundwater velocity of 0.5 m/y (Harvey et al., 2006), arsenic concentration of 1 μM (the approximate national average; BGS and DPHE, 2001), sedimentation rate of 1 cm/y, and 50 nmoles of arsenic mobilized per gram of surface sediment (~1/4 of typical surface sediment concentrations; Meharg et al., 2003; Swartz et al., 2004), the groundwater arsenic flux and input by sedimentation are comparable, both equal to 0.5 mmol As/m^2y. This suggests that steady groundwater concentrations could be sustained by sediment deposition in areas where groundwater velocities and dissolved arsenic concentrations are modest. However, where arsenic concentrations and groundwater fluxes are higher, such as our site in Munshiganj (8 μM and 1 m/y) (Harvey et al., 2002), or when sedimentation rates are lower, the observed arsenic concentrations suggest hydrologic or geochemical transience.

Our hydrologic data (Harvey et al., 2006) reveal residence times on the order of 80 y without irrigated agriculture; with irrigation pumping, residence times decrease to less than 40 y—the recent onset of irrigation pumping increases recharge rates by a factor of 2. The recent alteration in irrigation pumping has changed groundwater flow patterns, decreasing the residence time of groundwater and perhaps flushing arsenic (Harvey et al., 2003; McArthur et al., 2004) from the Holocene aquifer. Dry season rice cultivation,

now covering ~25% of the country (Hossain et al., 2003), is irrigated with ~1 m/y of groundwater (Harvey et al., 2006) which, assuming a porosity of 25%, causes an average downward component of groundwater velocity of ~1 m/y to the depth of well screens. The increased groundwater flow might explain current arsenic profiles but only if past groundwater residence times were sufficiently slow to impede even a single pore-volume of flushing since the inception of the aquifer. Therefore, if arsenic concentrations are to remain elevated an upstream source must be present.

3.3.5. Arsenic Release Through Deposition Combined with Redox Cycling

One potential upstream source of arsenic is the near-surface sediments, where, as noted above, sedimentation fluxes can sustain groundwater arsenic concentrations. Three pathways may lead to arsenic release within the surface and near-surface soils/sediments, all involving Fe and As reduction. First, recently deposited sediments containing As(V) associated with ferric (hydr)oxides will undergo reduction upon the following seasonal addition of organic carbon (surface derived) and flood waters. Solid-phase arsenic is deposited in association with detrital sulfides and ferric (hydr)oxides. Ferric (hydr)oxides dissolve, as illustrated by increasing Fe(II)/Fe_{total} ratios with depth (Horneman et al., 2004), in concert with As(V) reduction to As(III) as the sediments are buried to the depths of the grey aquifer material.

Second, seasonal cycling in aerobic/anaerobic conditions will lead to the destabilization of arsenic bearing sulfides, which contain more than 10 g/Kg of arsenic and are thus major repositories of this toxin. Seasonal water-table oscillations (BGS and DPHE, 2001; Harvey et al., 2002; Harvey et al., 2006) establish an oxic-anoxic cycle in

the surface and near-surface sediments. During the dry season, sulfide minerals will be oxidized leading to the repartitioning of arsenic into ferric (hydr)oxides (Mok and Wai, 1994), followed then by reductive dissolution of iron and arsenic during the ensuing wet season. Cyclic redox conditions in the near-surface sediments would therefore accelerate sulfide weathering and release of arsenic, consistent with processes noted for mining impacted environments (Moore, 1994). The presence of both detrital and authigenic sulfides demonstrates, in fact, that redox cycling is occurring, and fluctuating redox conditions have been proposed based on $\delta^{34}S$ measurements (Zheng et al., 2004).

Finally, a third means of arsenic liberation to the aqueous phase may result from changes in conditions that enhance the reducing intensity of the redox cycle, such as increased periods of field saturation. An area within the soil/sediment profile (down to depths of 80 m) consistently having arsenic concentrations greater than 10 mg/Kg exists within the upper 2-m of the surface—precisely where the greatest biogeochemical activity resides. Arsenic exists at concentrations in excess of 1000 mg/Kg (Breit et al., 2004) within iron bands created by past redox conditions (Brammer, 1966). Moreover, microbial reductive mobilization of arsenic from sediments of the oxic-anoxic boundary has been observed (Islam et al., 2004), demonstrating the potential for arsenic release under the onset of reducing conditions at the near-surface. Once partitioning into the aqueous phase, dissolved arsenic may then enter the aquifer during recharge.

3.4. SUMMARY AND CONCLUSIONS

Transport of carbon into the aquifer undoubtedly creates reducing conditions, and the high levels of dissolved molecular hydrogen and methane indicate that ferric iron no longer serves as a primary electron acceptor. High concentrations of young inorganic carbon correlate strongly with arsenic, ammonium, methane, calcium, and inversely with sulfate concentrations in the Holocene aquifer in Munshiganj (Harvey et al., 2002), implying that the most significant biological processes occur upgradient and mix during transport. Furthermore, the bell-shaped vertical profile of these solutes (Harvey et al., 2002) is typical of plume migration from a surface source. After solute enters an aquifer, plume movement is dominated by lateral transport away from the surface source, but recharge also displaces the plume downwards, so local sources create bell-shaped vertical solute profiles. Groundwater flow has a large lateral component because the distance between discharge areas (irrigation wells and river channels) is greater than the aquifer thickness. We therefore suggest that both inorganic carbon and arsenic are signatures of biological processes upgradient, likely reflecting surface and near-surface processes (anaerobic-aerobic cycles induced by the influx of carbon-rich surface waters following dry-season draw-down), that are transported along groundwater flow paths until reaching wells in the sandy aquifer. If a remnant band of ferric (hydr)oxide persists, such as Pleistocene aged material, within the flow-path, entry to organic carbon would induce reductive stabilization of arsenic as well. Organic carbon from the surface would be consumed rapidly, and arsenic, as arsenite, could easily be transported due to its low distribution coefficient in the sediments. Seasonal cycling in redox conditions coupled

with annual deposition could therefore account for the liberation of arsenic to the aqueous phase. We therefore hypothesize that surface and near-surface biogeochemical processes mobilize arsenic in Bangladesh and that these processes, coupled with arsenic transport through the aquifer, should be the focus of further research.

3.5. REFERENCES

Aggarwal, P. K., Basu, A. R. and Poreda R. J. (2002) Isotope hydrology of groundwater in Bangladesh: implications for characterization and mitigation of arsenic in groundwater. *IAEA-TC Project Report: BGD/8/016*, IAEA, Vienna.

Akai, J., Izumi, K., Fukuhara, H., Masuda, H., Nakano, S., Yoshimura, T., Ohfuji, H., Anawar, H. M., and Akai, K. (2004) Mineralogical and geomicrobiological investigations on groundwater arsenic enrichment in Bangladesh. *Appl. Geochem.* **19**, 215-230.

BGS and DPHE (2001) *Arsenic contamination of groundwater in Bangladesh, Vol. 2. Final report*. BGS technical report WC/00/19.

Brammer, H. (1966) *The Geography of the Soils of Bangladesh.* University Press Limited, Dhaka, Bangladesh.

Breit, G. N., Foster, A. L., Perkins, R. B., Yount, J. C., King, T., Welch, A. H., Whitney, J. W., Uddin, N., Muneem, A., and Alam., M. (2004) As-rich ferric oxyhydroxide enrichments in the shallow subsurface of Bangladesh. In Wanty, R. B. and Seal, R. R. II (eds.) *Water-Rock Interactions*. Taylor & Francis Group, London, 1457-1461.

Dowling, C. B., Poreda, R. J., Basu, A. R., Peters, S. L., and Aggarwal, P. K. (2002) Geochemical study of arsenic release mechanisms in the Bengal Basin groundwater. *Water Resour. Res.* **38**, 1173, doi: 10.1029/2001WR000968.

Hansel, C. M., Benner, S., Neiss, J., Dohnalkova, A., Kukkadapu, R. K., and Fendorf, S. (2003) Secondary mineralization pathways induced by dissimilatory iron

reduction of ferrihydrite under advective flow. *Geochim. Cosmochim. Acta* **67**, 2977-2992.

Harvey, C. F., Swartz, C. H., Badruzzaman, A. B. M., Keon-Blute, N., Niedan, V., Brabander, D., Oates, P. M., Ashfaque, K. N., Islam, S., Hemond, H. F., and Ahmed, M. F. (2002) Arsenic mobility and groundwater extraction in Bangladesh. *Science* **298**, 1602-1606.

Harvey, C. F., Swartz, C., Badruzzaman, A. B. M., Keon-Blute, N., Niedan, V., Brabander, D., Oates, P. M., Ashfaque, K. N., Islam, S., Hemond, H. F., and Ahmed, M. F. (2003) Response to comments on "Arsenic mobility and groundwater extraction in Bangladesh". *Science* **300**, 584d.

Harvey, C. F., Ashfaque, K. N., Yu, W., Badruzzaman, A. B. M., Ali, M. A., Oates, P. M., Michael, H., Neumann, R. B., Beckie, R., Islam, S., and Ahmed, M. F. (2006) Groundwater flow and arsenic biogeochemistry in Bangladesh: an analysis of transience and coupling. *Chemical Geology* **228**, 112-136.

Horneman, A., van Geen, A., Kent, D. V., Mathe, P. E., Zheng, Y., Dhar, R. K., O'Connell, S., Hoque, M. A., Aziz, Z., Shamsudduha, M., Seddique, A. A., and Ahmed, K. M. (2004) Decoupling of As and Fe release to Bangladesh groundwater under reducing conditions. Part I: Evidence from sediment profiles. *Geochim. Cosmochim. Acta* **68**, 3459-3473.

Hossain, M., Lewis, D., Bose, M., and Chowdhury, A. (2003) *Rice Research, Technological Progress, and Impacts on the Poor: The Bangladesh Case (Summary Report)*. International Food Policy Research Institute, Washington, DC.

Islam, F. S., Gault, A. G., Boothman, C., Polya, D. A., Chatterjee, D., and Lloyd, J. (2004) Direct evidence of arsenic release from Bengali sediments due to metal-reducing bacteria. *Nature* **430**, 68-71.

Lovley, D. R. and Anderson, R. T. (2000) Influence of dissimilatory metal reduction on fate of organic and metal contaminants in the subsurface. *Hydrogeology J.* **8**, 77-88.

McArthur, J. M., Banerjee, D. M., Hudson-Edwards, K. A., Mishra, R., Purohit, R., Ravenscroft, P., Cronin, A., Howarth, R. J., Chatterjee, A., Talukder, T., Lowry, D., Houghton, S., and Chadha, D. K. (2004) Natural organic matter in sedimentary basins and its relation to arsenic in anoxic ground water: the example of West Bengal and its worldwide implications. *Appl. Geochem.* **19**, 1255-1293.

Meharg, A. A. and Rahman, M. (2003) Arsenic contamination of Bangladesh paddy field soils: implications for rice contribution to arsenic consumption. *Environ. Sci. Technol.* **37**, 229-234.

Mok, W. M. and Wai, C. M. (1994) Mobilization of arsenic in contaminated river waters. p. 99-118. In Nriagu, J. O. (ed.). *Arsenic in the Environment. Part I. Cycling and Characterization*. Vol. **26**, Wiley Series in Advances in Environmental Science and Technology, Wiley-Interscience, 430 p.

Moore, J. N. (1994) Contaminant mobilization resulting form redox pumping in a metal-contaminated river-reservoir system. In: Baker, L.A. (Ed.), *Environmental Chemistry in Lakes and Reservoirs*, Vol. 237. American Chemical Society, Washington DC, pp. 451-471.

Nickson, R., McArthur, J., Burgess, W., Ahmed, K. M., Ravenscroft, P., and Rahman, M. (1998) Arsenic poisoning of Bangladesh groundwater. *Nature* **395**, 338.

Nickson, R. T., McArthur, J. M., Ravenscroft, P., Burgess, W. G., and Ahmed, K. M. (2000) Mechanism of arsenic release to groundwater, Bangladesh and West Bengal. *Appl. Geochem.* **15**, 403-413.

Smedley, P. L. and Kinniburgh, D. G. (2002) A review of the source, behaviour and distribution of arsenic in natural waters. *Appl. Geochem.* **17**, 517-568.

Swartz, C. H., Blute, N. K., Badruzzman, B., Ali, A., Brabander, D., Jay, J., Besancon, J., Islam, S., Hemond, H. F., and Harvey, C. F. (2004) Mobility of arsenic in a Bangladesh aquifer: inferences from geochemical profiles, leaching data, and mineralogical characterization. *Geochim. Cosmochim. Acta*, **68**, 4539-4557.

van Geen, A., Rose, J., Thoral, S., Garnier, M., Zheng, Y., Bottero, J. Y. (2004) Decoupling of As and Fe release to Bangladesh groundwater under reducing conditions. Part II: Evidence from sediment incubations. *Geochim. Cosmochim. Acta* **68**, 3475-3486.

Yu, W. H., Harvey, C. M., and Harvey, C. F. (2003) Arsenic in groundwater in Bangladesh: A geostatistical and epidemiological framework for evaluating health effects and potential remedies. *Water Resour. Res.* **39**, 1146, doi: 10.1029/2002WR001327.

Zheng, Y., Stute, M., van Geen, A., Gavrieli, I., Dhar, R., Simpson, H. J., Schlosser, P., and Ahmed, K. M. (2004) Redox control of arsenic mobilization in Bangladesh groundwater. *Appl. Geochem.* **19**, 201-214.

3.6. FIGURE CAPTIONS

Figure 3.1. Sulfate and arsenic concentrations measured at our study site (circular and square data points; Harvey et al., 2002), and mean, median, and 90-percentile of the shallowest 2848 samples from the country-wide BGS and DPHE (2001) report (shaded areas), binned into depth intervals of ~ 200 samples each. Similar dissolved arsenic peaks have been described at other sites (McArthur et al., 2004), although the country-wide data do not display a clear peak.

Figure 3.2. X-ray fluorescent images (left panel) and corresponding XANES spectra (right panel) of arsenic-bearing grains from 30 m depth of the Holocene aquifer. Light intensity corresponds with the highest arsenic concentrations in the image (left panel) and the scale bars represent 100 μm. (A) Arsenic concentrations within the grain range from 1 to 5.6% and are distributed within sulfide complexes (as noted by the first-derivative peak maxima between 11867 and 11869 eV) . (B) A weathered As-bearing sulfide grain containing ~ 0.7% arsenic composed of 17% orpiment-like, 55% arsenite-like, and 28% arsenate-like phases. White-line positions of arsenopyrite (FeAsS), realgar (AsS), orpiment (As_2S_3), arsenite (AsO_3^{3-}), and arsenate (AsO_4^{3-}) standards are depicted at 11867 eV, 11868 eV, 11869 eV, 11871 eV, and 11874 eV.

Figure 3.3. Arsenic desorption from Holocene aquifer sediments of 30-m depth after batch incubation for 2 (black bars) or 16 days (gray bars). Arsenic is released from sediments placed in deionized water and 1.5 mM DOC (as lactate). Aqueous arsenic

concentrations are suppressed with the addition of 0.04% ferrihydrite and are below detection limits with the addition of 0.2% ferrihydrite. Agreement of nonsterile results with gamma-irradiated control experiments indicates that desorption of arsenic observed here is not controlled by biological activity—neither reduction of iron or arsenic.

Figure 3.1.

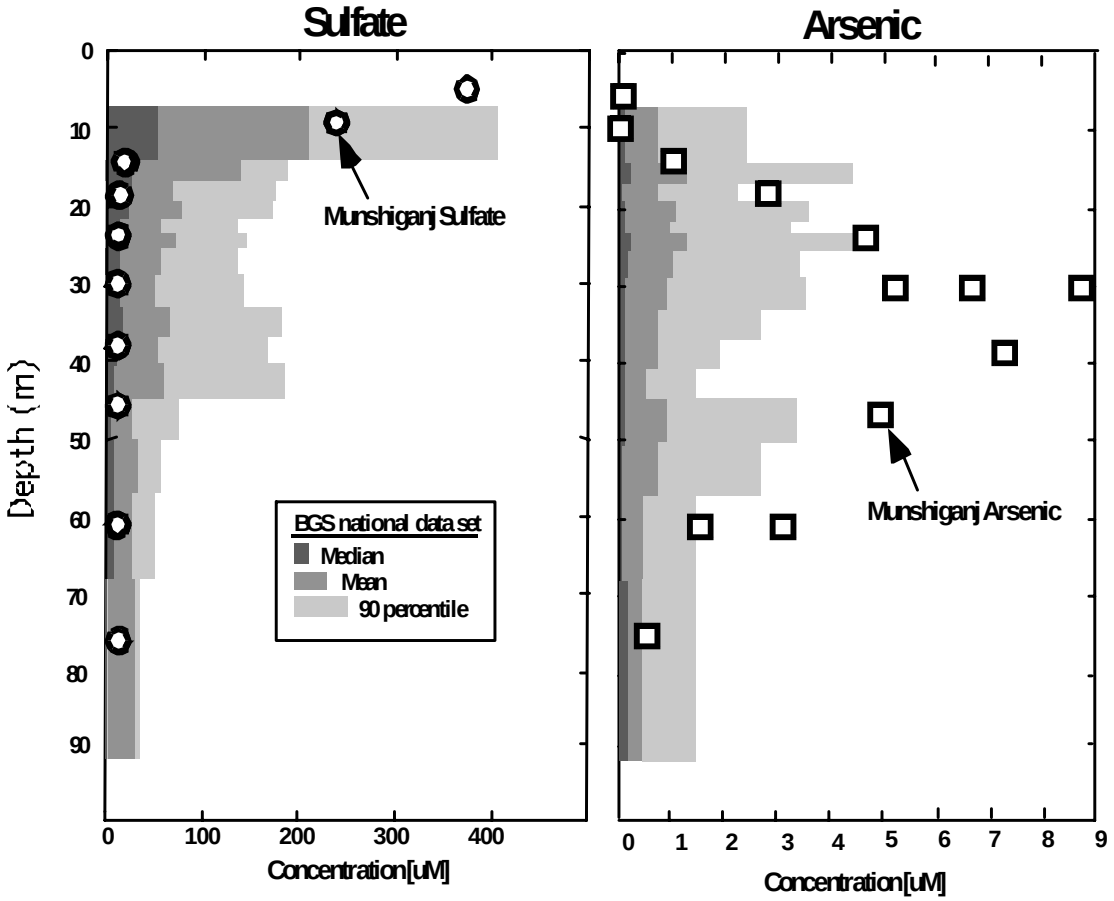
Sulfate
Arsenic
Depth (m)
0
10
20
30
40
50
60
70
80
90
Munshiganj Sulfate
BGS national data set
Median
Mean
90 percentile
0
100
200
300
400
Concentration [uM]
Munshiganj Arsenic
0
1
2
3
4
5
6
7
8
9
Concentration [uM]

Figure 3.2.

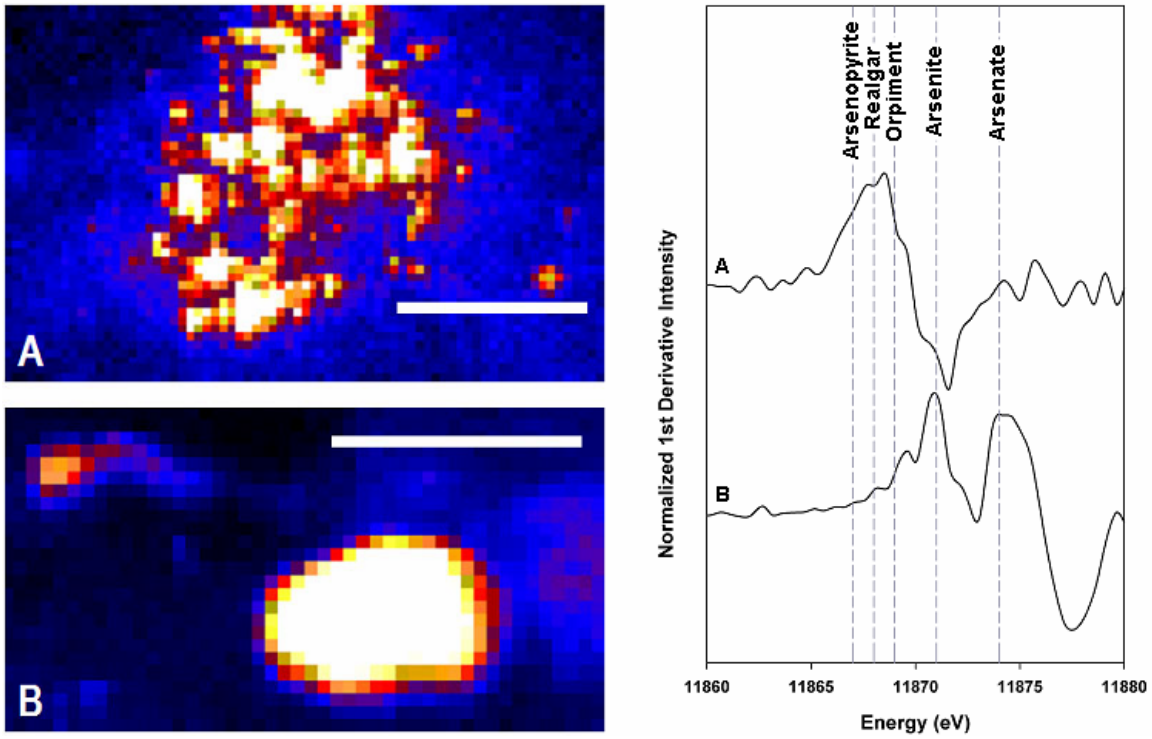
A
B
Arsenopyrite
Realgar
Orpiment
Arsenite
Arsenate
A
B
Normalized 1st Derivative Intensity
11860
11865
11870
11875
11880
Energy (eV)

Figure 3.3.

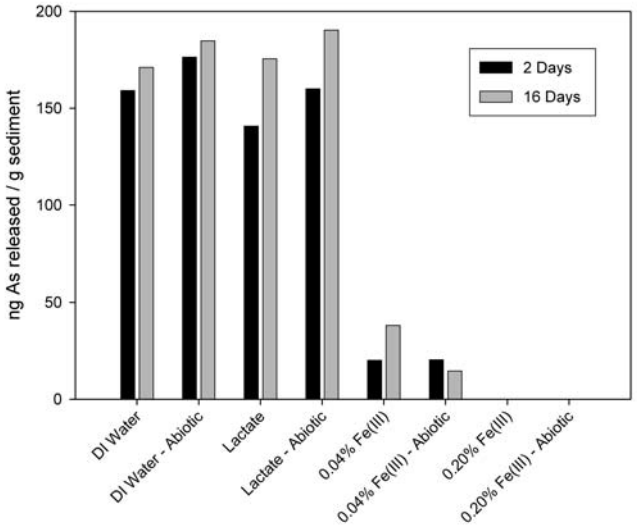
200
150
100
50
0
ng As released / g sediment
2 Days
16 Days
DI Water
DI Water - Abiotic
Lactate
Lactate - Abiotic
0.04% Fe(III)
0.04% Fe(III) - Abiotic
0.20% Fe(III)
0.20% Fe(III) - Abiotic

CHAPTER 4

Coupled Hydrologic and (Bio)geochemical Processes Controlling Arsenic Cycling in the Mekong Delta, Cambodia

ABSTRACT

The pervasive contamination of groundwater with arsenic in Southeast Asia necessitates a fundamental understanding of groundwater dynamics in the affected deltaic floodplains. Furthermore, potential links between hydrology and (bio)geochemistry need to be examined in order to understand arsenic cycling and the processes governing arsenic concentrations in groundwater. We have therefore undertaken a multifaceted study – including well installations, water level monitoring, particle size distributions, permeameter tests, slug tests, and isotopic and chemical analyses – to glean hydrologic flow and aquifer recharge information and to evaluate prevailing geochemical conditions at a field area in Cambodia. Hydraulic conductivities in the aquifer sediments are approximately 10^{-4} to 10^{-3} m/s, and those in the clay layer are 10^{-8} to 10^{-7} m/s. Variations in hydraulic gradients indicate seasonal reversals in flow directions, but net yearly flow is 1.3 m to 13 m from the aquifer to the Mekong River and 0.04 m to 0.43 m from inland surface ponds and wetlands downward to the aquifer. These yearly distances are supported by steady-state flux calculations as well as water budget analysis of wetland-pond water levels, evaporation rates, and rainfall data. Bulk aqueous chemistry supports the groundwater flux calculations, and arsenic concentration profiles illustrate arsenic transport along recharge flow paths. High arsenic concentrations are associated with high dissolved organic carbon, dissolved inorganic carbon, ammonium, ferrous iron, and phosphate concentrations in the initial portions of the flowpath (i.e., surface and near-surface soil/sediment), indicating a zone of biological activity and arsenic release; correlations diminish along the flowpath beyond the point of most prominent biological activity. Seasonal changes in near-river groundwater arsenic, ammonium, calcium,

magnesium, and sulfate concentrations are coincident with changes in flow directions. Arsenic concentrations are therefore controlled by coupled hydrological and biogeochemical processes within the aquifer, and accordingly, both factors must be assessed when evaluating arsenic in Southeast Asian groundwater.

4.1. INTRODUCTION

Use of groundwater is increasing in Cambodia, where, for generations, surface water derived water-borne diseases have inflicted the human population with numerous maladies, resulting in high infant mortality rates and low adult life expectancies. Between 1995 and 2004, groundwater tubewells increased approximately fourfold due to encouragement by the Cambodian government, international aid agencies, and NGOs (Fredericks, 2004).

Although well installations are rapidly increasing throughout the country, hydrological and geochemical knowledge about groundwater resources has advanced little, and, consequently, groundwater use often results in health risks. In particular, the occurrence of high concentrations of arsenic has slowly poisoned tens to hundreds of thousands of people, and, as in other parts of Southeast Asia where similar conditions exist, the causes for and distribution of arsenic in groundwater are not well understood. Moreover, throughout Southeast Asia, where high arsenic adversely affects as many as 100 million people (Ahmed et al., 2006), hydrologic influences on arsenic concentrations in groundwater remain unresolved (Harvey et al., 2002; van Geen et al., 2003b; Aggarwal et al., 2003; Harvey et al., 2003; McArthur et al., 2004; Harvey et al, 2006). Because human activities are strongly altering the natural hydrologic regimes of Asian deltas, resolving this issue has significant implications for effectively planning safe future groundwater use.

4.1.1. Arsenic in Southeast Asia

Within Southeast Asia, tens of millions of people routinely consume groundwater-derived drinking water with unsafe arsenic levels, while associated adverse health effects, such as arsenicosis and cancers, are increasing (Smith et al., 2000; Smedley and Kinniburgh, 2002; Yu et al., 2003; Milton et al., 2003; Ahmed et al., 2004; Berg et al., 2006; Ahmed et al., 2006). The majority of at-risk people live in rural Bangladesh and West Bengal, India where, in an effort to minimize the incidences of surface water-borne diseases, hand-pumped tubewells have been in place since the 1960s (BGS and DPHE, 2001; Chakraborti et al., 2002). Accordingly, most research concerning the causes of arsenic contamination has focused on areas of the Ganges-Brahmaputra-Meghna River system (Harvey et al., 2002; Dowlin et al., 2002; van Geen et al., 2003a; Anawar et al., 2003; McArthur et al., 2004; Islam et al., 2004; Akai et al., 2004), but unsafe groundwater arsenic concentration have also been observed in aquifers of the Mekong (Polya et al., 2003; Stanger et al., 2005; Polya et al., 2005; Berg et al., 2006; Buschmann et al., 2007) and Red River (Berg et al., 2001; Berg et al., 2006) sedimentary basins. In each contaminated basin high arsenic concentrations are found in association with reducing groundwaters. Moreover, the aquifers have similar compositions and depositional histories. They are typically characterized by thick sand units composed of eroded sediments transported from the Himalayas to the flat, low-lying alluvial basins (BGS/DHPE, 2001; Berg et al., 2001; JICA, 2002).

There is extensive debate concerning the processes responsible for hazardous arsenic levels in flood plain aquifers of Southeast Asia. There is general consensus that reduction of iron oxides and arsenic has resulted in the release of sorbed arsenic; in contrast, hydrological influences, the location of release within the vertical profile, and

anthropogenic influences on arsenic concentrations within aquifers are not resolved. It has been postulated that the microbial oxidation of carbon from sedimentary peat has fueled Fe(III) reduction at depth within the aquifer sediments (Berg et al., 2001; Dowling et al., 2002; McArthur et al., 2004; Polya et al., 2005; Buschmann et al., 2007). This model implies that human-induced hydrological perturbations (e.g. pumping, sediment excavation) have limited influence on arsenic release. It has also been suggested that arsenic liberation to porewaters via Fe(III) (and arsenic) reduction is promoted by downward migration of labile dissolved organic carbon from the surface to the aquifer (Harvey et al., 2002; Islam et al., 2004). Alternatively, arsenic liberation from soils and near-surface sediments, rather than within the aquifer sediments, and subsequent transport of dissolved arsenic to wells has also been proposed (Polizzotto et al., 2005).

Resolving the relative importance of these disparate mechanisms has proven difficult in Bangladesh for many reasons. Most prominently, pervasive groundwater pumping for irrigation has distorted the natural hydrology of the system (Harvey et al., 2002; Harvey et al., 2003; Harvey et al., 2006; Klump et al., 2006), and thus discerning groundwater flow and solute transport is challenging. Accordingly, arsenic concentrations are spatially variant over the scales of 100s of meters (van Geen et al., 2003a), and therefore deciphering chemical profiles along flowpaths is challenging. Finally, because wells have been installed in Bangladesh over the last 40 years but groundwater has been tested for arsenic only over the past 15 years, it is unknown to what extent anthropogenic perturbations have affected arsenic contamination (Harvey et al., 2002; Harvey et al., 2003; Aggarwal et al., 2003; van Geen et al., 2003b; McArthur et al., 2004; Harvey et al., 2006; Klump et al., 2006).

4.1.2. Hydrogeology of the Mekong River Delta

Cambodia is an ideal location to understand natural hydrological processes due to the lack of groundwater pumping for irrigation; additionally, the majority of wells that are in place have been installed within the past ten years and are used primarily for domestic use (Fredericks, 2004). Whereas groundwater pumping for irrigation is pervasive in many other countries of Southeast Asia, which may alter the hydrology of the river basins, Cambodia has one of the lowest irrigation water uses of any country in the region (Haddeland et al., 2006). Furthermore, studies of hydrologic and biogeochemical processes influencing groundwater composition are needed not only to understand arsenic contamination, but also to provide valuable information for future development and changes in land use.

Previous studies of groundwater in the Cambodian Mekong River Delta have provided valuable aquifer physical parameters. In the 1960s, the USGS engaged in a widespread project to evaluate groundwater resources in Cambodia through a USAID well-drilling program; the group analyzed well logs and determined yields, but the project was abruptly terminated in 1963 (Rasmussen and Bradford, 1977). The Japanese International Cooperation Agency (JICA, 2002) installed 1 to 5 wells per province in southern Cambodia and determined aquifer thickness, storativity, transmissivity, and hydraulic conductivity values; though wells were monitored yearly, the study examined individual wells over a large region, with 1 well per ~900 km^2, and wells were not spatially connected. Their focus was on static aquifer properties and individual well variations rather than groundwater flow, but their results demonstrate variations in

aquifer characteristics between wells. The paucity of spatially connected temporal water level data implicates the need for information concerning changing gradients and studies analyzing groundwater flow.

4.1.3. Resolving Arsenic Cycling in the Mekong Delta

Here we apply a multifaceted approach to characterize sediment stratigraphy, groundwater flow, and aqueous chemistry from a field area within the upper Mekong River Delta of Cambodia. Field and laboratory experiments, in concert with hydraulic gradients, allow us to determine net annual groundwater fluxes. Based upon routine groundwater and surface water sampling data, we examine spatial and temporal geochemical patterns, and reveal how they have been influenced by flow patterns. From our results we conclude that arsenic fate and transport within the surface and subsurface is controlled by coupled hydrological and biogeochemical processes, including liberation from sediments at recharge zones and transport by groundwater through the aquifer.

4.2. METHODS

4.2.1. Field Area

Our field site within the Mekong Delta is ~ 50 km^2 and located 20 km southeast of Phnom Penh in the Kandal Province of Cambodia. We have installed wells to monitor heads and groundwater chemistry, measured surface water chemistry and water levels, and collected sediment samples. A spatial key of well and sediment sample locations is shown in Figure 4.1. Well drilling, sediment collection, and water sampling methods are reported in Chapter 5 of this thesis. For each well drilled, core logs were obtained from

the displaced sediments. At select locations (Figures 4.1 and 4.2), preserved sediments were obtained in separate boreholes and the sedimentary profiles based on these collected samples were compared to those from the drill cuttings. In each case, the two profiles matched, although the collected samples gave more detail.

The subsurface within our field area is generally comprised of thick clay overlying sandy aquifer sediments. The clays separate inland ponds and wetlands from the aquifer. Fluctuations in water levels at our field area result in changing river-aquifer and pond-aquifer hydraulic gradients; during the wet season, flow directions are from the Mekong River to the aquifer to ponds and wetlands, but during the dry season these directions reverse and flow is from the ponds to the aquifer to the Mekong River (Figure 4.1 and Chapter 5). Within our field area, groundwater hydraulic gradients are impacted minimally by human land use practices and are therefore naturally derived. Until now, gradients and groundwater flow distances have not been quantified due to a lack of physical parameters.

4.2.2. Hydraulic Conductivities

4.2.2.1. Particle Size Analysis

Particle size separation was performed on aquifer sand samples in order to calculate hydraulic conductivity values. Prior to sieving, samples were dried in an anaerobic glove box. A known weight of each sediment sample was passed through sieves with openings of 0.707 mm, 0.5 mm, 0.354 mm, 0.25 mm, 0.177 mm, 0.125 mm, 0.088 mm, and 0.065 mm. Values for d_{10} and d_{60} – the grain sizes for which 10% and

60%, respectively, of the total grains are finer – were determined, and the uniformity coefficient, U, was computed as d_{60}/d_{10}.

On the basis of d_{10} and U values for the set of sediments, two methods were used to calculate hydraulic conductivities (K) from particle sizes. The Hazen method (Hazen, 1911; Kresic, 1997) is appropriate for well sorted samples with $U < 5$ and with $0.1 \text{ mm} < d_{10} < 3 \text{ mm}$. Based on the Hazen equation, $K = (g/v)C_h f(n) d_{10}^2$, where $C_h = 6x10^{-4}$, f(n) is a function of porosity (n) and f(n) = [1+10(n-0.26)], g is the gravitational constant, and v is the kinematic viscosity. For these analyses, n was varied from 0.2 to 0.3, and thus f(n) ranged from 0.4 to 1.4.

The Breyer method is used for heterogeneous samples with $1 < U < 20$ and $0.06 \text{ mm} < d_{10} < 0.6 \text{ mm}$. Hydraulic conductivities are computed by $K = (g/v)C_b d_{10}^2$, with $C_b = 6x10^{-4}\log(500/U)$ (Kresic, 1997).

4.2.2.2 Tidal Dampening of Water Levels

Water levels of the Mekong River and groundwater wells were monitored with Level Troll 500 and 700 pressure transducers (In-Situ Inc., USA). Transducers were secured > 2 m below the water surface and depths were recorded in one-minute intervals.

The propagation of the tidal signal from the Mekong source was used to calculate field-scale hydraulic conductivity values of the aquifer. Calculations were performed as developed by Ferris (1951) and utilized in Millham and Howes (1995), based on the proportion of amplitude dampening and time lag compared to the well distance from the Mekong River. Amplitude dampening is calculated by $H_x = H_o \exp[-x(\pi S/t_o T)^{0.5}]$, where H_o is the amplitude of the tidal source, H_x is the amplitude at a distance x, S is the aquifer

storativity, t_o is the tidal period, and T is the aquifer transmissivity. The time lag is calculated by $t_T = x(t_oS/4\pi T)^{0.5}$ where t_T is the time lag in the periodic tidal signal at distance x. Because K = T/b, where b is the aquifer thickness, for each equation, K can be calculated as a function of S and b. Thus the storativity and aquifer thickness values were varied in order to constrain a range of potential hydraulic conductivity values for the aquifer. Storativity values were varied from 0.01 to 0.2, based on single borehole tests within the Kandal province (JICA, 2002) and consistent with those for sandy aquifers. Aquifer thickness was ranged from 40 m, the depth of bedrock at one well location, to 100 m, approximately the maximum observed aquifer thickness in area boreholes (JICA, 2002).

In order to obtain field data, water levels in wells were monitored for > 4 tidal cycles coinciding with Mekong River water level measurements. Tidal amplitudes, tidal periods, and time lag data were averaged for the span of the measurements to provide parameters for hydraulic conductivity calculations.

4.2.2.3 Constant Head Permeameters

Constant head permeameter tests were performed on samples from the upper clay layer, with depths ranging from 6 m to 18 m, in order to calculate hydraulic conductivity values. Samples were dried in an anaerobic glove box and then packed into sealed flow cells, with lengths of 3.3 cm and cross-sectional areas of 24 cm^2. From a constant height, water was added to the bottom of the flow cell and allowed to flow upward. Flow was monitored and hydraulic conductivity values were calculated as K = QL/Ah, where Q is the flow rate, L is the sample length, A is the cross-sectional area, and h is the constant

head (Domenico and Schwartz, 1998). For each sample, the test was repeated with 3 to 6 different heads of pressure; for each trial at all depths at each site, results were within one order of magnitude of the average hydraulic conductivity.

4.2.2.4 Slug Tests

Slug displacement tests were performed on shallow (8-12 m) wells throughout the field site. Static water levels were measured and then a slug with a volume of 120 cm^3 or 260 cm^3 was dropped into the well. The initial displacement was measured and the falling head was monitored over time as the water level dropped back to equilibrium. Once equilibration was obtained, the slug was removed and the resulting rising head was monitored over time. The falling head and rising head tests were analyzed according to Hvorslev (1951), with $K = [r^2 \ln(L/R)/(2L(t_2-t_1))]\ln(H_1/H_2)$, where K is the hydraulic conductivity, r is the well casing radius, R is the radius of the gravel-packed well screen, L is the length of the well screen, and H_n is the head at time n (t_n). This method is applicable for $L/R > 8$, a quantity surpassed for each of the wells. The resulting K values for the falling head and rising head tests were typically within a factor of 2 from each other.

4.2.3. Flux Calculations

In order to determine net heads between wells and surface water bodies, water level hydrographs were interpolated in *Mathematica 5.2* (Wolfram Research, Inc., IL, USA) and the resulting function was integrated over one year. To determine groundwater flow distances between two points, data from weekly water level measurements were

interpolated and used in Darcy's Law with typical porosity values (0.2 for the aquifer and 0.5 for the clay; Domenico and Schwartz, 1998) to obtain daily groundwater flow distances; these were summed over one year.

4.2.4. Water Budget

Floating pans were deployed in ponds to measure evaporation. Rain-corrected evaporation was measured weekly and pans were subsequently refilled to a reference point. Temperature was monitored inside and outside the pans with Hobo temperature loggers; these temperatures were typically equivalent, indicating that measured evaporation and actual pond evaporation were comparable. Pan evaporation measurements of surface ponds are typically greater than evapotranspiration (ET) rates (Fetter, 2001), so our measurements constrain the maximum ET. Daily rainfall data were obtained from three Mekong River Commission rain gauge sites surrounding our field area. Weekly and monthly rainfall averages, maximums, and minimums were applied to our field area to help constrain the water budget. Infiltration and runoff were calculated by subtracting rainfall and ET from dry season pond drawdown rates.

4.2.5. Tritium and ^{14}C Dating. Age-dating of ^{3}H and ^{14}C in dissolved inorganic carbon was conducted at the University of Waterloo Environmental Isotope Laboratory.

4.3. RESULTS AND DISCUSSION

4.3.1. Physical Characterization of Field Area

4.3.1.1. Regional Topography

The regional topography on the Mekong Delta in Cambodia is gently sloped: the elevation at the field site is < 10 m above sea level, despite that the ocean coastline is > 250 km downstream. However, elevation variations perpendicular to the river are much more pronounced. As in most natural deltaic systems, the local topography is inverted, and surface elevations along riverbank levees are typically > 3 to 4 m higher than the inland wetland-occupied basins.

4.3.1.2. Sedimentary Profile

Sedimentary stratigraphy throughout the site is characterized by a clay-rich upper zone of underlain by a sand-rich lower zone (location of most drinking water tubewells). Sediments typically exhibit more reducing characteristics with depth (orange to grey) and tend towards finer material with distance from the river. General stratigraphic similarities in well cores are depicted in Figure 4.2 with white ovals, and these follow surface manifestations of historical river migration. Similar profiles are observed below the current river bank, adjacent to the oxbow lakes, and along previous riverbank levees. The bottom panel in Figure 4.2 shows a sedimentary cross-sectional profile from the Mekong River to the interior wetlands, based on the collected sediment cores.

Generally, textural and color transitions characterize near-surface sediments. Clayey sediments ubiquitously confine the aquifer sands throughout the field area. The uppermost sediments are red/brown in color while deeper sediments are typically grey, reflecting current redox conditions as well as those present during deposition. Generally, the red/brown sediments are oxidized and the grey sediments are reduced.

The primary water-producing fine, grey sand aquifer at the field site typically extends to > 60 m depth and is overlain by a 6-20 m clay unit (Figure 4.2). The lower portion of the clay unit is grey in color and contains abundant wood and organic material. The grey clay and grey sand are interpreted to represent an historic coastal beach and swamp depositional environment along a prograding coastline from ca. 6000 years ago (Nguyen, et al., 2000; Ta et al., 2002). These older units are overlain by red and grey clay overbank deposits, reflecting the current terrestrial deltaic depositional system. The overbank deposits are thickest adjacent to oxbow lakes, where natural levees have formed, and thin inland, where lower-elevation, variably-saturated wetlands dominate the landscape.

This generalized sedimentary profile has several discontinuous features, as depicted in Figure 4.2. Large conglomerates of woody debris were observed in the grey clays, but smaller pieces (< 0.5 cm) of woody tissue were also found in the top portion of the grey sands adjacent to the Mekong River; large peat deposits were not observed within the field site. In the northwestern part of our field area, and underneath an island in the Mekong, a grey clay layer exists at ~ 40 m. The sedimentary package typically coarsens downward to medium grey sands, and pebbles with diameters > 1 cm were collected between 40 and 45 m at sediment collection sites adjacent to the Mekong and Bassac Rivers. In the center of the wetlands, bedrock was encountered below grey sands at 40 m. Additionally, near the Mekong, the red-grey (oxidized-reduced) transition in sediments occurs in sand rather than clay. Finally, at wells adjacent to abandoned river channel oxbows, the clay-sand transition is characterized by a zone of thin, alternating clay and sand lenses up to 30 m depth.

4.3.1.3. Hydraulic Properties

Steep vertical gradients across the upper clay unit, combined with seasonally observed flowing wells, indicate that the sand aquifer is confined by overlying clay aquitard. Hydraulic conductivity values for the aquifer sand and upper clay aquitard sediments were each determined with one laboratory and one field methods. Hydraulic conductivities for the aquifer sand sediments were calculated based on the results of particle size analyses and tidal wave propagation in water levels. Constant head permeameter tests and slug tests were used to determine K of the clays. The employment of two techniques allows for a range of hydraulic conductivities to be obtained; while laboratory investigations are more easily controlled, the field methods account for heterogeneities in the sediments and flowpaths that are removed in the small sample sizes of the laboratory tests.

4.3.1.3.1. Particle Size Analysis of Aquifer Sediments. Two groups of sediments are apparent on the basis of grain-size analysis (Figure 4.3), those with $d_{10} < 0.2$ mm and those with $d_{10} > 0.2$ mm. The former group is representative of the fine to medium sands that dominate the aquifer; these samples are well sorted and as a group have small d_{10} and d_{60} ranges, despite being obtained from a variety of locations and depths throughout the field area. The latter group is composed of unique samples that were obtained at sites adjacent to the Mekong and Bassac Rivers. These samples are from layers and lenses of coarser sands.

Uniformity values are typically < 5, suggesting that the sediment samples are well-sorted, though calculations of U are not possible for the four coarse sand samples since their d_{60} grain sizes are unknown (Table 4.1). Both Hazen and Breyer hydraulic conductivities (Table 4.1) are in the range of fine to medium sands (Domenico and Schwartz, 1998). Breyer and Hazen values are within the same order of magnitude; however, Breyer hydraulic conductivities are preferable for fine and medium sands, while Hazen values are best for coarse sand samples (TH11-39, TE11-36, TE11-45, and BD11-45).

The fine and medium sand hydraulic conductivities are within approximately one order of magnitude, suggesting that the aquifer is relatively uniform with a hydraulic conductivity of ~ 10^{-4} m/s, but coarser sand zones having ten times the typical aquifer hydraulic conductivity (> 10^{-3} m/s) are noted.

4.3.1.3.2. Aquifer Hydraulic Conductivity from Tidal Signal Dampening. The Mekong River is tidal, with an average amplitude of 0.091 m (Table 4.2). A pressure wave propagates into the aquifer, which influences water levels in groundwater wells as a result of the tidal changes in river level. Wells screened in the aquifer sands exhibit daily fluctuating water levels in accordance with Mekong fluctuations (Figure 4.4), although these tidal signals are not observed in inland surface water or wells screened within the surficial clay. The Mekong River tidal period is 0.541 days. Wells adjacent to the Mekong (TH11 and TC11) exhibit tidal fluctuations with amplitude and timing more similar to those of the river, but as distance from the Mekong River increases (TC31 and

TC51), tidal amplitudes are dampened and occur longer after similar Mekong water level peaks (Figure 4.4).

For each set of S and b values determined from field measurement, K varies by approximately one order of magnitude for the four sites, with calculated hydraulic conductivities increasing with distance from the Mekong River (Table 4.2). Additionally, the average K values for the sets of S and b are between $1.7x10^{-3}$ m/s and $8.6x10^{-2}$ m/s, values 1 to 2 orders of magnitude greater than the hydraulic conductivities calculated from grain size analyses and indicative of coarse sand and gravel rather than fine and medium sands. Horizontal flow in sedimentary aquifers is primarily dominated by the most hydraulically conductive layers. Therefore, it would be expected that the hydraulic conductivities calculated by tidal dampening would likely be most consistent with the grain size analysis-based values for the coursest materials; that is what is observed here.

4.3.1.3.3. Constant Head Permeameter Tests of Near-Surface Clay Aquitard Sediments. Average clay layer hydraulic conductivity values obtained from constant head permeameter tests span three orders of magnitude (10^{-6}-10^{-9} m/s) across the entire field site (Table 4.3) and are consistent with silt to clay dominated sediments. These values, however, are distinguished by site type and location with respect to the Mekong and Bassac Rivers. Near-river samples – TH11, TE11, and BD11 – have hydraulic conductivities from 10^{-7} m/s to 10^{-6} m/s, values typical of silt-dominated samples (Domenico & Schwartz, 1998). As is typical for river systems, the upper floodplain sediments become finer moving progressively away from the river; hydraulic

conductivity values in wetland and abandoned oxbow ponds of the TC51, RDI well, and PE31 samples range from 10^{-9} m/s to 10^{-8} m/s.

4.3.1.3.4. Slug Tests of Shallow Wells. Average clay layer hydraulic conductivity values obtained from the falling head and rising head slug tests range from $8.6x10^{-8}$ m/s to $7.1x10^{-6}$ m/s (Table 4.4), also indicating clay and silt-dominated sediments. Slug test values approximately span the same range as the permeameter values but do not show a consistent spatial variation. The slug tests account for a greater volume of sediment in comparison to permeameter tests, and also encompass sediment structure and preferential flow paths. Because structural features often control flow through aquitards, the slug test values are likely a better estimate of field hydraulic conductivity values than laboratory based permeameter based values.

4.3.1.4. Groundwater Fluxes and Water Budget

Evaporation pan and rainfall data, in combination with recharge fluxes emanating from oxbow ponds, allow us to calculate average monthly water budgets for the inland oxbow ponds and wetlands during pond drawdown (Figure 4.5). In most months, surface water drawdown cannot be explained by maximum evapotranspiration minus rainfall alone, and thus infiltration and runoff play important roles in the pond water budget. The surface water network is controlled by flood gates, most notably in the wet season (August through October) when gates are opened and water flows into the basins from the rivers, resulting in rapidly increasing levels. The average infiltration plus runoff rate is 2.7 mm d^{-1} during drawdown. While this value does not constrain the minimum

amount of recharge, it does indicate that a significant amount of water is available for recharge.

Because flow is primarily vertical through aquitards and horizontal within aquifers, it is convenient to divide flux calculations accordingly. Although horizontal hydraulic gradients invert seasonally within the aquifer, net annual flow of groundwater is from the aquifer to the rivers (Table 4.5). Based on particle size analyses and water level response to tidal fluctuations, aquifer hydraulic conductivities are approximately 10^{-4} to 10^{-3} m/s (Tables 4.1 and 4.2). Using these values in Darcy's Law and analyzing multiple well-river head differences, the average net groundwater flow for March 2005 to March 2006 at our field site is 1.3 to 13 m. However, because of seasonal gradient reversals, groundwater flows 13 to 125 m from the aquifer towards the Mekong River in the dry season, but 11 to 113 m from the river to the aquifer during the wet season. These seasonal changes in flow have important implications for groundwater chemistry.

Like the underlying aquifer, vertical gradients across the aquitard invert annually, however the net annual gradient between the inland surface waters and the underlying aquifer is downward. Abandoned oxbows are connected in a network of ponds and sit above our wells at TH51, TE51, TC31, and TC45. However, because aquifer wells at TH51, TE51, and TC31 become artesian during the wet season, complete hydrographs were not obtainable. By using head hydrographs from TC45 and nearby wells TH31 and TC21, groundwater flow distances were estimated (Table 4.5). Hydraulic conductivities of 10^{-8} to 10^{-7} m/s (Tables 4.3 and 4.4) result in net flows of 0.04 to 0.4 m from the ponds to the aquifer, with 0.05 to 0.5 m downward flow in the dry season and 0.01 to 0.1 m upward flow during the wet season. Based on 0.5 m of total flow from the surface water

to the aquifer during the wet season, 1.4 mm of water infiltrates per day, a value that is supported by the water budget calculations.

Given our field area of ~ 6 km width and an aquifer thickness of 50 m, a cross-sectional aquifer area perpendicular to groundwater flow (parallel to the Mekong River) is $3x10^5$ m^2. With a net annual groundwater flow distance of 10 m, the net groundwater flux is $3x10^6$ m^3 y^{-1}. Our fieldsite is ~ 50 km^2 and if groundwater recharge is evenly distributed across this area, annual downward flow of 0.06 m y^{-1} maintains steady-state fluxes from the surface to the groundwater to the Mekong River. This value is within our range of calculated downward flow based on annual head differences. Recharge, however, is not evenly distributed across the entire field area but is restricted to oxbow ponds and wetlands; accordingly, the downward flow would be higher than 0.06 m yr^{-1}, perhaps approaching 0.4 m y^{-1}, the upper range of our calculations.

Isotopic measurements of groundwater samples support groundwater flux calculations and help to refine potential flow paths. Carbon-14 dating of dissolved inorganic carbon (DIC) indicates groundwater < 2,000 years old throughout the aquifer (Table 4.6), and given that the aquifer sediments were deposited > 6,000 years ago (Ta et al., 2002), the aquifer has been flushed multiple times by groundwater flow. DIC is youngest at TC11-25 with an age that is > 100% modern (Table 4.6). The next youngest groundwater samples are from TH11-37 and TC11-57, wells that are also next to the Mekong River. This suggests flow from the Mekong River into the aquifer. Because these samples were obtained towards the end of the wet season, they were collected near the peak of seasonal inflow. Groundwater flow calculations (with K = 10^{-3} m/s, Table 4.5) demonstrate that despite a net annual outflow to the river, river water may flow into

the aquifer over 100 m during the wet season, hence explaining the young ^{14}C ages we observe in wells near the Mekong River.

Dissolved inorganic carbon ^{14}C is older in wells adjacent to the wetlands (TC51) than wells next to abandoned oxbow ponds (TC31). This suggests either a chemical factor overriding net hydrological flow to the river or a hydraulic discontinuity between the ponds and wetlands. Indeed, aquifer heads in wells between the oxbow ponds and the Mekong River (e.g. TC11, TC21, TC31, TE11, TE51, TH11, TH31, and TH51) span a small range at any time point (Figure 1), but are much different than in wells inland of the oxbow ponds (e.g. TC45, TC51, TH71, PE51, and PW31), supporting the probability of a hydraulic discontinuity. Tritium was detectable (> 0.8 TU) in only two of seven well water samples examined in September and October, 2005: 26 m depth at wetland site TC51 (1.6 TU) and 25 m depth at TC11 adjacent to the Mekong River (1.9 TU).

Based on the minimum clay layer thickness (6 m) and maximum downward flow rates (0.4 m y^{-1}), surface water may reach the upper portion of the aquifer in as little as 15 y. While some flow lines may be altered by hydraulic discontinuities, annually, groundwater recharges from wetlands and ponds and discharges to rivers at our field site. Surface water infiltrates the near-surface clay layer and flows downward into the aquifer during the dry season, although flow directions temporarily reverse during the wet season. These flow analyses help describe aqueous chemical concentrations, including those of arsenic, within groundwater.

4.3.2. Aqueous Chemistry

4.3.2.1. Chemical Concentrations in Surface Water, Shallow Pore Water, and Aquifer Well Water

Arsenic concentrations are high throughout the aquifer and fewer than 10% of our installed wells (7 of 80 wells) have arsenic below the World Health Organization recommended standard of 10 $\mu g\ L^{-1}$. Groundwater arsenic concentrations in aquifer and shallow wells vary considerably across the field area and span a range of 0 to 1300 $\mu g\ L^{-1}$ (Figure 4.6A), similar to conditions reported elsewhere throughout Southeast Asia (BGS and DHPE, 2001; Berg et al., 2001; Smedley and Kinniburgh, 2002; van Geen et al., 2003a; Polya et al., 2005). Dissolved arsenic is typically found (> 80%) as the reduced arsenite species. Wells with As < 10 $\mu g\ L^{-1}$ are shallow wells (< 12 m depths) screened in surficial clay layers that are not productive for domestic use. Not all shallow wells, however, exhibit low arsenic concentrations; shallow wells adjacent to permanently saturated inland water bodies, such as oxbows of abandoned river channels (As concentrations ranging from 100 to 450 $\mu g\ L^{-1}$) and the central wetlands at well PE51 (As concentrations of up to 900 $\mu g\ L^{-1}$), have notably high arsenic concentrations. Aqueous arsenic concentrations do not obviously appear to correlate with solid-phase concentrations, which are at background levels (< 5 mg/Kg) in the aquifer sands and only slightly higher (< 12 mg/Kg) in the clays.

In addition to arsenic variations, the major ion compositions of aquifer groundwaters, shallow well waters (screened in clay), and surface waters are each chemically distinct from one another (Figure 4.7). Surface waters, including the rivers and wetlands, have a uniform bulk cation composition, indicating that there is little chemical change as river water floods the interior water bodies. A coupled decrease in

Ca^{2+} % and increase in $\{Na^{+} + K^{+}\}$ % support hydraulic flow from the surface to the aquifer (Table 4.7). Anionic charge in all water bodies is dominated by bicarbonate, with lesser concentrations of chloride and sulfate. Anionic composition is relatively uniform in the surface water, and the existing scatter is due to temporal variations between sampling (November, 2005 to February, 2006) rather than spatial variations. Aquifer wells have the highest bicarbonate percentages and the lowest sulfate, owing to anaerobic bacterial metabolism. Shallow wells typically have the lowest HCO_3^- percentages and highest SO_4^{2-} and Cl^- percentages (three shallow well data points in Figure 4.7 with HCO_3^- % > 85% are likely due to shallow wells that were partially screened within the aquifer).

Organic carbon is present in both the solid-phase sediments and in the aqueous phase. Dissolved organic carbon (DOC) concentrations in surface water are higher than those in the shallow wells, and then increase further in deeper well waters (average DOC in groundwater 6.9 mg/L) (Table 4.8). Sedimentary organic carbon was most notably observed at the bottom of the clay layers as dark bands and pieces of wood from historic mangrove swamps. While thick peat deposits were not observed within the aquifer sands, dispersed organic carbon is likely omnipresent at ~ 0.5-1%, as reported for Holocene sands in other areas of Southeast Asia (Swartz et al., 2004; McArthur et al., 2004). Increases in DOC concentration between the swallow and deep wells indicate that remnant detrital carbon continues to dissolve into passing waters.

Average dissolved inorganic carbon (DIC) concentrations increase from the surface water to the shallow wells, indicating carbon degradation in surface soils. Importantly, and in contrast to DOC profiles, DIC diminishes slightly in groundwater

(Table 4.8). The decrease in average concentration between the shallow wells and aquifer wells mimics the trend in bulk ions, including Ca^{2+} and Mg^{2+}. An increase in DOC but decrease in DIC in going from shallow to deeper wells indicates that recalcitrant solid phase organic carbon is continuing to dissolve into the aqueous phase and that bicarbonate and Ca and Mg are sorbing (adsorbing on mineral surfaces or precipitating) within the aquifer.

Across the set of shallow and aquifer wells, dissolved ammonium correlates strongly (R^2 = 0.7) with DOC (Figure 4.8), indicating that similar processes influence both species. Under the more reducing conditions of the aquifer, ammonium concentrations average 20 mg/L; they are 6.4 mg/L in the shallow wells, and are 0.8 mg/L in surface water. Ammonium is most likely produced as a product of microbial DOC oxidation, leading to the strong correlation between NH_4^+ and DOC, and indicating that where DOC and NH_4^+ are high, respiration has transpired (possibly at an upstream location, however). Dissolved phosphate is also highest in the aquifer and lowest in the surface water, suggesting that it too is liberated from solid phase organic matter. Nitrate is highest in the shallow wells with concentrations two orders of magnitude greater than in the surface water and aquifer well samples. Therefore nitrate is derived presumably via nitrification within soils and then consumed/removed, primarily by denitrification and possibly by assimilation, at deeper depths.

4.3.2.2. Spatial Variations in Chemical Concentrations

Hand-contoured cross-sectional spatial aqueous concentration profiles between the wetlands and Mekong River are depicted in Figure 4.6. Arsenic concentrations are

highest below the inland oxbow ponds and trend downward towards the Mekong River. The highest DOC, ammonium, DIC, phosphate, and ferrous iron concentrations are also found immediately below the ponds, although the spatial distributions differ slightly in other areas throughout the profile. Thus, chemical indicators of microbial processes are highest below the ponds, indicating enhanced biological activity at recharge zones.

Recharge zones, therefore, appear to be a source area for dissolved arsenic, DOC, ammonium, DIC, phosphate, and ferrous iron. Within the aquifer, arsenic exists as arsenite, its more mobile form particularly in silicate-dominated sediments. Consequently, high arsenic concentrations are maintained along flow paths between recharge and discharge zones. However, concentrations of DOC, ammonium, DIC, phosphate, and ferrous iron decline with distance from the zone of recharge, presumably as a result of varying reactivities of each species. Dissolved organic carbon may be further consumed during other microbial processes in the aquifer, or, more consistent with other chemical values, it may flocculate and partition back to the solid phase. Ferrous iron, phosphate, and DIC may precipitate as metal carbonate and phosphate phases; siderite, vivianite, and calcite (among other minerals) are typically at or above saturation within the aquifer. Dissolved inorganic carbon may also be consumed during methanogenesis. Additionally, each species sorbs to minerals and organic matter with different strengths. Finally, some species, such as DOC, may have alternate sources within other portions of the aquifer, thereby convoluting spatial trends. As a result, chemical profiles vary along flow paths further from recharge zones.

4.3.2.3. Seasonal Variations in Chemical Concentrations

Shifting hydraulic gradients also lead to temporal variations in aqueous concentrations. In particular, the variations are most notable at reservoir boundaries. Seasonal changes in surface water chemistry, coupled with infiltration and river water inflow, impact groundwater concentrations.

Interior ponds and wetlands of the basins are rapidly filled each year from river water inflow and local rains. River water enters during high stage levels when the river can breach the banks; inward flow is through natural channels, which, in some instances, are controlled by flood gates. Main channels can be > 5 m deep during high water stages. During the dry season, water levels drop due to evapotranspiration, infiltration, and runoff.

Aqueous concentrations of major cations and anions in surface waters of the basins (ponds and wetlands) are typically higher than those in rivers. Pond and wetland dissolved Cl^- (Figure 4.9A), SO_4^{2-}, HCO_3^-, Ca^{2+}, and Na^+ levels reach a maximum immediately prior to river water inflow, but then drop rapidly to river concentrations. Upon the onset of the dry season, major cation and anion levels increase due to evaporative concentration, as evidenced by $\delta^{18}O$ profiles (Figure 4.9B), and supported by net hydraulic gradients indicative of downward flow of surface water, thereby minimizing the possibility of a soil weathering source. Evaporative concentration in interior surface water is most appreciable in the summer during the hottest and driest months and when water levels are at their yearly minimum.

River chemistry concentrations also fluctuate during the year, although the magnitude of these changes is much less than in the interior surface waters. River concentrations exhibit evaporative concentration during the dry season when regional

gradients are smallest and the river is relatively stagnant. However, because river levels and regional gradients are controlled by Himalayan snowmelt and upstream monsoonal rainfall, rapid increase in river stage levels and subsequent chemical dilution occurs earlier than in the ponds and wetlands.

Within the aquifer, temporal variations in groundwater chemistry are most dramatic in wells near the Mekong River, reflecting the importance of groundwater movement on geochemistry. Arsenic concentrations from 25 m and 51 m depth at site TC11 are highest during the dry season, when flow is from the aquifer to the river; concentrations drop when the river is flowing into the aquifer (Figure 4.10). Because river water may flow > 100 m into the aquifer during the wet season, aqueous concentrations are impacted. The trends in arsenic are positively correlated with NH_4^+ and negatively with Ca, Mg, and S (SO_4^{2-}).

4.3.3. Coupled Processes Controlling Arsenic in the Subsurface

Arsenic is liberated to the aqueous solution in the surface or near-surface environment and then transported through the aquifer by groundwater flow. The concentration profile of arsenic (Figure 4.6) is indicative of highly mobile arsenic throughout much of the aquifer, rather than solely at wells TC11-25 and TC11-57. Arsenic concentrations of > 900 μg/L are maintained over kilometers and, within our field area, trend up from the river to the inland, oxbow ponds. Below the oxbow ponds, high arsenic concentrations are associated with some of the highest DOC, NH_4^+, DIC, Fe^{2+}, and PO_4^{3-} concentrations, all factors consistent with active microbial reduction and iron reduction. Moreover, arsenic release to the aqueous phase from the upper 4 m of

sediments near the oxbow ponds has been observed during seasonal times of downward groundwater flow (Chapter 5), further indicating that the area is a source of arsenic to the aquifer. The fact that spatial concentration profiles for DOC, NH_4^+, DIC, Fe^{2+}, and PO_4^{3-} do not coincide with that of arsenic further from recharge zones is likely a result of different precipitation and biotic reactivities along the flow path. In the absence of Fe (hydr)oxides in the aquifer, arsenite is the least reactive and most easily transported. Moreover, given the age of the aquifer and groundwater residence times, dissolved arsenic must be transported into the aquifer with groundwater recharge.

The decrease in arsenic concentrations at wells TC11-25 and TC11-57 during the wet season suggests that the river or river-aquifer interface are not source areas for arsenic, since flow from the river to the aquifer corresponds to a decrease in dissolved arsenic. Arsenic is derived, then, from an upgradient source, a condition that has allowed dissolved arsenic to remain in the aquifer despite net groundwater flow from the aquifer to the river. The rapid response of arsenic to changes in groundwater flow direction at the aquifer near the river suggests that arsenic is mobile (limited retardation) within at least the grey aquifer sands. Similar observations have also been noted in laboratory investigations of arsenic desorption from Bangladeshi aquifer sediments (Polizzotto et al., 2005).

If arsenic is released by the reductive dissolution of Fe (hydr)oxides, and if this process is fueled by the oxidation of sedimentary organic matter (McArthur et al., 2004), the results of this process are masked by the overriding importance of arsenic transport. Hydraulically, the buildup of arsenic in groundwater solely due to reductive dissolution requires relatively stagnant groundwater; such a process would also lead to minimal

temporal changes in arsenic concentrations – conditions we do not observe. Spatial and temporal patterns of arsenic are inconsistent with it being bound strongly to aquifer solids, such as would be expected for arsenic adsorbed on ferric (hydr)oxides, and instead are indicative of a surface to near-surface source with aqueous phase and labile complexes of arsenic.

4.4. CONCLUSIONS AND IMPLICATIONS

The composite of hydrological and (bio)geochemical data illustrate arsenic release to porewater upon the onset of anaerobic conditions in the upper soil/sediment profile, transport of arsenic down in the profile with groundwater recharge, and transport through the aquifer with groundwater flow. Arsenic is released from the solid phase in soil and near-surface sediments, and it is transported primarily from oxbow ponds down in the profile. Within our field area of the Mekong delta, natural groundwater flow has transported arsenic from the near-surface, through the aquifer and towards the river, causing dissolved arsenic concentrations to be dangerously high in many tubewells.

Previous studies of arsenic in Southeast Asia have left the mechanisms of arsenic release and the hydrological influences on arsenic concentrations unresolved. We have revealed that, in Cambodia, arsenic mobilization arises due to microbial reductive processes driven by changes in hydraulic gradients, and groundwater flow delivers arsenic to aquifers. Environmental similarities imply that the coupled processes controlling arsenic in Cambodia also control arsenic throughout Southeast Asia. Therefore, confounding factors observed in other countries, such as spatial variance in arsenic concentrations, may be a result of groundwater flowpaths, which, in Bangladesh,

have been distorted by extensive dry season irrigation pumping. Finally, we have demonstrated here that arsenic concentrations are a result of natural processes. However, while anthropogenic activities are unnecessary to generate dangerous levels of arsenic, they may impact arsenic concentrations; this is an important avenue for future investigation.

In addition to those concerning arsenic, the results herein also provide information about water resources within the Mekong delta on a spatial scale that has previously been overlooked. The Mekong River is both the main source and recipient of groundwater. During high stages, river water combines with local rains to fill wetlands; these interior water levels then decline during the dry season due to runoff, evapotranspiration, and infiltration to the aquifer. Groundwater from infiltration then flows back to the rivers, carrying arsenic with it. The local water cycle is an important driver of nutrient chemistry; it is essential for fish and plant growth, and therefore the livelihood of people who depend on the rivers and wetlands for survival.

4.5. REFERENCES

Aggarwal, P. K., Basu, A. R., and Kulkarni., K. M. (2003) Comment on "Arsenic mobility and groundwater extraction in Bangladesh" (I). *Science* **300**, 584b.

Ahmed, K. M., Bhattacharya, P., Hasan, M. A., Akhter, S. H., Alam, S. M. M, Bhuyian, M. A. H., Imam, M. B., Khan, A. A., and Sracek, O. (2004) Arsenic enrichment in groundwater of the alluvial aquifers in Bangladesh: an overview. *Appl. Geochem.* **19**, 181-200.

Ahmed, M. F., Ahuja, S., Alauddin, M., Hug, S. J., Lloyd, J. R., Pfaff, A., Pichler, T., Saltikov, C., Stute, M., and van Geen, A. (2006) Ensuring safe drinking water in Bangladesh. *Science* **314**, 1687-1688.

Akai, J., Izumi, K., Fukuhara, H., Masuda, H., Nakano, S., Yoshimura, T., Ohfuji, H., Anawar, H.M., and Akai, K. (2004) Mineralogical and geomicrobiological investigations on groundwater arsenic enrichment in Bangladesh. *Appl. Geochem.* **19**, 215-230.

Anawar, H. M., Akai, J., Komaki, K., Terao, H., Yoshioka, T., Ishizuka, T., Safiullah, S., and Kata, K. (2003) Geochemical occurrence of arsenic in groundwater of Bangladesh: source and mobilization processes. *J. Geochem. Explor.* **77**, 109-131.

Berg, M., Tran, H. C., Nguyen, T. C., Pham, H. V., Schertenlieb, R., and Giger, W. (2001) Arsenic contamination of groundwater and drinking water in Vietnam: A human health threat. *Environ. Sci. Technol*. **35**, 2621-2626.

Berg, M., Stengel, C., Trang, P. T. K., Viet, P. H., Sampson, M. L., Leng, M., Samreth, S., and Fredericks, D. (2006) Magnitude of arsenic pollution in the Mekong and Red River Deltas — Cambodia and Vietnam. *Sci. Tot. Environ.* **372**, 413-425.

Buschmann, J., Berg, M., Stengel, C., and Sampson, M. L. (2007) Arsenic contamination in Cambodia: confined risk areas controlled by 'mirco-topography' in the Upper Mekong Delta. *Environ. Sci. Technol*. in press.

BGS and DPHE. (2001) *Arsenic contamination of groundwater in Bangladesh,* Final Report. British Geological Survey Report WC/00/19; Kinniburgh, D. G. and Smedley, P. L., Eds.; British Geoilogical Survey: Keyworth, Vol. 2.

Chakraborti, D., Rahman, M. M., Paul, K., Chowdhury, U. K., Sengupta, M. K., Lodh, D., Chanda, C. R., Saha, K. C., and Mukherjee, S. C. (2002) Arsenic calamity in the Indian subcontinent – What lessons have been learned? *Tantala*, **58**, 3-22.

Domenico, P. A. and Schwartz, F. W. (1998) *Physical and Chemical Hydrogeology*. John Wiley & Sons, New York. 506 p.

Dowling, C. B., Poreda, R. J., Basu, A. R., Peters, S. L., and Aggarwal, P. K. (2002) Geochemical study of arsenic release mechanisms in the Bengal Basin groundwater. *Water Resour. Res.* **38**, 1173, doi: 10.1029/2001WR000968.

Ferris, J. G. (1951) Cyclic fluctuations of water level as a basis for determining aquifer transmissibility. *Int. Assoc. Sci. Hydrol. Pub.* **33**, 148-155.

Fetter, C. W. (2001) *Applied Hydrogeology*. Prentice Hall, New Jersey. 598 p.

Fredericks, D. (2004) *Situation analysis: arsenic contamination of groundwater in Cambodia.* Unpublished Report to Arsenic Inter-Ministerial Sub-Committee, Cambodia, July 2004, 54 p.

Haddeland, I., Lettenmaier, D. P., and Skaugen, T. (2006) Effects of irrigation on the water and energy balances of the Colorado and Mekong river basins. *J. Hydr.* **324**, 210-233.

Harvey, C. F., Swartz, C. H., Badruzzaman, A. B. M., Keon-Blute, N., Niedan, V., Brabander, D., Oates, P. M., Ashfaque, K. N., Islam, S., Hemond, H. F., and Ahmed, M.F. (2002) Arsenic mobility and groundwater extraction in Bangladesh. *Science* **298**, 1602-1606.

Harvey, C. F., Swartz, C., Badruzzaman, A. B. M., Keon-Blute, N., Niedan, V., Brabander, D., Oates, P. M., Ashfaque, K. N., Islam, S., Hemond, H. F., and Ahmed, M. F. (2003) Response to comments on "Arsenic mobility and groundwater extraction in Bangladesh". *Science* **300**, 584d.

Harvey, C. F., Ashfaque, K. N., Yu, W., Badruzzaman, A. B. M., Ali, M. A., Oates, P. M., Michael, H., Neumann, R. B., Beckie, R., Islam, S., and Ahmed, M. F. (2006) Groundwater flow and arsenic biogeochemistry in Bangladesh: an analysis of transience and coupling. *Chemical Geology* **228**, 112-136.

Hazen, A. (1911) Discussion: Dams on sand foundations. *Transactions, American Society of Civil Engineers* **73**, 199.

Hvorslev, M. J. (1951) *Time lag and soil permeability in groundwater observations.* U.S. Army Corps of Engineers Waterway Experimentation Station, Bulletin 36, Vicksburg, Miss.

Islam, F. S., Gault, A. G., Boothman, C., Polya, D. A., Chatterjee, D., and Lloyd, J. (2004) Direct evidence of arsenic release from Bengali sediments due to metal-reducing bacteria. *Nature* **430**, 68-71.

JICA (Japanese International Cooperation Agency) (2002). *The study on groundwater development in Southern Cambodia.* Final Report by Kokusai Kogyo Co., Ltd. To Ministry of Rural Development, Cambodia.

Klump, S., Kipfer, R., Cirpka, O. A., Harvey, C. F., Brennwald, M. S., Ashfaque, K. N., Hug, S. J., and Imboden, D. M. (2006) Groundwater dynamics and arsenic mobilization in Bangladesh assessed using noble gases and tritium. *Ennviron. Sci. Technol.* **40**, 243-250.

Kresic, N. (1997) *Quantitative Solutions in Hydrogeology and Groundwater Modeling*. CRC, Boca Raton. 480 p.

McArthur, J. M., Banerjee, D. M., Hudson-Edwards, K. A., Mishra, R., Purohit, R., Ravenscroft, P., Cronin, A., Howarth, R. J., Chatterjee, A., Talukder, T., Lowry, D., Houghton, S., and Chadha, D. K. (2004) Natural organic matter in sedimentary basins and its relation to arsenic in anoxic ground water: the example of West Bengal and its worldwide implications. *Appl. Geochem.* **19**, 1255-1293.

Millham, N. P. and Howes, B. L. (1995) A comparison of methods to determine K in a shallow coastal aquifer. *Ground Water* **33**, 49-57.

Milton, A. H., Hasan, Z., Rahman, A, and Rahman, M. (2003) Non-cancer effects of chronic arsenicosis in Bangladesh. Preliminary results. *J. Environ. Sci. Health, Part A*, **A38**, 301-305.

Nguyen, V. L., Ta, T. K. O., and Tateishi, M. (2000) Late Holocene depositional environmentsl and coastal evolution of the Mekong River Delta, Southern Vietnam. *J. Asian Earth Sci.* **18**, 427-439.

Polizzotto, M. L., Harvey, C. F., Sutton, S. R., and Fendorf, S. (2005) Processes conducive to the release and transport of arsenic into aquifers of Bangladesh. *Proc. Nat. Acad. Sci.* **102**, 18819-18823.

Polya. D. A., Lythgoe, P. R., Abou-Shakra, F., Gault, A. G., Brydie, J. R., Webster, J. G., Brown, K. L., Nimfopolous, M. K., and Michailidis, K. M. (2003) IC-ICP-MS and IC-ICP-HEX-MS determination of arsenic speciation in surface and groundwaters: preservation and analytical issues. *Mineral. Mag.* **67**, 247-262.

Polya, D. A., Gault, A. G., Diebe, N., Feldman, P., Rosenboom, J. W., Gilligan, E., Fredericks, D., Milton, A. H., Sampson, M., Rowland, H. A. L., Lythgoe, P. R., Jones, J. C., Middleton, C., and Cooke, D. A. (2005) Arsenic hazard in shallow Cambodian groundwaters. *Mineral. Mag.* **69**, 807-823.

Rasmussen, W. C. and Bradford, G. M. (1977) *Ground-Water Resources of Cambodia*. U.S. Geological Survey Water-Supply Paper 1608-P. 122 p.

Smedley, P. L. and Kinniburgh, D. G. (2002) A review of the source, behaviour and distribution of arsenic in natural waters. *Appl. Geochem.* **17**, 517-568.

Smith, A. H., Lingas, E. O., and Rahman, M. (2000) Contamination of drinking-water by arsenic in Bangladesh: a public health emergency. *Bulletin World Health Organization* **78**, 1093-1103.

Stanger, G., Truong, T. V., Ngoc, K. S. L. T. M., Luyen, T. V., and Thanh, T. T. (2005) Arsenic in groundwaters of the Lower Mekong. *Environ. Geochem. Health* **27**, 341-357.

Swartz, C. H., Blute, N. K., Badruzzman, B., Ali, A., Brabander, D., Jay, J., Besancon, J., Islam, S., Hemond, H. F., Harvey, C. F. (2004) Mobility of arsenic in a Bangladesh aquifer: inferences from geochemical profiles, leaching data, and mineralogical characterization. *Geochim. Cosmochim. Acta*, **68**, 4539-4557.

Ta, T. K. O., Nguyen, V. L., Tateishi, M., Kobayashi, I., Tanabe, S., and Saito, Y. (2002) Holocene delta evolution and sediment discharge of the Mekong River, southern Vietnam. *Quaternary Sci. Rev*. **21**, 1807-1819.

van Geen, A., Zheng, Y., Versteeg, R., Stute, M., Horneman, A., Dhar, R., Steckler, M., Gelman, A., Small, C., Ahsan, H., Graziano, J. H., Hussain, I., and Ahmed, K. M. (2003a) Spatial variability of arsenic in 6000 tube wells in a 25 km^2 area of Bangladesh. *Water Resour. Res.* **39**, 1140, doi: 10.1029/2002WR001617.

van Geen, A., Zheng, Y., Stute, M., and Ahmed, K. M. (2003b) Comment on "Arsenic mobility and groundwater extraction in Bangladesh" (II). *Science* **300**, 584c.

Yu, W. H., Harvey, C. M., and Harvey, C. F. (2003) Arsenic in groundwater in Bangladesh: A geostatistical and epidemiological framework for evaluating health effects and potential remedies. *Water Resour. Res.* **39**, 1146, doi: 10.1029/2002WR001327.

4.6. FIGURE CAPTIONS

Figure 4.1. A. Field area with labeled well and surface water monitoring locations. B. Aquifer heads in sediments from 20-25 m (red) and surface water heads (yellow) during the wet season with inflow from the Mekong River to the aquifer. C. Aquifer and surface water heads during the dry season with groundwater outflow from the aquifer to the Mekong River.

Figure 4.2. Upper panel: Field area map with well and sediment collection sites. White ovals indicate areas with equivalent sedimentary profiles and dotted yellow line depicts transect for the lower panel cross-section. Lower panel: Sedimentary cross-section of field area.

Figure 4.3. Grain size distributions from sandy aquifer sediments.

Figure 4.4. Propagation of Mekong River tidal signal into aquifer well water levels.

Figure 4.5. Water budget of surface ponds. Pond drawdown values are based on weekly measurements of pond water levels (background). Rainfall data are averaged from three Mekong River Commission rain gauge stations surrounding our field area and error bars represent data from the station with the maximum rainfall. Maximum evapotranspiration (ET) is based on rainfall-corrected floating pan evaporation measurements. Infiltration plus runoff is equivalent to pond drawdown minus evaporation plus rainfall.

Figure 4.6. Cross-section depictions of aqueous chemical concentrations. Numbers represent measured concentrations. A. Arsenic. B. Dissolved organic carbon. C. Ammonium. D. Bicarbonate. E. Phosphate. F. Ferrous iron.

Figure 4.7. Major ion aqueous chemistry in surface water, shallow wells, and aquifer wells.

Figure 4.8. Correlation of dissolved inorganic carbon and ammonium in well water samples.

Figure 4.9. Upper panel: Temporal changes in Cl^- concentrations in surface water. Middle panel: Temporal changes in $\delta^{18}O$ signatures of surface water. Lower panel: Wetlands and Mekong River water levels.

Figure 4.10. Temporal changes in groundwater chemistry from depths of 25 m and 57 m at site TC11, adjacent to the Mekong River.

Table 4.1. Hydraulic conductivities of aquifer sediments from particle size analysis.

Sample	*D_{10} (mm)*	*d_{60} (mm)*	*U*	*Hazen K (m/s)*	*Breyer K (m/s)*
TH11-12	0.140	0.235	1.68	$4.0x10^{-5}$ - $1.4x10^{-4}$	$2.5x10^{-4}$
TH11-27	0.100	0.194	1.94	$2.1x10^{-5}$ - $7.2x10^{-5}$	$1.2x10^{-4}$
TH11-39	0.351	>0.707	NA	$2.5x10^{-4}$ - $8.9x10^{-4}$	NA
TE11-33	0.041	0.218	5.32	$3.5x10^{-6}$ - $1.2x10^{-5}$	$1.7x10^{-5}$
TE11-36	0.485	>0.707	NA	$4.9x10^{-4}$ - $1.7x10^{-3}$	NA
TE11-45	>0.707	>0.707	NA	$>10^{-3}$	NA
TE61-48	0.070	0.236	3.37	$1.0x10^{-5}$ - $3.5x10^{-5}$	$5.5x10^{-5}$
PE31-24	0.030	0.096	3.20	$1.9x10^{-6}$ - $6.5x10^{-6}$	$1.0x10^{-5}$
TC51-33	0.068	0.235	3.46	$9.5x10^{-6}$ - $3.3x10^{-5}$	$5.2x10^{-5}$
TC51-39	0.175	0.302	1.73	$6.3x10^{-5}$ - $2.2x10^{-4}$	$3.9x10^{-4}$
TC51-48	0.149	0.218	1.46	$4.6x10^{-5}$ - $1.6x10^{-4}$	$2.9x10^{-4}$
BD11-24	0.116	0.202	1.74	$2.8x10^{-5}$ - $9.7x10^{-5}$	$1.7x10^{-4}$
BD11-44	0.156	0.248	1.59	$5.0x10^{-5}$ - $1.8x10^{-4}$	$3.1x10^{-4}$
BD11-45	0.212	>0.707	NA	$9.3x10^{-5}$ - $3.2x10^{-4}$	NA
Average	**0.2**	**0.358**		**$1.5x10^{-4}$ - $5.3x10^{-4}$**	
Fine sand average	**0.105**	**0.218**		**$2.7x10^{-5}$ - $9.6x10^{-5}$**	**$1.7x10^{-4}$**

Table 4.2. Hydraulic conductivities of aquifer sediments from tidal dampening analyses.

Site	*Distance (m)*	*Tidal period (d)*	*River Amplitude (m)*	*Well Amplitude (m)*	*Time Lag (d)*	*Kb/S – amplitude (m^2/s)*	*Kb/S – time lag (m^2/s)*	*Average Kb/S (m^2/s)*	*K (m/s)* **S=0.01, b=100 m**	*K (m/s)* **S=0.01, b=40 m**	*K (m/s)* **S=0.2, b=100 m**	*K (m/s)* **S=0.2, b=40 m**
TH11	106	0.544	0.095	0.019	0.040	$2.6x10^{4}$	$3.1x10^{5}$	$1.7x10^{5}$	$1.9x10^{-4}$	$4.8x10^{-4}$	$3.8x10^{-3}$	$9.6x10^{-3}$
TC11	170	0.520	0.083	0.031	0.031	$1.8x10^{5}$	$1.3x10^{6}$	$7.2x10^{5}$	$8.4x10^{-4}$	$2.1x10^{-3}$	$1.7x10^{-2}$	$4.2x10^{-2}$
TC31	916	0.536	0.092	0.008	0.101	$8.6x10^{5}$	$3.5x10^{6}$	$2.2x10^{6}$	$2.5x10^{-3}$	$6.3x10^{-3}$	$5.1x10^{-2}$	$1.3x10^{-1}$
TC51	2649	0.564	0.092	0.005	0.564	$4.7x10^{6}$	$9.9x10^{5}$	$2.8x10^{6}$	$3.3x10^{-3}$	$8.2x10^{-3}$	$6.6x10^{-2}$	$1.6x10^{-1}$
Average		**0.541**	**0.091**			**$1.4x10^{6}$**	**$1.5x10^{6}$**	**$1.5x10^{6}$**	**$1.7x10^{-3}$**	**$4.3x10^{-3}$**	**$3.4x10^{-2}$**	**$8.6x10^{-2}$**

Table 4.3. Hydraulic conductivities of clay sediments from constant head permeameter tests.

Site	Site Type	Depths (m)	Average K (m/s)
TC51	Wetland	9, 12	4.5×10^{-8}
TH71	Wetland	9, 15	2.9×10^{-8}
PE31	Pond	12, 18	3.0×10^{-9}
TH11	Near River	9, 15	7.7×10^{-7}
TE11	Near River	12	1.7×10^{-6}
BD11	Near River	6	7.4×10^{-7}

Table 4.4. Hydraulic conductivities in clay sediments from slug tests.

Site	*Average K (m/s)*
TC11	4.4×10^{-7}
TC31	1.5×10^{-7}
TC41	2.2×10^{-6}
TC45	8.6×10^{-8}
TE51	5.1×10^{-7}
TE61	4.6×10^{-7}
TH51	2.0×10^{-7}
BD11	8.3×10^{-7}
BD31	6.5×10^{-7}
BD51	2.4×10^{-7}
PE31	3.6×10^{-6}
PE51	1.2×10^{-6}
PE71	1.5×10^{-7}
PW11	7.1×10^{-6}
PW51	4.8×10^{-7}

Table 4.5. Calculated horizontal and vertical groundwater flow distances.

Sites	*dL (m)*	*n (-)*	*K (m/s)*	*Net yearly flow (m)*	*Flow out (m)*	*Flow in (m)*
TH11 – Mekong	106	0.2	10^{-4} 10^{-3}	0.1 1.1	15.8 158.5	15.7 157.4
TH31 – Mekong	352	0.2	10^{-4} 10^{-3}	1.6 15.6	14.2 141.9	12.6 126.3
TC21 – Mekong	621	0.2	10^{-4} 10^{-3}	0.7 6.7	7.2 71.9	6.5 65.1
TC45 – Mekong	1749	0.2	10^{-4} 10^{-3}	1.9 19.0	11.7 116.6	9.8 97.6
TH31 – TH11	246	0.2	10^{-4} 10^{-3}	2.2 21.8	13.9 139.0	11.7 117.2
Aquifer - Mekong Average			**10^{-4}** **10^{-3}**	**1.3** **12.8**	**12.6** **125.6**	**11.3** **112.7**
Pond – TH31	20	0.5	10^{-8} 10^{-7}	0.04 0.45	0.06 0.60	0.02 0.15
Pond – TC21	20	0.5	10^{-8} 10^{-7}	0.04 0.45	0.06 0.61	0.02 0.16
Pond – TC45	20	0.5	10^{-8} 10^{-7}	0.04 0.39	0.04 0.39	0 0
Pond – Aquifer Average			**10^{-8}** **10^{-7}**	**0.04** **0.43**	**0.05** **0.53**	**0.01** **0.10**

Table 4.6. Dissolved inorganic carbon ^{14}C age data.

Site	Depth (m)	DIC ^{14}C age (ybp)	% Modern
TH11	37	404	95%
TC11	25	-401	104%
TC11	57	981	88%
TC31	20	1178	86%
TC31	51	986	88%
TC51	26	1846	79%
TC51	49	2151	76%

Table 4.7. Average aqueous bulk ion proportions within aquifers.

	Ca^{2+} %	Mg^{2+} %	$(Na^{+}+K^{+})$ %	HCO_3^- %	SO_4^{2-} %	Cl^- %
Surface Water	56.4	24.0	19.6	74.0	5.6	**20.4**
Shallow Wells	46.4	30.0	23.7	58.9	14.6	**26.5**
Aquifer Wells	**46.0**	**24.9**	**29.1**	**86.7**	**3.6**	**9.6**

Table 4.8. Average aqueous As and nutrient concentrations.

	Surface Water	Shallow Wells	Aquifer Wells
As (µg/L)	< 5	160	**500**
DOC (mg/L)	4.4	3.3	**6.9**
NH_4^+-N (mg/L)	0.8	6.4	**20**
HCO_3^- (mg/L)	40	320	**260**
PO_4^{3-} (mg/L)	< 0.4	1.1	**3.2**
NO_3^--N (mg/L)	**0.01**	**2.8**	**0.03**

Figure 4.1.

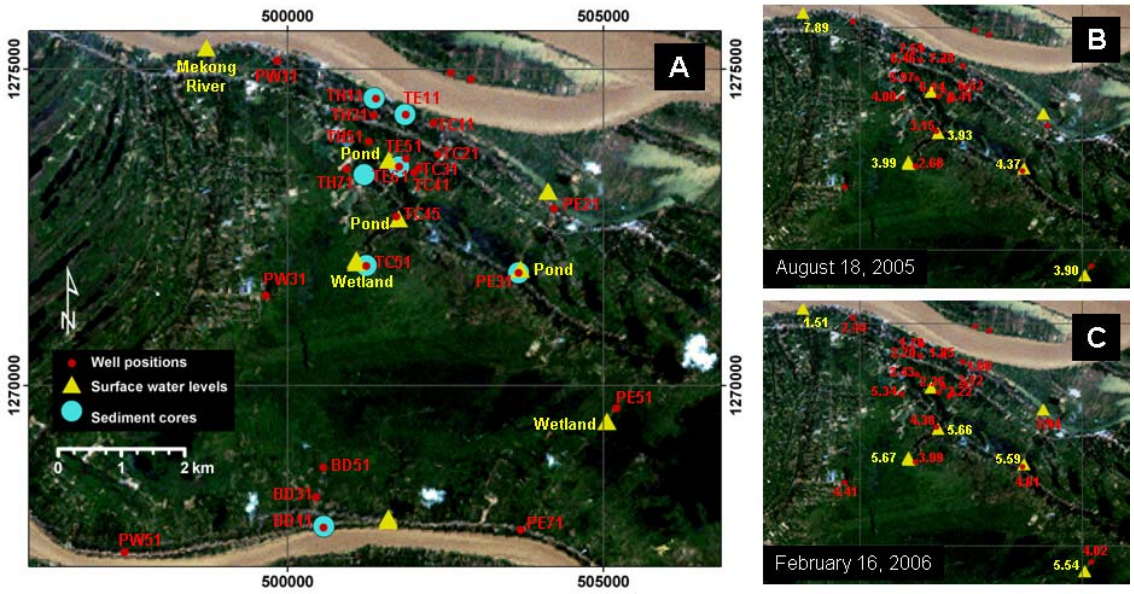
A
B
C
500000
505000
1275000
1270000
Mekong River
PW11
TH11
TE11
TH21
TE21
TH61
TE51
TC21
Pond
TC31
TH71
TE71
TC41
PE21
Pond
TE45
TC51
Wetland
PW31
PE31
Pond
PE51
Wetland
BD51
BD31
BD11
PW51
PE71
Well positions
Surface water levels
Sediment cores
0
1
2 km
N
August 18, 2005
February 16, 2006

Figure 4.2.

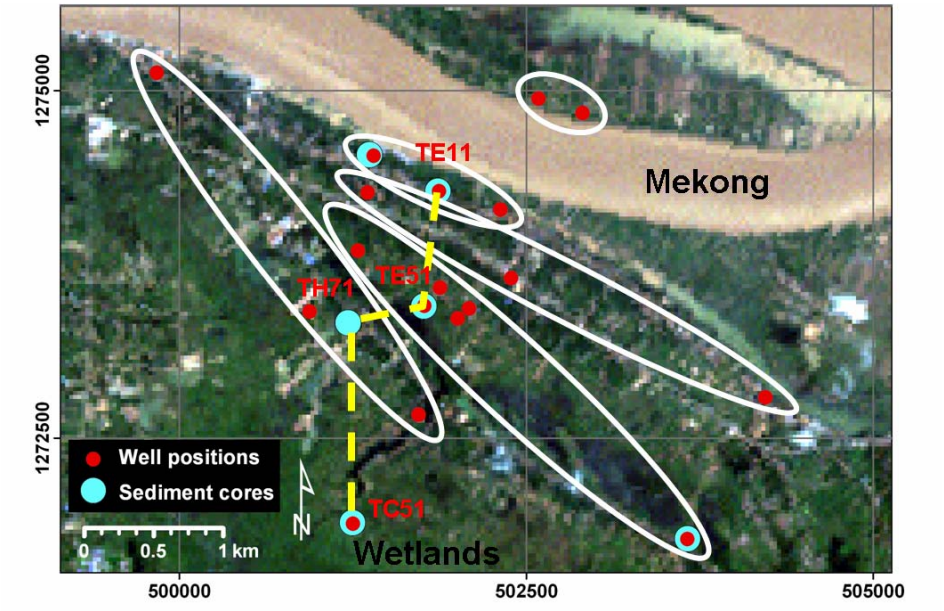
1275000
1272500
500000
502500
505000
TE11
Mekong
TH71
TE51
TC51
Wetlands
Well positions
Sediment cores
0
0.5
1 km
N

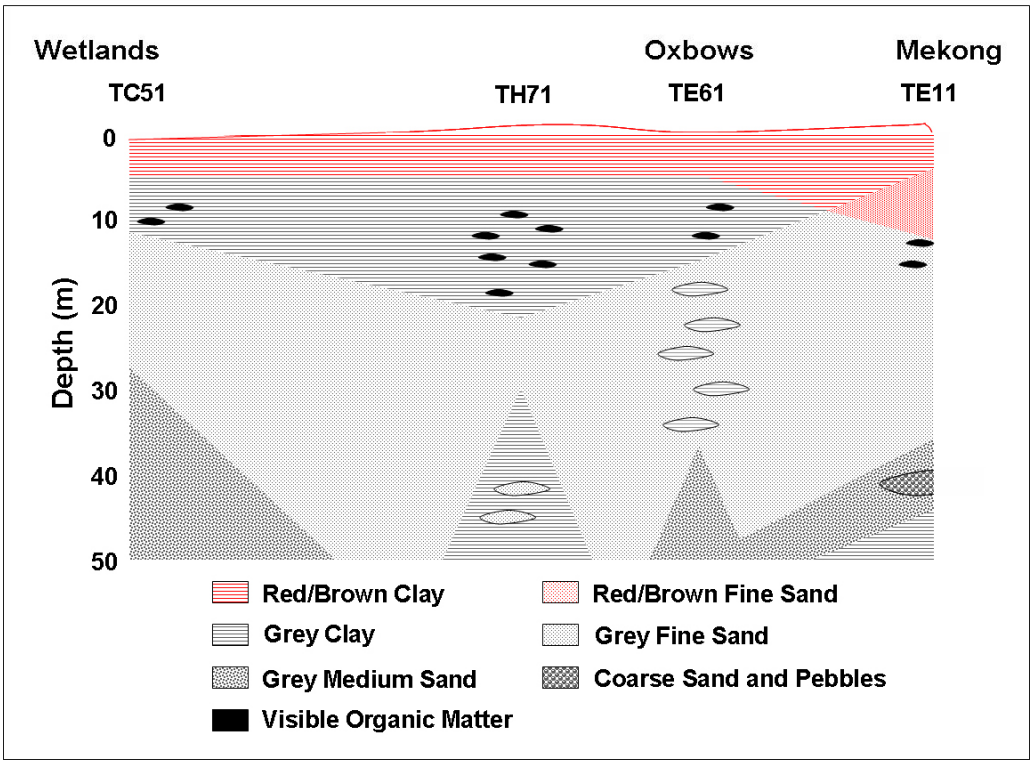
Wetlands
Oxbows
Mekong
TC51
TH71
TE61
TE11
0
10
20
30
40
50
Depth (m)
Red/Brown Clay
Red/Brown Fine Sand
Grey Clay
Grey Fine Sand
Grey Medium Sand
Coarse Sand and Pebbles
Visible Organic Matter

Figure 4.3.

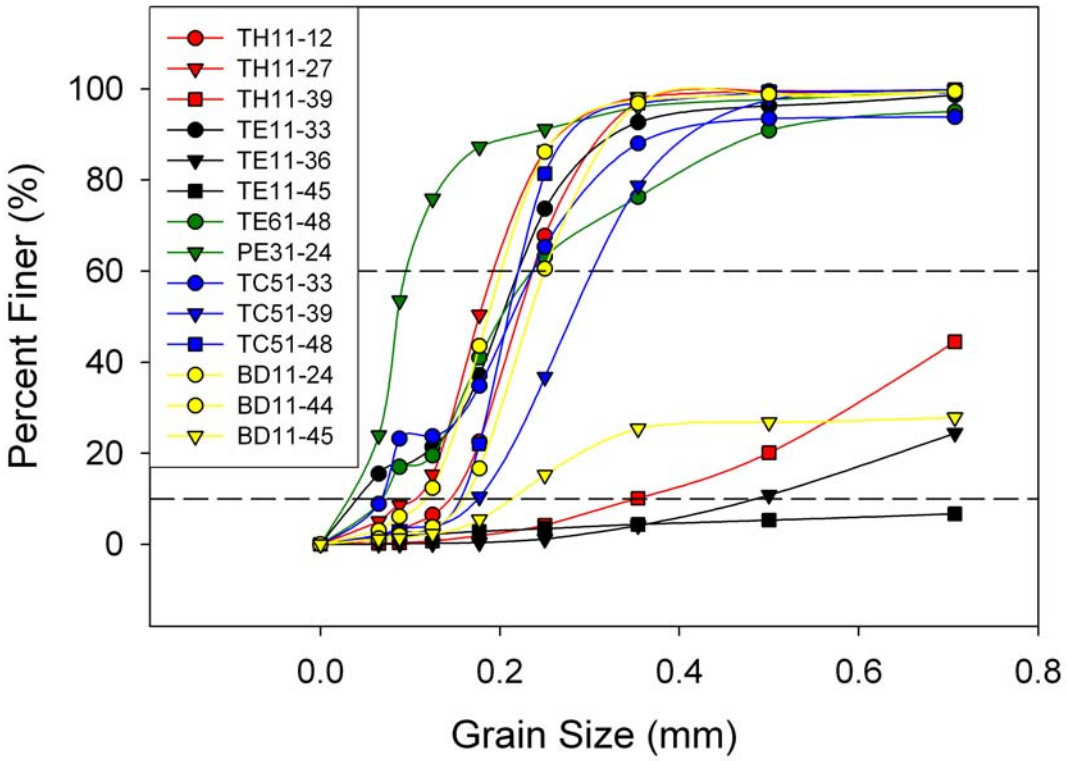
TH11-12
TH11-27
TH11-39
TE11-33
TE11-36
TE11-45
TE61-48
PE31-24
TC51-33
TC51-39
TC51-48
BD11-24
BD11-44
BD11-45
Percent Finer (%)
100
80
60
40
20
0
0.0
0.2
0.4
0.6
0.8
Grain Size (mm)

Figure 4.4.

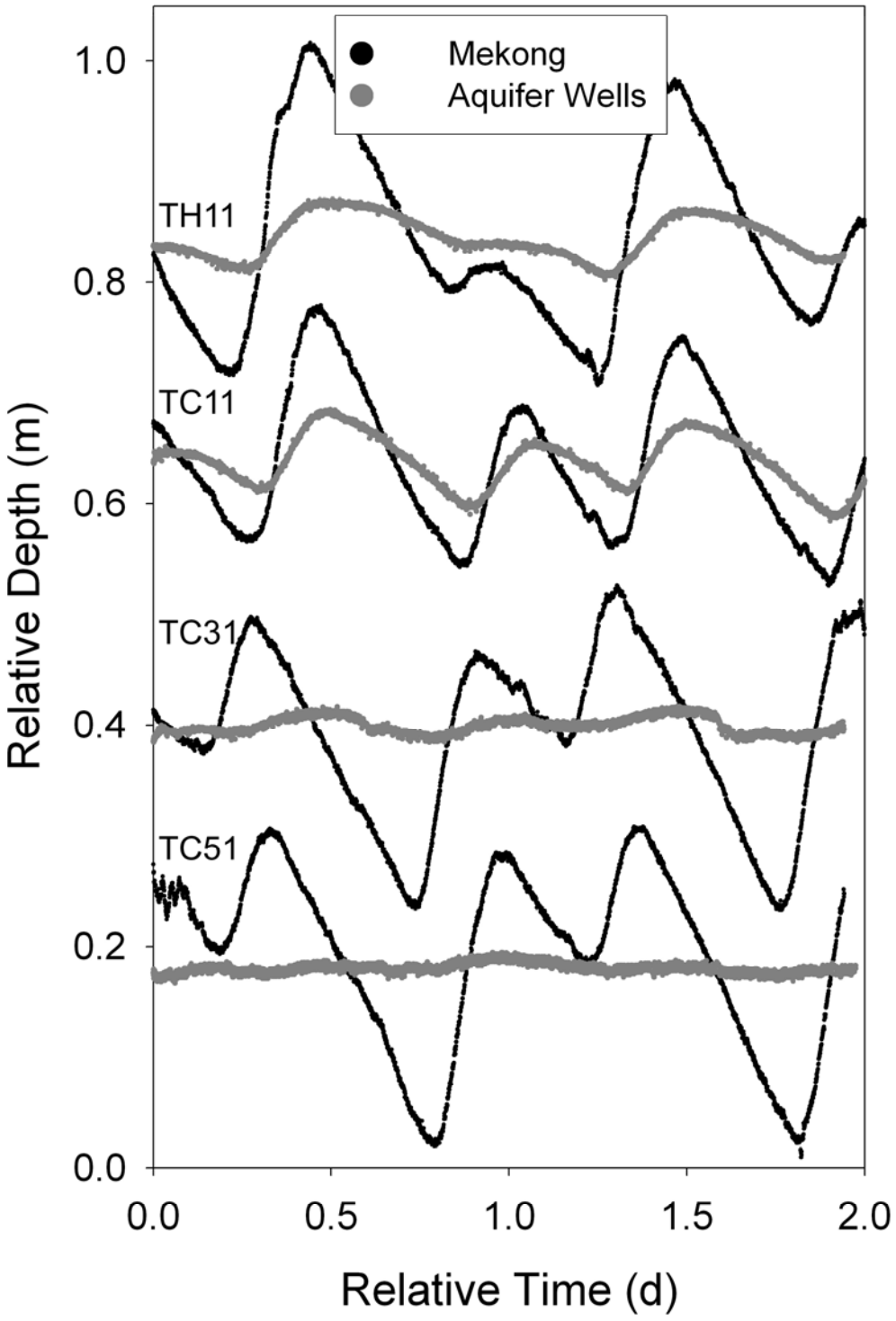
Mekong
Aquifer Wells
TH11
TC11
TC31
TC51
Relative Depth (m)
1.0
0.8
0.6
0.4
0.2
0.0
0.0
0.5
1.0
1.5
2.0
Relative Time (d)

Figure 4.5.

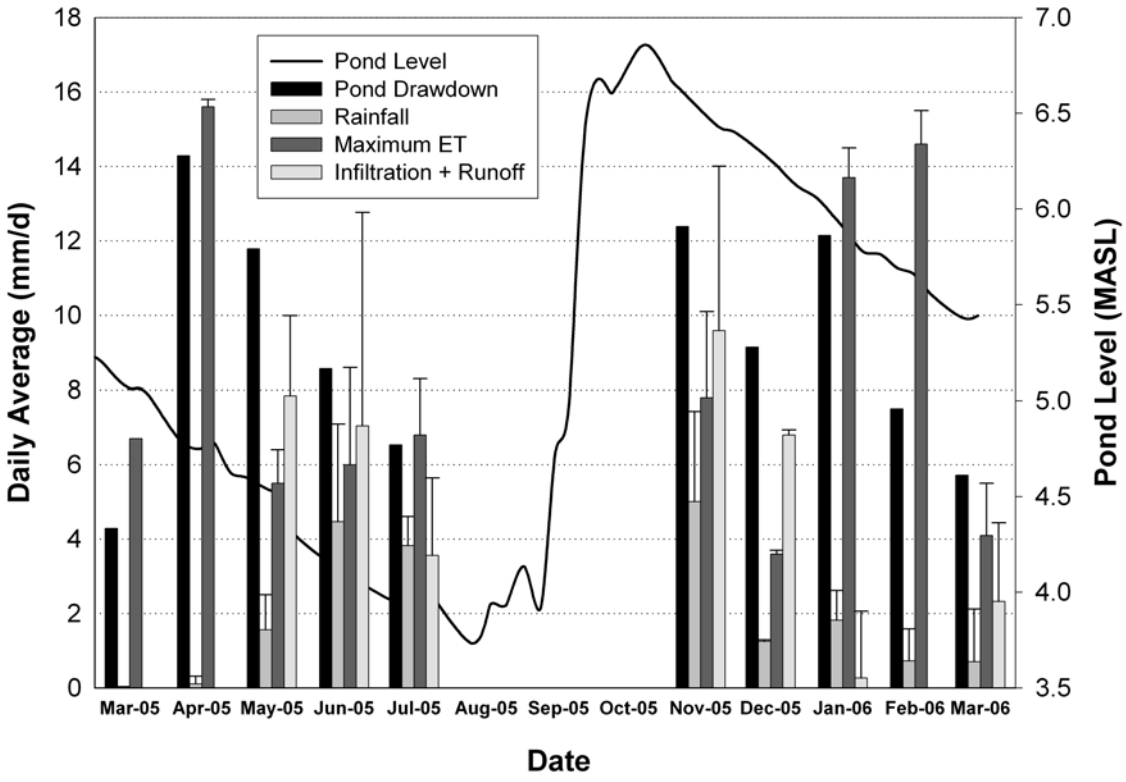
Pond Level
Pond Drawdown
Rainfall
Maximum ET
Infiltration + Runoff
Daily Average (mm/d)
Pond Level (MASL)
Date
0
2
4
6
8
10
12
14
16
18
3.5
4.0
4.5
5.0
5.5
6.0
6.5
7.0
Mar-05
Apr-05
May-05
Jun-05
Jul-05
Aug-05
Sep-05
Oct-05
Nov-05
Dec-05
Jan-06
Feb-06
Mar-06

Figure 4.6 A-C.

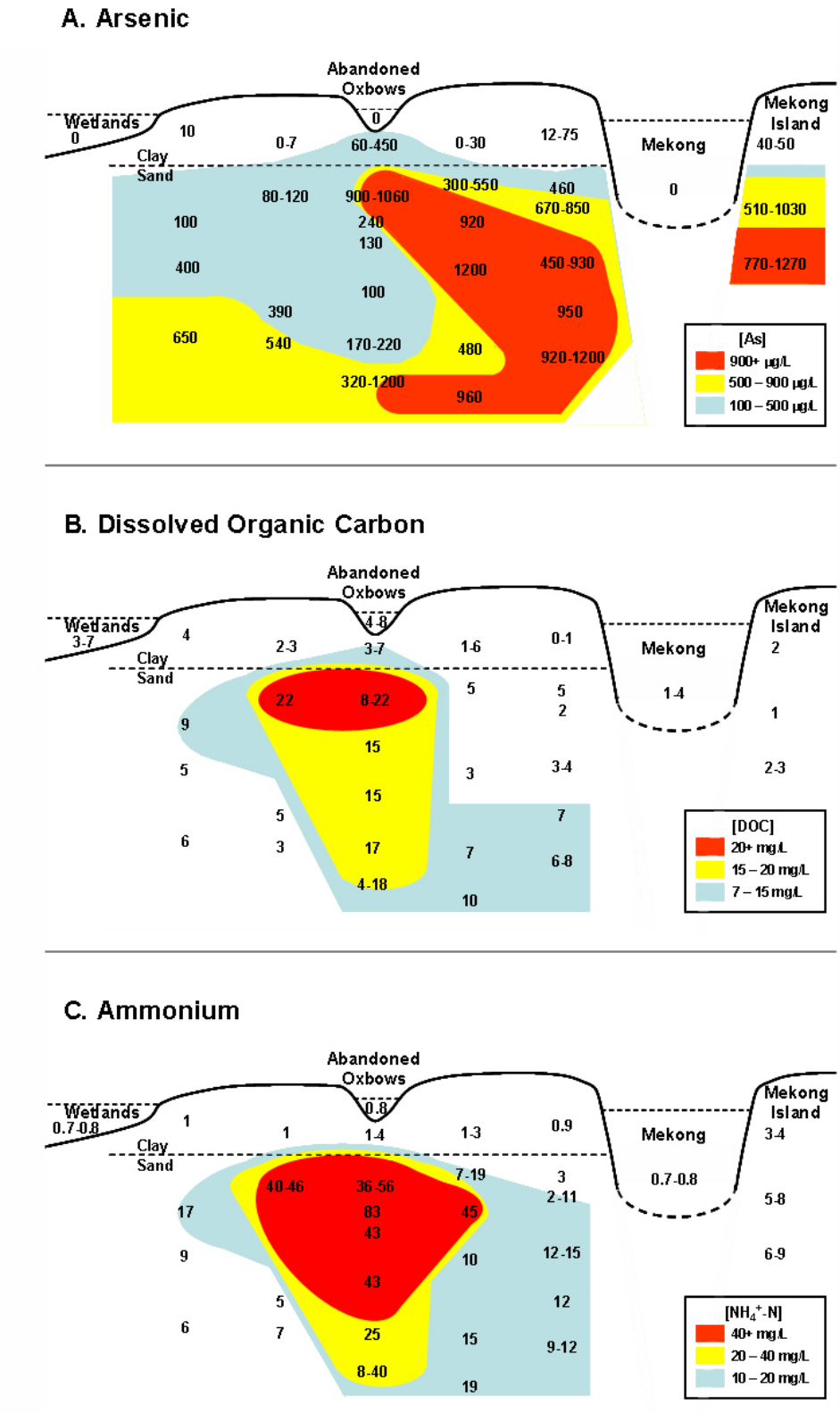
A. Arsenic
Abandoned Oxbows
Wetlands
Clay
Sand
Mekong
Mekong Island
0
10
0-7
60-450
0-30
12-75
40-50
80-120
900-1060
300-550
460
670-850
100
240
920
130
400
1200
450-930
100
390
950
650
540
170-220
480
920-1200
320-1200
960
510-1030
770-1270
[As]
900+ µg/L
500 – 900 µg/L
100 – 500 µg/L
B. Dissolved Organic Carbon
Abandoned Oxbows
Wetlands
Clay
Sand
Mekong
Mekong Island
3-7
4
2-3
3-7
1-6
0-1
2
22
8-22
5
5
2
1-4
1
9
15
5
3
3-4
2-3
15
7
5
6
3
17
7
6-8
4-18
10
[DOC]
20+ mg/L
15 – 20 mg/L
7 – 15 mg/L
C. Ammonium
Abandoned Oxbows
Wetlands
Clay
Sand
Mekong
Mekong Island
0.7-0.8
1
1
1-4
1-3
0.9
3-4
40-46
36-56
7-19
3
0.7-0.8
17
83
45
2-11
5-8
43
9
10
12-15
6-9
43
5
12
6
7
25
15
9-12
8-40
19
[NH4+-N]
40+ mg/L
20 – 40 mg/L
10 – 20 mg/L

Figure 4.6 D-F.

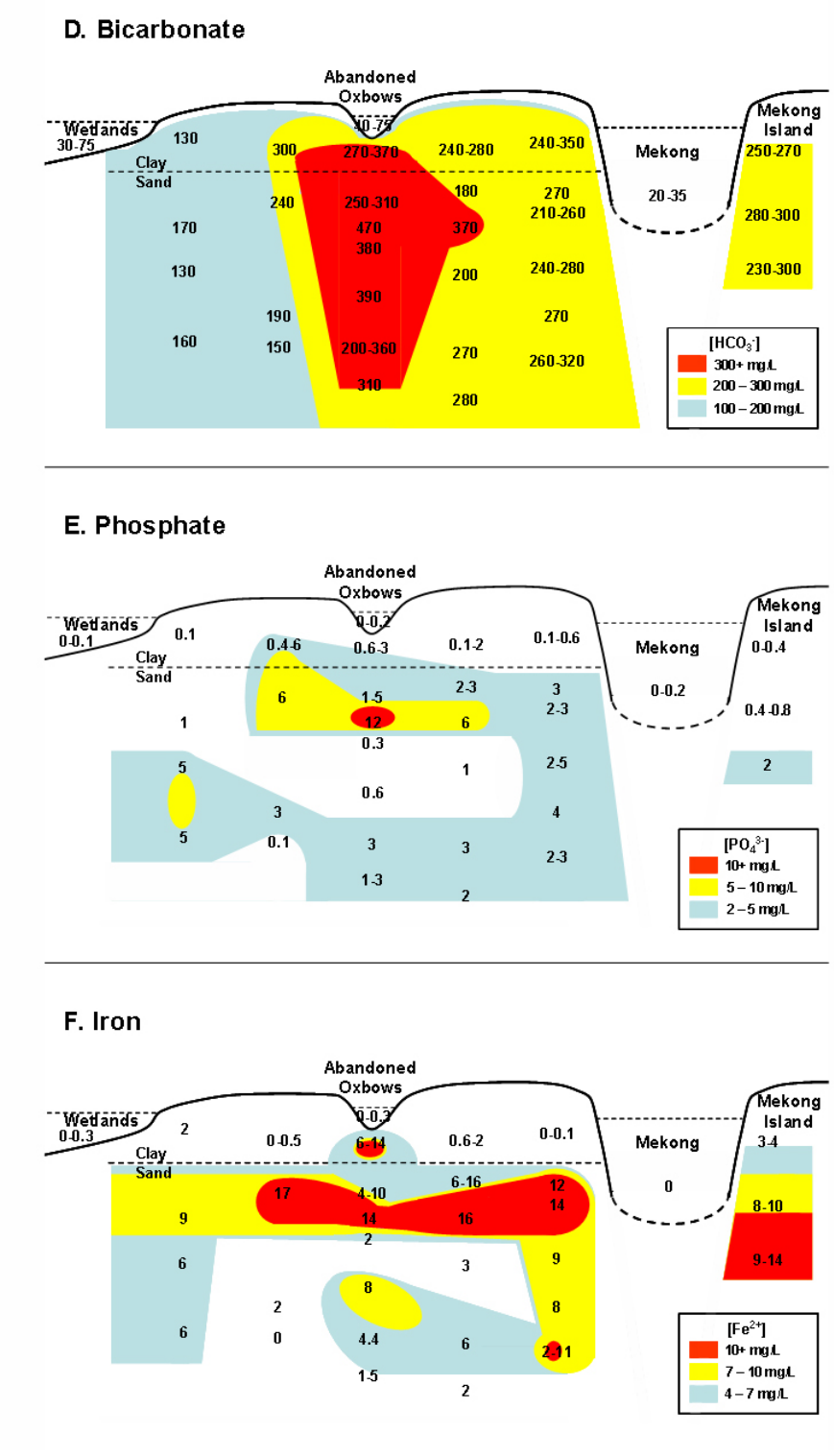
D. Bicarbonate
Abandoned Oxbows
Wetlands
30-75
Clay
Sand
Mekong
Mekong Island
130
300
270-370
240-280
240-350
250-270
240
250-310
180
270
210-260
20-35
280-300
170
470
370
380
130
200
240-280
230-300
390
190
270
160
150
200-360
270
260-320
310
280
[HCO3-]
300+ mg/L
200 – 300 mg/L
100 – 200 mg/L
E. Phosphate
Abandoned Oxbows
Wetlands
0-0.1
Clay
Sand
Mekong
Mekong Island
0.1
0.4-6
0.6-3
0.1-2
0.1-0.6
0-0.4
6
1.5
2-3
3
0-0.2
1
12
6
2-3
0.4-0.8
0.3
5
1
2-5
2
0.6
3
4
5
0.1
3
3
2-3
1-3
2
[PO4 3-]
10+ mg/L
5 – 10 mg/L
2 – 5 mg/L
F. Iron
Abandoned Oxbows
Wetlands
0-0.3
Clay
Sand
Mekong
Mekong Island
2
0-0.5
6-14
0.6-2
0-0.1
3-4
17
4-10
6-16
12
0
14
8-10
9
14
16
2
6
3
9
9-14
8
2
8
6
0
4.4
6
2-11
1-5
2
[Fe2+]
10+ mg/L
7 – 10 mg/L
4 – 7 mg/L

.

Figure 4.7.

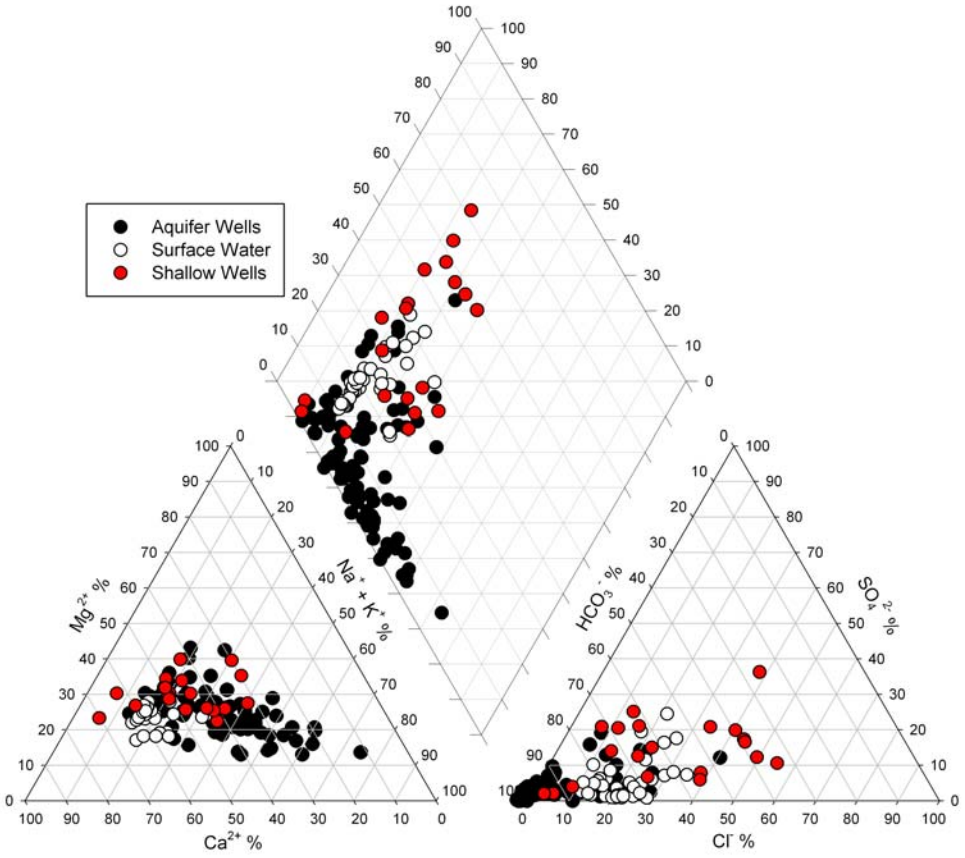
Aquifer Wells
Surface Water
Shallow Wells
Mg2+ %
Na+ + K+ %
Ca2+ %
HCO3- %
SO4 2- %
Cl- %

Figure 4.8.

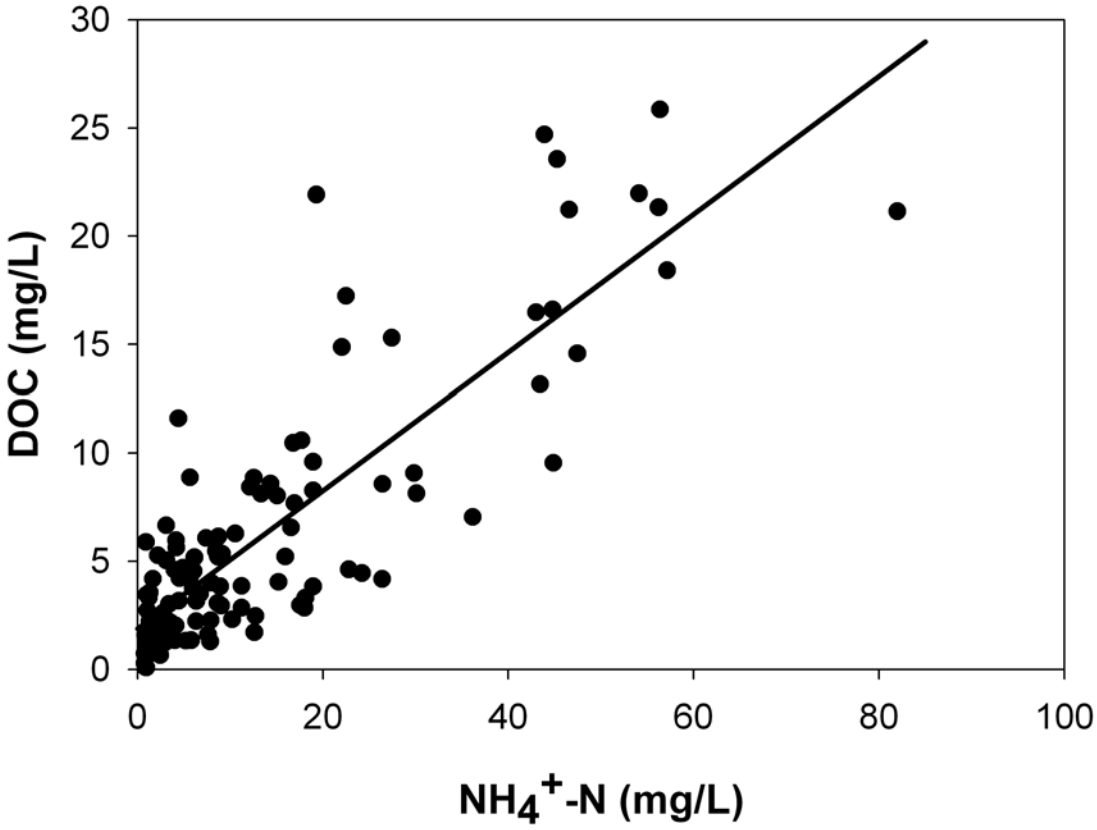

Figure 4.9.

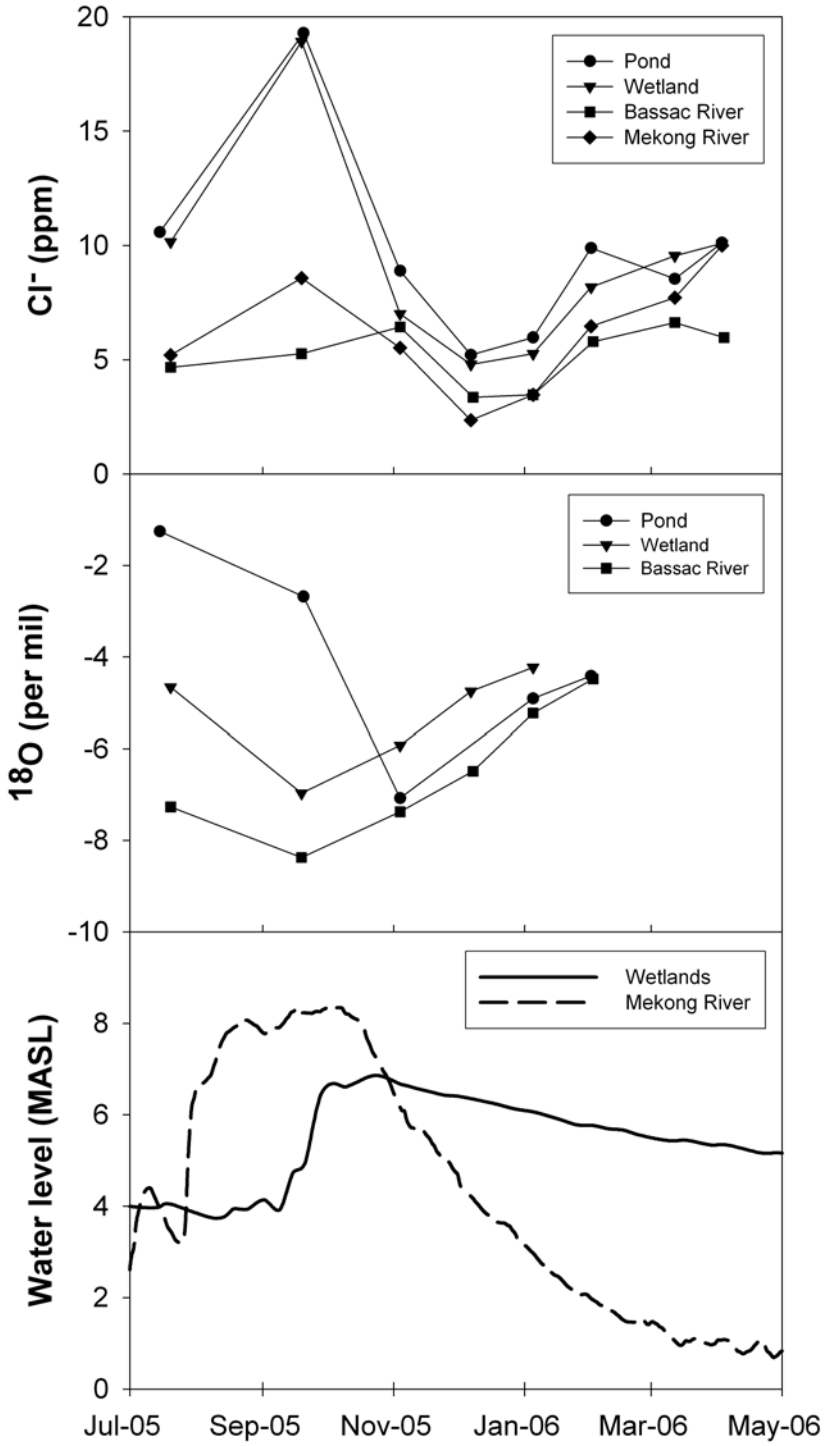
Cl- (ppm)
20
15
10
5
0
Pond
Wetland
Bassac River
Mekong River
18O (per mil)
-2
-4
-6
-8
-10
Pond
Wetland
Bassac River
Water level (MASL)
8
6
4
2
0
Wetlands
Mekong River
Jul-05
Sep-05
Nov-05
Jan-06
Mar-06
May-06

Figure 4.10.

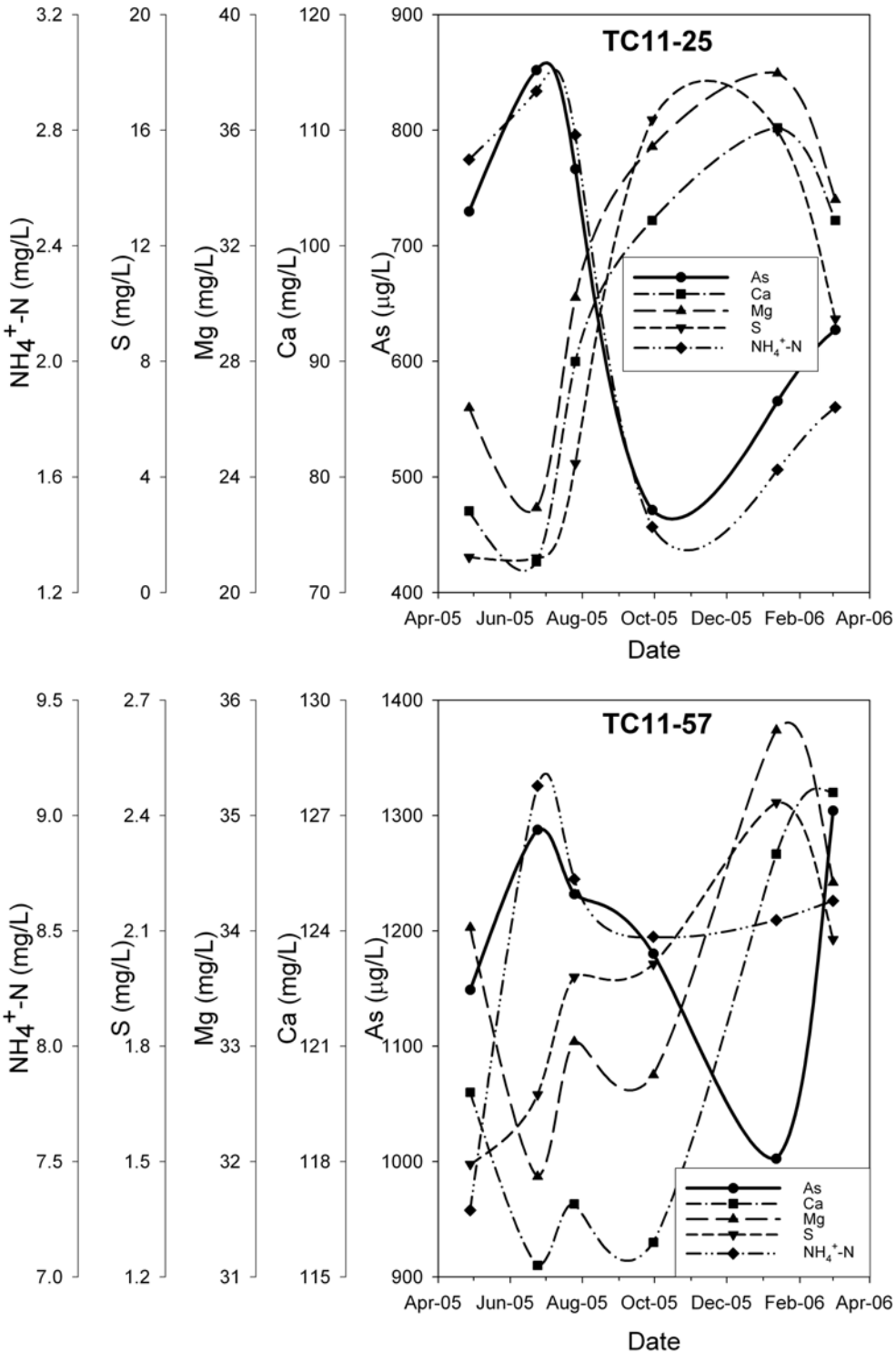
TC11-25
NH_4^+-N (mg/L)
S (mg/L)
Mg (mg/L)
Ca (mg/L)
As (µg/L)
As
Ca
Mg
S
NH_4^+-N
Apr-05 Jun-05 Aug-05 Oct-05 Dec-05 Feb-06 Apr-06
Date
TC11-57
NH_4^+-N (mg/L)
S (mg/L)
Mg (mg/L)
Ca (mg/L)
As (µg/L)
As
Ca
Mg
S
NH_4^+-N
Apr-05 Jun-05 Aug-05 Oct-05 Dec-05 Feb-06 Apr-06
Date

CHAPTER 5

Contributions of Natural Arsenic Cycling and Human Disturbance to History's Largest Mass Poisoning

ABSTRACT

Mass poisoning by arsenic contaminated groundwater is occurring throughout Southeast Asia. Arsenic transported in Himalayan-derived river sediment is deposited in sedimentary basins of the region and released to the groundwater as a result of unresolved processes. We reveal that hydrologic variations between rivers and adjacent wetlands drive both biogeochemical arsenic release to the shallow pore water and centurial-scale transport through the underlying aquifer back to the river. Although the natural hydrologic cycle responsible for hazardous levels of arsenic in aquifers has persisted for millennia, it is sensitive to presently occurring and impending human-induced land use changes.

5.1. INTRODUCTION

Tens of millions of people in Southeast Asia routinely consume well water with unsafe arsenic levels (Smith et al., 2000; Yu et al., 2003; Ahmed et al., 2006). Research concerning the causes of arsenic contamination has focused primarily on areas of the Ganges-Brahmaputra-Meghna River system, where the problem is most acute, but debate persists concerning the biogeochemical mechanisms controlling arsenic within the subsurface, the role of hydrology on arsenic and solute transport, and the anthropogenic influence on arsenic cycling (Harvey et al., 2002; Aggarwal et al., 2003; van Geen et al., 2003a; vanGeen et al., 2003b; Harvey et al., 2003; McArthur et al., 2004; Polizzotto et al., 2005). Recently, the occurrence of arsenic in deltaic aquifers of the Mekong (Stanger et al., 2005; Polya et al., 2005; Berg et al., 2006) and Red River (Berg et al., 2001; Berg et al., 2006) sedimentary basins has come to light, where similarities in geologic deposition, aquifer source rock, and regional hydrological gradients to those of Bangladesh (Berg et al., 2001; JICA, 2002) suggest that common processes control arsenic within the groundwater. However, because land use practices, especially irrigation with groundwater, differ greatly from country to country, local hydrogeologic flow currently varies. Understanding key processes and differences between regional settings with different land uses may allow us to glean important information on the mechanisms controlling arsenic liberation to, and transport within, groundwater, and will help identify changes in dissolved arsenic that result with alterations in land use. Here we develop a self-consistent, quantitative hydrological model of the Kandal province, Cambodia that, when coupled with geochemical profiles, demonstrates that arsenic contamination predates human perturbation of the surface-subsurface environment, that

seasonal arsenic cycling is linked to changing hydraulic gradients, and that arsenic concentrations can be maintained for millennia.

5.2. MATERIALS AND METHODS

5.2.1. Field area

Our field site in the Kandal province of Cambodia comprises approximately 50 km^2 between the Mekong and Bassac Rivers (Figure 5.1) and is typical of the Mekong floodplain system. The region between the two rivers is encompassed by native wetlands, and arsenic concentrations in groundwater can be greater than 100 times the World Health Organization's (WHO) recommended guideline of 10 μg L^{-1}. A network of 80 installed wells and 10 surface water monitoring sites are distributed throughout the field area, and a ~ 5 km^2 focused study area includes near-surface lysimeters and a subset of closely spaced wells for more detailed spatial analyses.

The Mekong River is a broad river that carries the seventh largest sediment load in the world (Nguyen et al., 2000), the majority of which is discharged during the wet season. The delta floodplain is roughly 62, 500 km^2 (Nguyen et al., 2000) and the upper 10-35 m of sediment has been deposited in the past 5000 y (Ta et al., 2002) following the most recent sea level highstand. Below surficial overbank clays, Holocene sediments representing delta progradation include organic-rich silts, sands, and clays (ESCAP, 1993); these sediments encompass the majority of wells within our field area and are those with which high dissolved As concentrations are typically associated. Quarternary sediments underlay the Holocene sediments and are were deposited during delta aggradation (Ta et al., 2002).

5.2.2. Well installation, core collection, and lysimeter installation

Wells were installed using a local drilling method by manually rotating a 1.5" diameter pipe with a 4" diameter open cutting tip. Lengths of 3 m were added sequentially to extend the pipe to desired well depths (up to 60 m), and water was pumped downward through the middle to physically displace the sediment. Once drilling was complete, the pipe was removed from the hole and 1.25" diameter PVC tubing was installed to create the wells. At each location, 3 to 5 wells were put in spanning the following depths: shallow (8 to 12 m), medium (20 to 30 m), and deep (36 to 60 m). Discrete, pre-fabricated well screens were used at the bottom of the PVC; screening intervals were 6 to 8 m for shallow wells and 4 m for medium and deep wells. Once the PVC was installed, holes were backfilled with coarse-sand and capped with clay and/or cement.

Because of the potential for homogenization and oxidation of drill cuttings, an alternate, intact coring procedure was used at select locations for sediment retrieval. A 0.75" open core device (AMS, Idaho, USA) fitted with a polycarbonate sleeve and core-catcher was deployed through the drilling pipe at 3 m intervals and driven into the undisturbed sediment below the drilling tip. Once retrieved, samples were immediately capped and sealed in O_2-impermeable pouches with AnaeroPacks (Mitsubishi Gas Chemical, Japan) to prevent oxidation of the sediments. Sediment samples were stored and transported at 4^oC.

In order to monitor near-surface porewater chemistry in a zone of variable redox conditions, ceramic cup lysimeters (Prenart Equipment ApS, Denmark) were installed in

a sediment profile underneath an ephemeral wetland within an abandoned river channel (oxbow) at depths of 1, 2, and 4 m. Holes were dug with a hand auger and soil cores were collected in undisturbed sediments below the extent of augering; samples were preserved as above. Following lysimeter installation, holes were first backfilled with native clay material for approximately 5 to 10 cm, and then sealed with bentonite and native clay.

5.2.3. Water level measurements

Hydraulic heads in each well were measured weekly with a Solinst Mini 101 Water Level Meter (Solinst Canada Ltd., Ontario, Canada). Surface water levels were also measured weekly with a weighted measuring tape from points of fixed height. All reference points for water level measurements were spatially linked by vertical surveying with a Leica Auto Level NA720 (Leica Geosystems AG, Switzerland); manufacturer accuracy per double km run is 2.5 mm and measurements between reference points were verified by completing surveying circles <5 mm.

Elevations were referenced with Mekong River stage levels provided by the Mekong River Commission. Distance-weighted averages from the Phnom Penh Port (upstream of our site) and the Neak Luong (downstream) stations were used to calibrate the absolute elevation of our water level monitoring site in the Mekong River, and, following elevation surveying, the remainder of the water level measurements throughout our field area were adjusted accordingly. Based on recent historic Mekong River level fluctuations, the river levels we show here are representative of a typical year, midway between recent maximum flood and drought year levels.

5.2.4. Water sampling

Wells were sampled with a Geopump II peristaltic pump (Geotech Environmental Equipment, Inc., Colorado, USA), with flow rates of ~ 1 L/min. A YSI 556 multiparameter probe equipped with a flow-through cell (YSI, Inc., Ohio, USA) was placed in the outflow line to monitor dissolved oxygen (DO), pH, conductivity, temperature, and Eh. Wells were purged before sample collection until multiparameter stabilization was observed (typically 30 to 130 minutes). If a well could not be pumped continuously (i.e. low yield), it was pumped dry and re-infiltrated water was collected on the following day.

Groundwater samples were filtered with 0.45 μm filters (Geotech) and collected in acid-washed bottles. Samples for cations and total arsenic concentrations were acidified with trace-metal grade HCl to pH < 2. Samples for anion analyses were pretreated with a Bio-Rad AG50W-X8 cation exchange resin in hydrogen form (Bio-Rad Laboratories, California, USA) to prevent oxidative metal precipitation and subsequent anion scavenging. Arsenic speciation in the field was performed by acidification of groundwater to pH 3, followed by treatment with a Bio-Rad AG1-X8 anion exchange resin in acetate form to remove As(V). Dissolved inorganic carbon (DOC), nitrate, and ammonium samples were acidified with HCl and sterilized with $HgCl_2$.

Lysimeters were allowed to equilibrate with porewater for 30 days prior to sample collection; during this time, samples were routinely collected and discarded. Each lysimeter was subsequently sampled bimonthly from August 2005 to March 2006.

Porewater was drawn by suction (-800 mBar) into bottles, each containing 15 mL of trace-metal grade 3 M HCl for preservation of As and Fe.

Surface water was collected in a churn bucket at the water-air interface and sampling was performed as with the groundwater samples.

5.2.5. Analytical measurements

Measurements on aqueous samples were conducted in the field and in the laboratory. Field measurements were performed for arsenic, alkalinity, ferrous iron, nitrate, sulfate, and sulfide; all but alkalinity and dissolved sulfide were duplicated in the laboratory. Arsenic was measured with the Hach 5-reagent low range arsenic test kit (Hach Company, Colorado, USA). Alkalinity measurements were performed by titration with 1.6 M H_2SO_4 to a colorimetric endpoint using a digital titrator and a bromcresol green – methyl red indicator (Hach). Ferrous iron, nitrate, sulfate, and sulfide were measured with a DR 2400 Portable Spectrophotometer (Hach) using manufacturer dedicated reagents and defined protocols.

In the laboratory, aqueous-phase arsenic concentrations were analyzed by hydride generation inductively-coupled-plasma atomic emission spectroscopy (HG-ICP-AES) with a Thermal Jarrell Ash ICP-AES (Thermo Electron Corporation, Massachusetts, USA). Arsenate was reduced to arsenite with KI, and arsine gas was subsequently formed by reaction with a 0.6% NaBH4/0.5% NaOH solution. Detection limits were 5 $\mu g\ L^{-1}$ arsenic. Dissolved Al, Ca, K, Fe, Mg, Mn, Na, P, S, and Si were measured by ICP-AES, and quality control standards were monitored throughout the course of the analyses. Fluoride, Cl^-, NO_3^-, PO_4^{3-}, and SO_4^{2-} analyses were performed on a Dionex

500DX Ion Chromatograph fitted with an AS9 Ion Pac column and an AG9 4-mm guard column (Dionex Corporation, California, USA); the flow rate was 1.0 mL min^{-1} of a 9 mM Na_2CO_3 eluent. Dissolved organic carbon (DOC) was measured as non-purgeable organic carbon on a Shimadzu TOC-5000A analyzer (Shimadzu Corporation, Japan); measurements were detected with a non-dispersive infrared gas analyzer after samples were acidified and dissolved inorganic carbon was sparged. Nitrate and ammonium were analyzed colorimetrically with an Alpkem Continuous-Flow Analyzer (OI Corporation, Texas, USA).

Elemental solid-phase concentrations were determined after microwave digestion according to EPA method 3052 (EPA, 1994). Sediment samples were chemically dissolved in 3:1 concentrated HNO_3:concentrated HF and the resulting solution was evaporated to dryness. Following reconstitution in HCl, concentrations were measured by ICP-AES.

5.3. RESULTS AND DISCUSSION

Both the Ganges-Brahmaputra-Meghna and Mekong River systems include massive deltas draining the Himalayan uplift that have formed following the rise in sea level 6,000 to 10,000 years ago. Each system has distinct inverted deltaic topography and associated hydrology that is strongly influenced by the monsoonal-driven rise and fall of its respective rivers. Moreover, the general stratigraphy of our field site is similar to that in Bangladesh: the primary water-producing fine, grey sand aquifer at our field site typically extends to > 60 m depth and is overlain by a 6 to 20 m thick red and grey clay unit, of which the lower portion is grey and contains abundant wood and organic

material. Additionally, each system contains diffuse, near crustal-average solid-phase arsenic concentrations.

Groundwater chemistry at our field site is similar to that in other arsenic-contaminated aquifers throughout Southeast Asia. Dissolved arsenic concentrations are associated with reducing and circumneutral pH conditions (Table 5.1), with an average Eh of 70 mV (relative to the standard hydrogen electrode), pH of 7.1, dissolved O_2 < 1 mg/L, Fe^{2+} of 8.0 mg/L, SO_4^{2-} of 8.2 mg/L, and often detectable (> 1 μg/L) HS^-. Groundwaters have high alkalinities such that HCO_3^- provides > 70% of the bulk anionic charge in all but 5 of the wells, while Ca^{2+} is the dominant cation and contributes an average of 46% of the bulk cationic charge. Ammonium concentrations average 20 mg/L and correlate with dissolved organic carbon which averages 6.9 mg/L.

Unlike many other areas where arsenic has been studied in Asia, land use alteration is minimal within our field site. Use of groundwater for irrigation is limited and thus retrieval, which is essentially negligible, is primarily for domestic use; in fact, in the Kandal province, most tubewells have been installed within the past 10 years (Fredericks, 2004). These conditions provide an opportunity to investigate arsenic behavior in an aquifer subjected to limited anthropogenic disturbance. In appreciable areas of Bangladesh, near-surface clay sediments, which may be as thin as 2 m, have been removed and piled in order to raise village levels above flood levels and structure rice fields, leaving ponds that, along with irrigation fields, may act as sources of aquifer recharge (Harvey et a;., 2006). At our field site in Cambodia, the majority of people live on natural river levees and therefore the near-surface sediment structure is much less distorted. Thus, while (bio)geochemical conditions at our field site may be similar to

those of other arsenic-contaminated sites, the hydrology of our system remains governed by natural rather than anthropogenic processes, allowing us to devise a unified spatiotemporal model of arsenic within the subsurface.

Dissolved arsenic concentrations vary spatially, range from 15 to 1300 μg L^{-1} in aquifer groundwater, can be > 400 μg L^{-1} in near-surface (0-2 m depth) porewater, and are typically < 10 μg L^{-1} in surface water. Solid-phase arsenic concentrations are < 12 mg Kg^{-1} in the oxidized layers of surficial clays, and decrease in the deeper (> 3 m) grey clays to an average of ~ 4 mg Kg^{-1}. In the aquifer sediments from where domestic wells retrieve water, solid-phase arsenic concentrations average ~ 3 mg Kg^{-1} and are typically less than 5 mg Kg^{-1}. Aqueous arsenic concentrations are not well correlated with solid-phase arsenic concentrations; rather, the solid-phase concentrations are relatively uniform while dissolved concentrations in groundwater are more spatially variable. However, within our detailed study area, dissolved arsenic concentrations are generally constant at equivalent depths parallel to the Mekong River. While arsenic concentrations greatly exceed the WHO standard in wells below 15 m, the consistently highest arsenic concentrations occur in locations from which the Mekong River has recently migrated, as indicated by surficial expression of abandoned oxbow features. In particular, the highest arsenic concentrations are observed immediately below (~ 20 m depth) present-day oxbow wetland-ponds, and concentrations of > 900 μg L^{-1} trend downward towards deeper (40-57 m) wells adjacent to the Mekong River (Figure 5.2), where aquifer sediments are often coarser than the typical fine sands, and at depths from where pebbles up to 1 cm in diameter have been recovered.

River levels fluctuate approximately 8 m annually, steadily declining from mid-October to early June and then steeply rising in July due to upstream monsoonal rains and Himalayan snowmelt (Figure 5.1). Inland surface water bodies, including the wetlands and abandoned river channel oxbow wetland-ponds, also undergo seasonal fluctuations driven by the monsoonal climate but exhibit trends distinct from those observed in the Mekong River. Sharp increases in inland surface water levels occur from late September to early October when local rains combine with increasing river levels to flood inland areas. With the onset of the dry season, surface water levels decline due to a combination of infiltration, evapotranspiration, and runoff. While the relative elevations of the wetlands and the river levels invert semi-annually, the wetlands are higher than the river for 9 out of the 12 months of the year.

Seasonal changes in groundwater levels most closely mimic river levels, and the amplitude of the fluctuations decreases with distance from the Mekong River, suggesting a strong hydrologic connection between the aquifer and the river. The hydraulic gradient between the aquifer and river inverts annually: during rising river-stage, the subsurface gradient is from the river to the floodplain aquifer, but during falling river-stage, the gradient is towards the river. Local hydraulic gradients between rivers and the adjacent floodplain aquifer are two-orders of magnitude greater than the regional gradient extending parallel with the river towards the ocean, suggesting that groundwater hydrology is controlled by the temporally variable gradient perpendicular to the Mekong River. The hydrologic connection between the overlying wetlands and underlying aquifer is apparently limited by surfacial clay, and surface water level changes are clearly distinct

from those observed at depth. However, these changes produce temporally variable but strong vertical gradients between the surface water and underlying aquifer.

Although hydraulic gradients between the aquifer and the river and between the wetlands and the aquifer invert seasonally, net gradients indicate that the annual flow direction is from the wetlands to the aquifer (gradient of 0.07 m/m) and from the aquifer to the river (gradient of $7x10^{-5}$ m/m). Importantly, differences in hydraulic head both horizontally and vertically are typically on the scale of decimeters to meters, while our measurement error was sub-centimeter, providing a high degree of certainty for the net gradient calculations.

Although there is uncertainty in the hydraulic conductivities within the aquifer, the measured gradients provide an internally consistent driving force for steady-state mass balance of water flux downwards from the wetlands and horizontally from the aquifer to the river. In-field slug tests and laboratory permeameter tests result in hydraulic conductivities of the matrix ranging from 10^{-8} to 10^{-7} m/s in the clay layer separating the aquifer sands from surface water, and thus, with a porosity of 0.5, net annual vertical flow distances are 0.04 to 0.4 m from the wetland-ponds to the aquifer. If groundwater recharge was evenly distributed across our entire field area, annual downward fluxes would range from $2x10^{6}$ to $2x10^{7}$ m^3 y^{-1}. Particle size and tidal dampening analyses indicate typical aquifer hydraulic conductivities of 10^{-4} to 10^{-3} m/s, and assuming a porosity of 0.2, net annual horizontal groundwater flow to the river ranges from 1.3 to 13 m. Given our field site of ~ 6 km width and an aquifer thickness of 50 m, the net annual horizontal groundwater flux within the aquifer ranges from $4x10^{5}$ to $4x10^{6}$ m^3 y^{-1}. While the flow velocities, especially within the upper clay units remain uncertain, these mass

balance calculations provide additional support for the steady-state flow of water from the wetlands to the aquifer and from the aquifer to the river. This trend in groundwater flow is similar to model-predicted results for the Bangladeshi aquifer without groundwater pumping (Harvey et al., 2006).

Our estimates therefore suggest that the travel time from the wetlands to the river is in the range of 200-2000 y. The age of the aquifer, and associated sedimentary organic carbon, is greater than 6000-8000 years based on both ^{14}C dating and regional geologic history (Ta et al., 2002). This suggests that the aquifer has likely been flushed by as many as 30 pore volumes. Carbon-14 dating indicates that dissolved inorganic carbon (DIC) is younger than 1800 years old throughout the aquifer. These dates suggest that the majority of this DIC must have been derived from surface rather than sedimentary organic carbon and are indicative of aquifer residence times of < 1800 years. Both observations are consistent with surface recharge and aquifer flushing. The lack of an alkalinity gradient within the aquifer and along the flowpath is also illustrative of limited carbon oxidation at depth.

The seasonal fluctuations in vertical and horizontal hydraulic gradients result in temporal variations of geochemical conditions at both the near surface zone of recharge and the zone of discharge to the river. A subset of the field site wells was sampled monthly, and wells exhibiting both temporally variant and invariant arsenic concentrations were observed. Wells adjacent to the Mekong River (Figure 5.3A) demonstrate seasonally changing arsenic concentrations coincident with changes in hydraulic gradients. In a 25 m well, inflow of groundwater from the Mekong towards the aquifer during July through November results in a decline in arsenic concentrations by

nearly 50%, but as gradients reverse during outflow, arsenic concentrations rebound. Such seasonal trends in arsenic concentrations are also observed at 57 m, and in each case, changes in arsenic are positively correlated with changes in dissolved NH_4^+ and negatively correlated with SO_4^{2-}. The temporal variation in arsenic concentrations at locations near the Mekong River is controlled by flowing groundwater, a result of arsenic transport when flow direction is towards the river or groundwater dilution with river water during high river stages. In contrast, wells within the aquifer at greater distance from the river do not exhibit seasonal variations in arsenic concentrations.

Within near-surface porewater, temporal variations in arsenic concentrations coincide with changes in vertical hydraulic gradients. Lysimeters were installed at the edge of an abandoned river channel oxbow pond to monitor porewater in a zone with fluctuating water-table and redox conditions. Following the onset of downward gradients in November, arsenic is detected in the porewater and there is a trend toward higher arsenic concentrations with increasing depth (Figure 5.3B), with concentrations reaching ~ 500 μg L^{-1} at 2 m. As water levels drop, arsenic concentrations subsequently decrease and by March arsenic concentrations are < 50 μg L^{-1} in all lysimeter samples. Dissolved Fe(II) concentrations track those of arsenic, while SO_4^{2-} trends are reversed, suggesting changing redox conditions. Arsenic cycling observed in the redox-variable soil (upper 2 m) indicates a near-surface zone of arsenic release from the solids, and because arsenic is released during downward flow, it is likely transported towards the aquifer.

The observed seasonal variations in arsenic concentrations within shallow clay and deeper aquifer porewaters reflect biogeochemical cycling and, in association, movement of waters of variable arsenic concentrations. They further illustrate that arsenic

cycling is occurring at distinct spatial scales, each of which may impact water quality. Moreover, the correspondence of changes in aqueous chemistry to changes in hydraulic gradients signifies that local hydrology is a critically important driver of geochemical conditions, particularly arsenic concentrations (Figure 5.4). Furthermore, because groundwater pumping is minimal and large areas remain undeveloped and uncultivated at our field site, observed hydrologic and geochemical gradients are naturally derived and contrast with local gradients dominated by groundwater pumping, such as those in Bangladesh. Therefore, at our field site, arsenic cycling predates human influence. Hydraulic data from a site in the Munshiganj district of Bangladesh illustrate similar patterns to those observed here for the Mekong Delta for two months after wet season floods, but upon initiation of dry season groundwater pumping, aquifer water levels fall below those of the river, altering groundwater flow (Harvey et al., 2006). While site to site variations are likely present, the similarity between the general conditions of the Ganges-Brahmaputra-Meghna and Mekong Deltas, along with the similarities in local hydrologic data noted here, suggest that throughout much of Southeast Asia arsenic contamination existed prior to land use changes.

The potential for downward transport of arsenic observed at the near-surface has important implications for arsenic in well water. Because groundwater flow has effectively flushed the aquifer, either an upstream source of arsenic must exist or arsenic must be continually released from the aquifer solid-phase — or a combination of both must occur — for arsenic to persist within the aquifer. Based on our yearly aquifer groundwater fluxes and an aqueous As concentration of 500 μg L^{-1}, $2x10^{11}$ to $2x10^{12}$ μg of As is removed from the aquifer system annually via transport to the river. Chemical

gradients indicate that arsenic is primarily released from near-surface sediments, where present-day hydrologic-biogeochemical cycling is observed. Carbon-14 dates indicate an average clay layer deposition rate of ~ 3.3 mm/y over the last 6000 years, yielding a delivery rate of approximately $3x10^{12}$ μg As to the system annually. Accordingly, As influx (via sediment deposition) and efflux (from the aquifer to the river) are comparable, indicating the system is in a steady-state with respect to arsenic content.

Aquifer arsenic concentrations are controlled by biogeochemical processes in the near-surface that release it from soil/sediment solids and hydrologic factors that presently deliver arsenic at levels comparable to its efflux from the aquifer, and, as a result, changes in land use that disrupt the hydrologic regime will have significant consequences on arsenic in the aquifer. Arsenic accumulation within soils or near-surface sediments – for example, by irrigation with groundwater or landfill disposal of arsenic-laden water filters – would result in enhanced arsenic concentrations being drawn to the aquifer by natural groundwater flow. However, in contrast, clay excavation may remove arsenic from the system and result in lower arsenic within recharge waters. Similarly, upstream river damming, as projected for the Mekong River, would reduce floodplain sediment deposition as well as the magnitude of flooding, thereby diminishing the influx of arsenic to the system. No matter the specific perturbation, land use changes will modify the existing hydrologic and biogeochemical conditions and change dissolved arsenic concentrations. Only with continued or accelerated aquifer flushing without an upstream arsenic source can groundwater arsenic concentrations decrease.

5.4. REFERENCES

Aggarwal, P. K., Basu, A. R., and Kulkarni., K. M. (2003) Comment on "Arsenic mobility and groundwater extraction in Bangladesh" (I). *Science* **300**, 584b.

Ahmed, M. F., Ahuja, S., Alauddin, M., Hug, S. J., Lloyd, J. R., Pfaff, A., Pichler, T., Saltikov, C., Stute, M., and van Geen, A. (2006) Ensuring safe drinking water in Bangladesh. *Science* **314**, 1687-1688.

Berg, M., Tran, H. C., Nguyen, T. C., Pham, H. V., Schertenlieb, R., and Giger, W. (2001) Arsenic contamination of groundwater and drinking water in Vietnam: A human health threat. *Environ. Sci. Technol*. **35**, 2621-2626.

Berg, M., Stengel, C., Trang, P. T. K., Viet, P. H., Sampson, M. L., Leng, M., Samreth, S., and Fredericks, D. (2006) Magnitude of arsenic pollution in the Mekong and Red River Deltas — Cambodia and Vietnam. *Sci. Tot. Environ.* **372**, 413-425.

EPA (1994) *Method 3052: Microwave assisted acid digestion of siliceous and organically based matrices,* 3rd ed. U.S. Environmental Protection Agency: Washington, DC, Vol. 2004.

ESCAP (1993) *Atlas of Mineral Resources of the ESCAP Region. Vol. 10. Cambodia.* United Nations, New York, 87 pp.

Fredericks, D. (2004) *Situation analysis: arsenic contamination of groundwater in Cambodia.* Unpublished Report to Arsenic Inter-Ministerial Sub-Committee, Cambodia, July 2004, 54 p.

GLCF. Global Land Cover Facility, University of Maryland, *http://www.landcover.org*.

Harvey, C. F., Swartz, C. H., Badruzzaman, A. B. M., Keon-Blute, N., Niedan, V., Brabander, D., Oates, P. M., Ashfaque, K. N., Islam, S., Hemond, H. F., and

Ahmed, M.F. (2002) Arsenic mobility and groundwater extraction in Bangladesh. *Science* **298**, 1602-1606.

Harvey, C. F., Swartz, C., Badruzzaman, A. B. M., Keon-Blute, N., Niedan, V., Brabander, D., Oates, P. M., Ashfaque, K. N., Islam, S., Hemond, H. F., and Ahmed, M. F. (2003) Response to comments on "Arsenic mobility and groundwater extraction in Bangladesh". *Science* **300**, 584d.

Harvey, C. F., Ashfaque, K. N., Yu, W., Badruzzaman, A. B. M., Ali, M. A., Oates, P. M., Michael, H., Neumann, R. B., Beckie, R., Islam, S., and Ahmed, M. F. (2006) Groundwater flow and arsenic biogeochemistry in Bangladesh: an analysis of transience and coupling. *Chemical Geology* **228**, 112-136.

JICA (Japanese International Cooperation Agency) (2002). *The study on groundwater development in Southern Cambodia.* Final Report by Kokusai Kogyo Co., Ltd. To Ministry of Rural Development, Cambodia.

McArthur, J. M., Banerjee, D. M., Hudson-Edwards, K. A., Mishra, R., Purohit, R., Ravenscroft, P., Cronin, A., Howarth, R. J., Chatterjee, A., Talukder, T., Lowry, D., Houghton, S., and Chadha, D. K. (2004) Natural organic matter in sedimentary basins and its relation to arsenic in anoxic ground water: the example of West Bengal and its worldwide implications. *Appl. Geochem.* **19**, 1255-1293.

Nguyen, V. L., Ta, T. K. O., and Tateishi, M. (2000) Late Holocene depositional environmentsl and coastal evolution of the Mekong River Delta, Southern Vietnam. *J. Asian Earth Sci.* **18**, 427-439.

Polizzotto, M. L., Harvey, C. F., Sutton, S. R., and Fendorf, S. (2005) Processes conducive to the release and transport of arsenic into aquifers of Bangladesh. *Proc. Nat. Acad. Sci.* **102**, 18819-18823.

Polya, D. A., Gault, A. G., Diebe, N., Feldman, P., Rosenboom, J. W., Gilligan, E., Fredericks, D., Milton, A. H., Sampson, M., Rowland, H. A. L., Lythgoe, P. R., Jones, J. C., Middleton, C., and Cooke, D. A. (2005) Arsenic hazard in shallow Cambodian groundwaters. *Mineral. Mag.* **69**, 807-823.

Smith, A. H., Lingas, E. O., and Rahman, M. (2000) Contamination of drinking-water by arsenic in Bangladesh: a public health emergency. *Bulletin World Health Organization* **78**, 1093-1103.

Stanger, G., Truong, T. V., Ngoc, K. S. L. T. M., Luyen, T. V., and Thanh, T. T. (2005) Arsenic in groundwaters of the Lower Mekong. *Environ. Geochem. Health* **27**, 341-357.

Ta, T. K. O., Nguyen, V. L., Tateishi, M., Kobayashi, I., Tanabe, S., and Saito, Y. (2002) Holocene delta evolution and sediment discharge of the Mekong River, southern Vietnam. *Quaternary Sci. Rev*. **21**, 1807-1819.

van Geen, A., Zheng, Y., Versteeg, R., Stute, M., Horneman, A., Dhar, R., Steckler, M., Gelman, A., Small, C., Ahsan, H., Graziano, J. H., Hussain, I., and Ahmed, K. M. (2003a) Spatial variability of arsenic in 6000 tube wells in a 25 km^2 area of Bangladesh. *Water Resour. Res.* **39**, 1140, doi: 10.1029/2002WR001617.

van Geen, A., Zheng, Y., Stute, M., and Ahmed, K. M. (2003b) Comment on "Arsenic mobility and groundwater extraction in Bangladesh" (II). *Science* **300**, 584c.

Yu, W. H., Harvey, C. M., and Harvey, C. F. (2003) Arsenic in groundwater in Bangladesh: A geostatistical and epidemiological framework for evaluating health effects and potential remedies. *Water Resour. Res.* **39**, 1146, doi: 10.1029/2002WR001327.

5.5. FIGURE CAPTIONS

Figure 5.1. Our field site is located ~ 20 km southeast of Phnom Penh, Cambodia, situated in the Upper Mekong Delta. We have installed wells in transects across the field site from the Mekong River to the Bassac River and each multi-level well symbol represents 3 to 5 wells screened at varying depths. The base map (GLCF) is a "true color" composite of a Landsat image taken July 11, 2001, approximately the onset of the wet season; the white dotted line shows the areal extent of the central wetlands, and abandoned river channel oxbow lakes are indicated. Selected wells (TC11, TC21, and TC31) and surface water body (Mekong River, abandoned river channel oxbow wetland-ponds, and central wetlands) water level monitoring sites are labeled in the field map, and respective year-long hydrographs are shown in the graph to the right. The plateau at the peak of the TC31 hydrograph reflects a period when that well became artesian following nearby surface water inundation and soil/sediment compression.

Figure 5.2. Field site cross-section with groundwater arsenic concentrations. Well nests with equivalent distances and sedimentological relationship in regards to the Mekong River show similar arsenic depth profiles in groundwater. Well water arsenic concentrations are depicted with numbers within the cross-section; temporal variations within wells have been averaged and ranges are representative of wells of equivalent depths and location. Shallow wells screened in clay and medium and deep wells screened in aquifer sands are separated by the clay-sand dotted line. Other than from adjacent to the abandoned oxbow ponds, arsenic concentrations from wells screened in the clay are

typically < 100 μg/L, while As > 100 μg/L in all but one aquifer sample. Mekong River bottom sediments are fine to coarse sands; the Mekong River depth profile is unknown and depicted with a dotted line here, but Mekong River Commission cross-sections indicate river depths of typically 20-25 m below the adjacent shores.

Figure 5.3. Dissolved arsenic concentrations vary temporally within the aquifer and near-surface porewaters in coincidence with hydraulic gradients. (A) In the aquifer, arsenic concentrations vary by as much as 50% in a 25 m deep well adjacent to the Mekong River (Near River, TC11-25). Concentrations rise when aquifer horizontal gradients are positive, indicating flow towards the river, and decrease during inflow from the river. Such changes are also observed in the 57 m deep well at the same well site, and while temporal fluctuations in arsenic concentrations are observed at other wells, they are most pronounced adjacent to the Mekong River. Arsenic concentrations in a 49 m, far-river well (Far from River, TC51-49) adjacent to the inner wetlands exhibit smaller changes. (B) In the near-surface porewaters from 1 m (inset) and 2 m lysimeter samples, arsenic concentrations rise as vertical hydraulic gradients change from upward flow (negative gradients) to downward flow (positive gradients), and concentrations reach ~500 mg/L in 2 m samples.

Figure 5.4. Conceptual cross-sectional profile of field site with the hydrogeochemical processes influencing arsenic. Magnitudes and directions of hydraulic gradients fluctuate seasonally and are denoted by relative arrow thicknesses and orientations; double-headed arrows indicate periods of gradient reversals. Red shading designates the temporally-

variable oxidized zone while green specifies the reduced zone. Arsenic distribution contours from Figure 5.2 are superimposed on the central net annual cycling figurette. Cross-section represents depths to 60 m.

Table 5.1. Aqueous concentrations from aquifer well, shallow well, and surface water samples collected November, 2005 – February, 2006.

		Aquifer Wells (n = 48)				**Shallow Wells** (n = 25)				**Surface Water** (n = 24)			
		Min	**Max**	**Average**	**Median**	**Min**	**Max**	**Average**	**Median**	**Min**	**Max**	**Average**	**Median**
As	μg/L	15	1300	500	480	0.00	1000	160	50	0.0	9.8	1.4	0.0
pH		6.3	9.1	7.1	7.1	6.5	7.4	6.8	6.7	6.2	7.6	6.8	6.8
Eh	mV	-190	290	70	41	-86	350	110	140	240	450	310	310
TDS	μS/cm	43	2300	1100	1100	100	3900	1600	1800	11	230	130	130
DO	mg/L	< 1	1.4	< 1	< 1	< 1	2.0	< 1	< 1	< 1	7.5	3.7	3.6
Al	mg/L	< 0.01	0.03	< 0.01	< 0.01	< 0.01	< 0.01	< 0.01	< 0.01	< 0.01	0.15	0.03	< 0.01
Ca	mg/L	22	130	71	65	60	290	130	110	11	27	19	19
K	mg/L	0.88	9.3	3.8	3.2	0.27	36	4.2	1.9	0.20	4.0	1.9	1.8
Fe	mg/L	0.00	24	8.0	8.0	0.0	26	4.0	2.3	0.0	0.37	0.08	0.04
Mg	mg/L	8.7	43	24	22	16	120	51	43	2.5	8.1	4.6	4.5
Mn	mg/L	0.01	3.2	0.79	0.55	0.00	4.9	1.6	1.5	0.00	0.38	0.05	0.03
Na	mg/L	8.4	110	44	43	12	210	83	74	2.4	8.9	5.7	5.7
P	mg/L	0.04	4.2	1.2	0.91	0.04	1.9	0.49	0.20	0.00	0.09	0.02	0.02
S	mg/L	0.47	22	2.4	1.4	1.5	160	28	18	0.59	1.7	0.97	0.99
Si	mg/L	5.3	37	17	13	7.6	30	16	15	2.3	7.0	5.2	5.4
F^-	mg/L	< 0.3	1.0	<0.3	<0.3	< 0.3	1.5	< 0.3	< 0.3	< 0.3	< 0.3	< 0.3	< 0.3
Cl^-	mg/L	3.5	160	19	9.1	5.2	340	110	58	2.4	9.9	5.9	5.8
PO_4^{3-}	mg/L	< 0.4	13	3.2	2.7	< 0.4	5.6	1.1	< 0.4	< 0.4	< 0.4	< 0.4	< 0.4
SO_4^{2-}	mg/L	< 0.5	58	8.2	5.6	4.7	440	76	52	0.84	3.8	2.0	2.0
NO_3-N	mg/L	< 0.02	0.08	0.03	0.03	< 0.02	15	2.8	0.10	< 0.02	0.06	0.01	< 0.02
NH_4-N	mg/L	1.6	84	20	13	0.75	29	6.4	1.4	0.72	0.88	0.80	0.80
DOC	mg/L	1.0	24	6.9	5.2	0.09	19	3.3	2.2	2.2	7.1	4.4	4.6
Alkalinity	mg/L $CaCO_3$	200	760	420	420	210	860	530	480	39	96	67	69
Sulfide	μg/L	< 1	96	7.4	2.7	< 1	19	2.2	1.0	NA	NA	NA	NA

Figure 5.1.

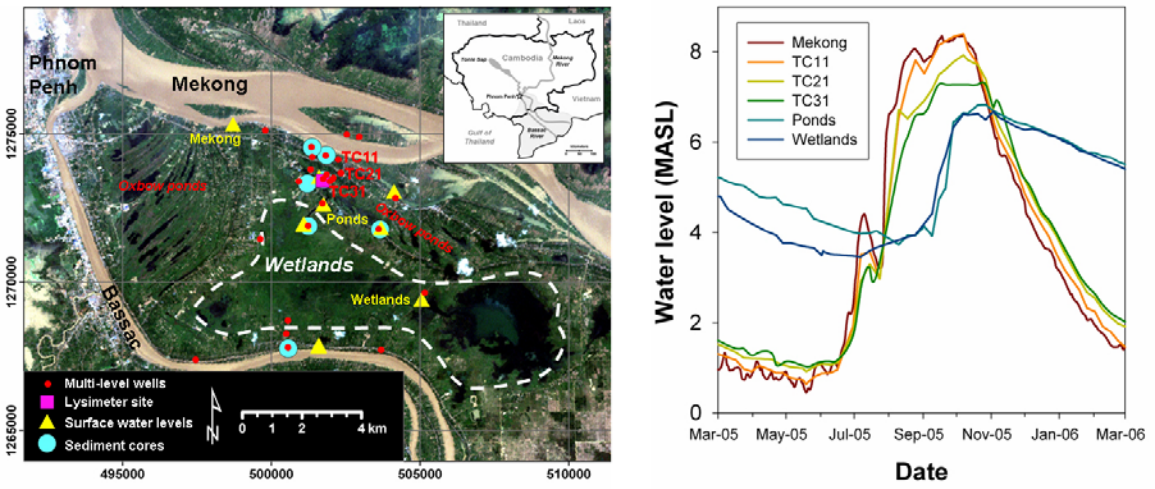
Phnom Penh
Mekong
Mekong
TC11
TC21
TC31
Ponds
Wetlands
Wetlands
Oxbow ponds
Oxbow ponds
Bassac
Multi-level wells
Lysimeter site
Surface water levels
Sediment cores
N
0 1 2 4 km
1275000
1270000
1265000
495000
500000
505000
510000
Thailand
Laos
Cambodia
Vietnam
Gulf of Thailand
Water level (MASL)
Mekong
TC11
TC21
TC31
Ponds
Wetlands
0
2
4
6
8
Mar-05
May-05
Jul-05
Sep-05
Nov-05
Jan-06
Mar-06
Date

Figure 5.2.

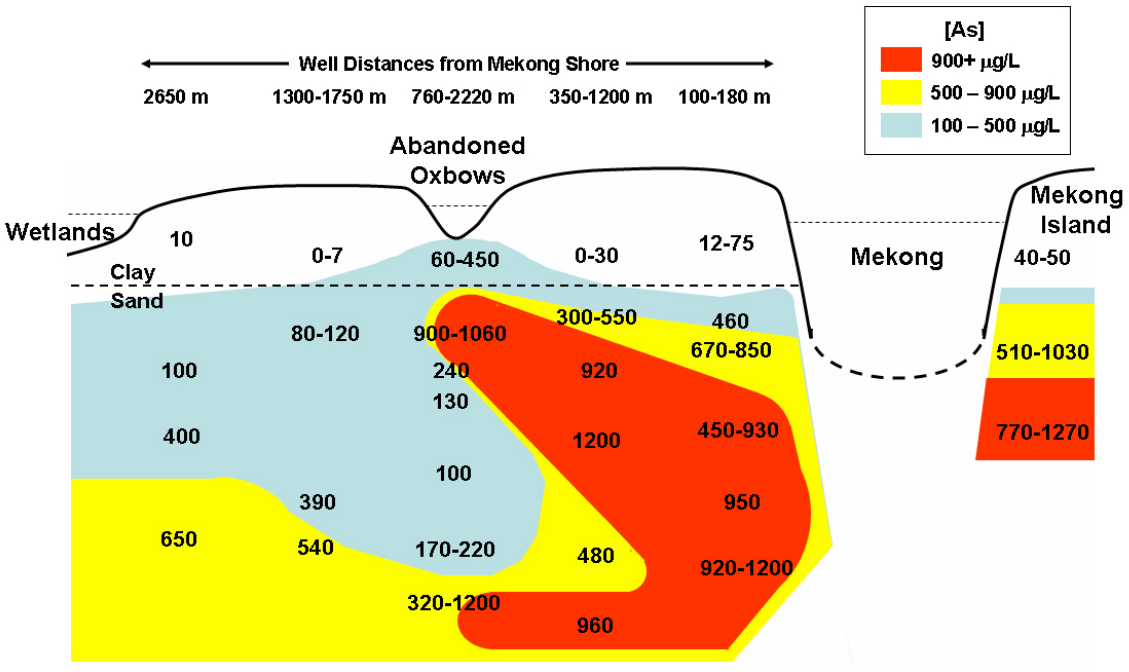
[As]
900+ µg/L
500 – 900 µg/L
100 – 500 µg/L
Well Distances from Mekong Shore
2650 m
1300-1750 m
760-2220 m
350-1200 m
100-180 m
Abandoned Oxbows
Wetlands
Mekong
Mekong Island
Clay
Sand
10
0-7
60-450
0-30
12-75
40-50
80-120
900-1060
300-550
460
670-850
100
240
920
130
510-1030
400
1200
450-930
770-1270
100
390
950
650
540
170-220
480
920-1200
320-1200
960

Figure 5.3.

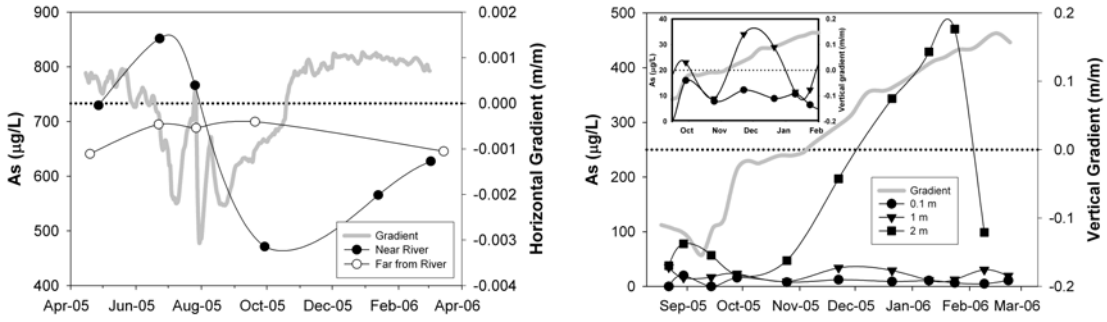
As (µg/L)
Horizontal Gradient (m/m)
Gradient
Near River
Far from River
Apr-05
Jun-05
Aug-05
Oct-05
Dec-05
Feb-06
Apr-06
As (µg/L)
Vertical Gradient (m/m)
Gradient
0.1 m
1 m
2 m
Sep-05
Oct-05
Nov-05
Dec-05
Jan-06
Feb-06
Mar-06

Figure 5.4.

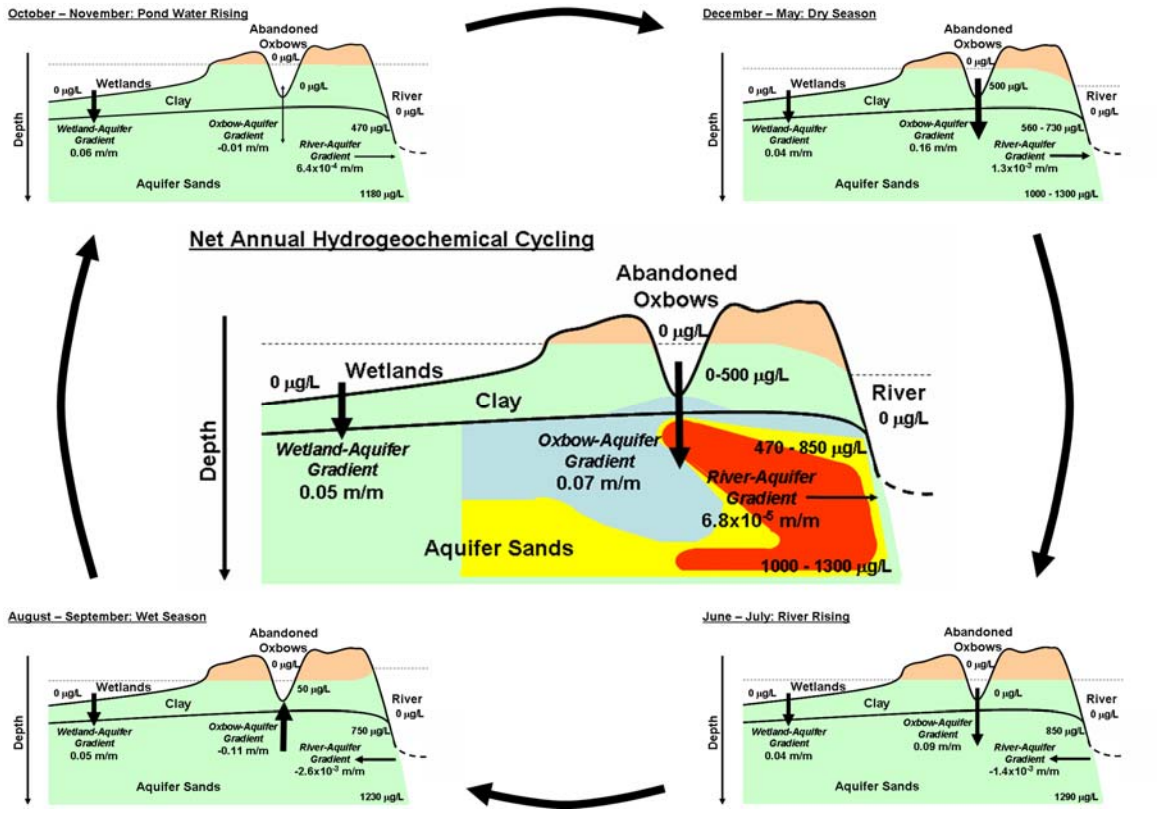
October – November: Pond Water Rising
Abandoned Oxbows
0 µg/L
Wetlands
0 µg/L
Clay
0 µg/L
River
0 µg/L
Depth
Wetland-Aquifer Gradient
0.06 m/m
Oxbow-Aquifer Gradient
-0.01 m/m
470 µg/L
River-Aquifer Gradient
6.4x10-4 m/m
Aquifer Sands
1180 µg/L
December – May: Dry Season
Abandoned Oxbows
0 µg/L
Wetlands
0 µg/L
Clay
500 µg/L
River
0 µg/L
Depth
Wetland-Aquifer Gradient
0.04 m/m
Oxbow-Aquifer Gradient
0.16 m/m
560 - 730 µg/L
River-Aquifer Gradient
1.3x10-3 m/m
Aquifer Sands
1000 - 1300 µg/L
Net Annual Hydrogeochemical Cycling
Abandoned Oxbows
0 µg/L
Wetlands
0 µg/L
Clay
0-500 µg/L
River
0 µg/L
Depth
Wetland-Aquifer Gradient
0.05 m/m
Oxbow-Aquifer Gradient
0.07 m/m
470 - 850 µg/L
River-Aquifer Gradient
6.8x10-5 m/m
Aquifer Sands
1000 - 1300 µg/L
August – September: Wet Season
Abandoned Oxbows
0 µg/L
Wetlands
0 µg/L
Clay
50 µg/L
River
0 µg/L
Depth
Wetland-Aquifer Gradient
0.05 m/m
Oxbow-Aquifer Gradient
-0.11 m/m
750 µg/L
River-Aquifer Gradient
-2.6x10-3 m/m
Aquifer Sands
1230 µg/L
June – July: River Rising
Abandoned Oxbows
0 µg/L
Wetlands
0 µg/L
Clay
0 µg/L
River
0 µg/L
Depth
Wetland-Aquifer Gradient
0.04 m/m
Oxbow-Aquifer Gradient
0.09 m/m
850 µg/L
River-Aquifer Gradient
-1.4x10-3 m/m
Aquifer Sands
1290 µg/L

CHAPTER 6

Conclusions

6.1. ARSENIC CYCLING UNDER NATURAL CONDITIONS IN SOUTHEAST ASIA

Contamination of groundwater in Southeast Asia represents the largest mass poisoning in history (Smith et al., 2000): up to 100 million people are drinking water contaminated with hazardous concentrations of arsenic (Ahmed et al., 2006). In this thesis, I show that arsenic is liberated from soil and near-surface sediments rather than in the aquifer. After displacement from solids in the surface/near-surface, arsenic is subsequently transported to depth by groundwater flow. Sediment deposition during annual monsoonal floods provides a continual source of fresh arsenic to the hydrologic system that continues to replenish arsenic displaced by groundwater flow to the rivers.

Eroded Himalayan sediments, including arsenic-bearing ferric (hydr)oxides and sulfides, are deposited by major rivers in floodplain deltas of Southeast Asia (Figure 6.1). Following sediment deposition, fluctuating water levels at the near-surface create seasonally variable redox conditions that destabilize arsenic, liberating it to solution. During the dry season, sulfide minerals are oxidized, forming additional ferric (hydr)oxides with adsorbed arsenate. As water levels rise in the wet season, reducing conditions stimulate arsenic release from solid-phases. Arsenate reduction to arsenite and ferric (hydr)oxide reductive dissolution cause desorption and, under hydrodynamic conditions, enhanced mobility of arsenic. Arsenic liberation to solution results from microbial reduction processes in soil and near-surface sediments, and dissolved arsenic is associated with high dissolved inorganic carbon and ferrous iron, and low sulfate concentrations. Anaerobic bacterial reduction processes are coupled with oxidation of organic carbon in surface/near-surface sediments.

While redox conditions fluctuate in the surface and near-surface environment (approximately 0 to 4 m in depth), within the contaminated aquifers, strongly reducing conditions persist continuously. Dissolved arsenic is found predominantly as arsenite; groundwater has low oxidation-reduction potentials, and dissolved sulfide, hydrogen, and methane are detectable. Aquifer sediments are dominated by grey silicate sands, and solid-phase arsenic concentrations within the aquifer are at or below crustal averages of 1-20 mg/Kg (Smedley and Kinniburgh, 2002). Up to 60% of the solid-phase arsenic is found in sulfide minerals, including detrital grains remaining from original sediment deposition and authigenic sulfides precipitated within the aquifer. The remainder of solid-phase arsenic is diffusely distributed and exists as adsorbed complexes on mineral surfaces. Ferric (hydr)oxides are not detected within the aquifer sediments, and based on hydrogen and methane concentrations, are not presently serving as electron acceptors in microbial respiration. Therefore, in contrast to the accepted paradigm, arsenic is not released to solution following the microbial reductive dissolution of ferric (hydr)oxides within the aquifer sediments. Furthermore, due to the lack of iron oxide minerals and the predominance of arsenite, arsenic is mobile within the aquifer. Batch incubation experiments confirm the lability of arsenic within aquifer sands.

Owing to hydrologic flow, the mobility of arsenic within the aquifer has implications for the extent of groundwater contamination. Groundwater flow in Southeast Asia is governed by seasonally fluctuating hydraulic gradients between rivers and ponds/wetlands. During the wet season, high river levels breach banks, flooding interior land areas and filling peripheral ponds and wetlands. Additionally, river water enters the aquifer via subsurface flow at the onset of the wet season when groundwater

heads are higher than those for ponds and wetlands. Flow is reversed during the dry season. Flood waters recede by infiltration to the aquifer and surface runoff to rivers, while groundwater discharges to rivers. Despite seasonal reversals in flow directions, net annual groundwater flow is from wetlands and ponds, through the aquifer, and to rivers; hydraulic fluxes indicate steady-state groundwater flow. Arsenic is released from near-surface sediments at recharge zones (ponds and wetlands) following seasonal flooding, which corresponds to the onset of reducing conditions and the steepest downward hydraulic gradients. Thus, arsenic is liberated and drawn into the aquifer below. Once in the aquifer, arsenic, as arsenite, is transported relatively unimpeded through the sandy aquifer. Groundwater flow is governed by natural (Cambodia) or human-induced (Bangladesh) hydraulic gradients, and arsenic is discharged to rivers annually. As a consequence, wells obtaining water along these flow paths are contaminated with arsenic.

Geochemical profiles support arsenic release in the surface and near-surface environment and subsequent transport down to and through the aquifer. Chemical indicators of microbial activity (dissolved organic carbon, dissolved inorganic carbon, phosphate, and ammonium), and specifically Fe(III) and As(V) reduction (Fe^{2+}, H_3AsO_3), are also highest below recharge zones. Furthermore, on the basis of carbon-14 dating, dissolved inorganic carbon (< 2000 years old) in groundwater is younger than the aquifer sediments (> 6000 years old), indicating that the aquifer has been flushed multiple times. Thus, for arsenic concentrations to remain high within the aquifer, arsenic must be continuously entering the aquifer.

High arsenic concentrations are maintained along flow paths between recharge and discharge zones in the aquifer. At discharge zones, arsenic concentrations fluctuate

seasonally due to flow reversals and wet season influx of river water into the aquifer. However, groundwater ultimately discharges into rivers where arsenic is likely oxidized and adsorbed on (or possibly co-precipitated with) newly formed ferric (hydr)oxides in the hyporheic zone. Arsenic-bearing ferric (hydr)oxides formed in the river channel may be transported downstream and then possibly redeposited in the floodplain further downstream. It is possible that one arsenic atom may cycle through groundwater many times before it ultimately reaches the ocean. However, arsenic appears to be at steady-state within the aquifer system. Arsenic influx via sedimentation and efflux via groundwater discharge are equivalent, and groundwater concentrations are maintained despite aquifer flushing. Arsenic has been present in the groundwater for millennia, and under natural conditions, it is poised to remain as a contaminant in Southeast Asian groundwater indefinitely.

6.2. CHANGES TO ARSENIC CONCENTRATIONS FOLLOWING LAND USE ALTERATION

Arsenic concentrations in groundwater are governed by sedimentation, biogeochemical release of arsenic to the aqueous phase, and groundwater flow. Although arsenic contamination of the aquifers has arisen from natural processes, land use alterations that distort the natural hydrologic regime, biogeochemistry, or solid-phase inputs will change arsenic concentrations. The most significant change that has taken place to date is groundwater pumping for irrigation; while irrigation pumping is absent in Cambodia, pumping is extensive in Bangladesh. Dry season pumping in Bangladesh has severely convoluted flow paths and has caused wells to replace rivers as discharge zones

(Harvey, 2006). Furthermore, pumping has decreased groundwater residence times and increased the rate at which surface water recharges the aquifer. Widespread irrigation pumping will ultimately cause average arsenic groundwater concentrations to decrease over time since sediment input remains the same but the aquifer is flushed more rapidly, thereby discharging a greater quantity of arsenic annually.

The placement of wells also impacts the distribution of arsenic. When multiple irrigation wells are screened at the same depth in a local area, recharge waters are drawn to that depth and maximum arsenic concentrations are found there; evidence for this scenario is observed at the BUET-MIT field site in Munshiganj, Bangladesh (Harvey et al., 2002). However, when irrigation wells are of variable depth, the spatial distribution of arsenic becomes more random. Finally, and importantly, irrigation pumping will shift recharge paths owing to anisoptropy in hydraulic conductivities.

Excavation of surface sediment is another common alteration in Bangladesh. Surface clays are used to build roads and villages above wet season flood levels, and excavation leaves depressions in the land surface. The holes become ponds and with the thinned clay serve as local recharge zones. In areas where excavation is common, flow paths are convoluted since a few large recharge areas are replaced by many small ones. Moreover, as sediments are removed, arsenic is also removed and input to groundwater diminished. Indeed, areas in Bangladesh without a surficial clay layer exhibit lower arsenic concentrations than in comparable areas with a clay surface layer (Métral et al., 2007).

Finally, upstream river damming, as is proposed for upper reaches of the Mekong River, will also impact arsenic concentrations in groundwater. River levels are controlled

by Himalayan monsoonal rains and snowmelt, and it is the large fluctuations in river levels that drive the floodplain hydrology. With the installation of dams, downstream water stage level amplitudes will be drastically reduced. As a result, hydraulic gradients will be gentler, flooding will cease, and groundwater flow will become more stagnant. Additionally, dams will trap sediments, reducing downstream river suspended loads. Combined with a lack of flooding, floodplain sedimentation will decrease and arsenic inputs will drop. Thus, upstream damming will result in decreased arsenic concentrations in groundwater.

Bangladesh and Cambodia represent end-member cases in terms of anthropogenic land use alterations. In Bangladesh, the dense population is dependent on dry-season rice crops, and irrigation covers over 25% of the nation's land surface (Hossain et al., 2003). Additionally, yearly flooding throughout the nation has led to widespread sediment excavation for road and village development. In many areas wells have replaced rivers as discharge zones. As a result, natural groundwater flow paths are distorted and the spatial variability of arsenic is high (van Geen et al., 2003). In contrast, land use alterations are minimal in Cambodia, and groundwater flow is governed by natural gradients. Accordingly, the distribution of arsenic is dictated by decipherable flow patterns. However, while arsenic concentrations may be decreasing in Bangladesh due to aquifer flushing by irrigation pumping and excavation of arsenic-bearing surface sediments, arsenic concentrations remain at high levels in Cambodia.

Elevated arsenic concentrations in Bangladesh groundwater were only discovered following the mass use of groundwater for irrigation, and due to the resultant changes in the hydrologic regime, processes controlling arsenic were not fully elucidated. However,

because land use alterations are minimal, Cambodia serves as a view to the past of Bangladesh, prior to irrigation pumping and sediment excavation. Recognition of the near-surface source of arsenic and the sensitivity of arsenic to changes in flow paths explains the spatial variability in arsenic concentrations observed in Bangladesh. Moreover, understanding the natural coupled hydrological and biogeochemical processes governing arsenic concentrations is an essential starting point for effectively planning future groundwater use strategies in Bangladesh.

While the influence of human-induced alterations to arsenic sedimentary inputs, biogeochemical release mechanisms, and groundwater flow is currently negligible in Cambodia, the country is poised for rapid population growth and future development. Changes in land use are imminent and arsenic concentrations will be altered accordingly. In this regard, Bangladesh serves as a view towards Cambodia's future. By observing how arsenic concentrations have changed under different land uses in Bangladesh, arsenic concentrations resulting from similar human-induced land use alterations may be better predicted in Cambodia.

6.3. REFERENCES

Ahmed, M. F., Ahuja, S., Alauddin, M., Hug, S. J., Lloyd, J. R., Pfaff, A., Pichler, T., Saltikov, C., Stute, M., and van Geen, A. (2006) Ensuring safe drinking water in Bangladesh. *Science* **314**, 1687-1688.

Harvey, C. F., Swartz, C. H., Badruzzaman, A. B. M., Keon-Blute, N., Niedan, V., Brabander, D., Oates, P. M., Ashfaque, K. N., Islam, S., Hemond, H. F., and Ahmed, M.F. (2002) Arsenic mobility and groundwater extraction in Bangladesh. *Science* **298**, 1602-1606.

Harvey, C. F., Ashfaque, K. N., Yu, W., Badruzzaman, A. B. M., Ali, M. A., Oates, P. M., Michael, H., Neumann, R. B., Beckie, R., Islam, S., and Ahmed, M. F. (2006) Groundwater flow and arsenic biogeochemistry in Bangladesh: an analysis of transience and coupling. *Chemical Geology* **228**, 112-136.

Hossain, M., Lewis, D., Bose, M., and Chowdhury, A. (2003) *Rice Research, Technological Progress, and Impacts on the Poor: The Bangladesh Case (Summary Report)*. International Food Policy Research Institute, Washington, DC.

Métral, J., Charlet, L., Bureau, Mallik, S. B., Chakraborty, S., Ahmed, K. M., Rahman, M. W., Cheng, Z., and van Geen, A. (2007) Impact of local recharge on arsenic concentrations in shallow aquifers of Chakdaha, India, and Araihazar, Bangladesh. *Geochem. Trans.,* in press.

Smedley, P. L. and Kinniburgh, D. G. (2002) A review of the source, behaviour and distribution of arsenic in natural waters. *Appl. Geochem.* **17**, 517-568.

Smith, A. H., Lingas, E. O., and Rahman, M. (2000) Contamination of drinking-water by arsenic in Bangladesh: a public health emergency. *Bulletin World Health Organization* **78**, 1093-1103.

van Geen, A., Zheng, Y., Versteeg, R., Stute, M., Horneman, A., Dhar, R., Steckler, M., Gelman, A., Small, C., Ahsan, H., Graziano, J. H., Hussain, I., and Ahmed, K. M. (2003) Spatial variability of arsenic in 6000 tube wells in a 25 km^2 area of Bangladesh. *Water Resour. Res.* **39**, 1140, doi: 10.1029/2002WR001617.

6.4. FIGURE CAPTION

Figure 6.1. Processes controlling the fate and transport of arsenic in Southeast Asia.

Figure 6.1.